Short range reconnaissance unmanned aerial vehicle

S.J. KERSOP

B. ENG. (ELECTRONIC ENGINEERING)

Dissertation submitted in fulfilment of the requirements for the degree:
MASTERS of ENGINEERING at the North West University

PROMOTER: **DR M. KLEINGELD**

NOVEMBER 2009

PRETORIA

ABSTRACT

Title:	Short Range Reconnaissance Unmanned Aerial Vehicle
Author:	Stefanus Jacobus Kersop
Promoter:	Dr M. Kleingeld
School:	Electrical and Electronic Engineering
Faculty:	Engineering
Degree:	Masters of Engineering
Search terms:	Unmanned Aerial Vehicles (UAV), Unmanned Aerial Systems (UAS), Man-portable, autopilot, data link, mini-UAV, small UAV, cameras, RF transmitters.

Unmanned aerial vehicles (UAVs) have been used increasingly over the past few years. Special Forces of various countries utilise these systems successfully in war zones such as Afghanistan. The biggest advantage is rapid information gathering without endangering human lives.

The South African National Defence Force (SANDF) also identified the need for local short range aerial reconnaissance and information gathering. A detailed literature survey identified various international players involved in the development of small hand-launch UAV systems. Unfortunately, these overseas systems are too expensive for the SANDF. A new system had to be developed locally to comply with the unique requirements, and budget, of the SANDF.

The survey of existing systems provided valuable input to the detailed user requirement statement (URS) for the new South African development. The next step was to build a prototype using off-the-shelf components. Although this aircraft flew and produced good video images, it turned out to be unreliable.

The prototype UAV was then replaced with a standard type model aircraft, purchased from Micropilot. Some modifications were needed to ensure better compliance with the URS. Laboratory and field tests proved that the aircraft can be applied for aerial images, within a

range of 10 km from the ground control station (GCS). The major limitation is that it can only fly for 40 minutes. Furthermore, the airframe is not robust, needing repairs after only 15 flights.

Although the system has shortcomings, it has already been used successfully. It is expected that improved battery technologies and sturdier light-weight materials will further help to improve the system beyond user specifications.

SAMEVATTING

Titel:	Kortafstand onbemande verkenningsvliegtuig
Outeur:	Stefanus Jacobus Kersop
Promotor:	Dr M. Kleingeld
Skool:	Skool vir Elektriese en Elektroniese Ingenieurswese
Fakulteit:	Ingenieurswese
Graad:	Magister Engeneriae
Sleutelterme:	Unmanned Aerial Vehicles (UAV), Unmanned Aerial Systems (UAS), Man portable, autopilot, data link, mini-UAV, small UAV, cameras, RF transmitters

Onbemande lugvoertuie (UAV's) is die afgelope paar jaar toenemend gebruik. Spesiale Magte van verskillende lande wend hierdie sisteme suksesvol in oorlogsgeteisterde gebiede soos Afghanistan aan. Die grootste voordeel hiervan, is dat inligting spoedig ingewin word sonder om menselewens in gevaar te stel.

Die Suid-Afrikaanse Nasionale Verdedigingsmag (SANDF) het die behoefte na 'n plaaslike, kortafstand, lugverkenning en inligtingsversameling geïdentifiseer. 'n Gedetaileerde literatuuroorsig het getoon dat verskeie internasionale rolspelers betrokke is in die ontwikkeling van klein hand-loods UAV sisteme. Ongelukkig is hierdie oorsese sisteme te duur vir die SANDF om aan te skaf. 'n Nuwe sisteem is plaaslik ontwikkel om aan al die unieke vereistes te voldoen en binne die begroting van die SANDF te bly.

Die oorsig van bestaande sisteme het 'n waardevolle bydrae tot die gedetaileerde gebruikervereistestaat (URS) vir die nuwe Suid Afrikaanse ontwikkeling gelewer. Die volgende stap was om 'n prototipe te bou, deur plaaslike bekombare komponente te gebruik. Alhoewel hierdie vliegtuig wel gevlieg het, en goeie beeldmateriaal gelewer het, was dit onbetroubaar.

Die prototipe UAV is vervang met 'n standaard modelvliegtuig, aangekoop by Micropilot. Dit was noodsaaklik om sekere veranderings aan te bring om te verseker dat dit aan die

vereistes van die URS voldoen. Laboratorium- en veldtoetse het bewys dat die vliegtuig aangewend kan word vir die inwin van lugfotos binne 'n afstand van 10 km vanaf die grondbeheerstasie (GCS). Die grootste beperking was dat dit slegs vir 40 minute kan vlieg en dat die lugraam nie sterk genoeg was nie. Verder word herstelwerk benodig na net 15 vlugte.

Alhoewel die sisteem tekortkominge het, is dit alreeds suksesvol aangewend. Daar word verwag dat verbeterde batterytegnologie en sterker liggewigmateriale die sisteem kan verbeter en gebruiker spesifikasies ver oortref.

ACKNOWLEDGEMENTS

There are several people I would like to thank for their help and support during this study:

a. To God, for my abilities and to be able to enjoy life.

b. To my wife Yolandé, for her support, understanding and motivation.

c. To my study leader Dr Marius Kleingeld, for his motivation, patience and guidance.

d. To the Council of Scientific and Industrial Research (CSIR) who sponsored my studies financially and in giving me the time to do most of my work during working hours.

e. To Trevor Kirsten and Klaus Muller, my managers, for encouraging me to work on my studies during times project deliverables were urgent.

f. Dr Bennie Broughton and Mr John Monk at CSIR DPSS Aeronautics Systems for the aeronautical designs, calculations and field test support.

g. To everyone else who also made a contribution and were not mentioned.

TABLE OF CONTENTS

Abstract i
Samevatting iii
Acknowledgements v
List of tables vii
List of figures viii
List of abbreviations xi
List of terminologies xiii

1 INTRODUCTION 14

1.1 Preamble 15
1.2 Existing UAV Technologies 15
1.3 Payload technologies for mini-UAV's 19
1.4 Wireless communications technologies 21
1.5 Need for new development 28
1.6 Purpose of this study 29
1.7 Outline of this study 30

2 REQUIREMENTS for a mini-UAV system 32

2.1 Preamble 33
2.2 Operational Requirements 35
2.3 Training requirements 39
2.4 Maintenance and support requirements 40
2.5 Environmental requirements 40
2.6 Summary 41

3 DESIGN AND IMPLEMENTATION 42

3.1 Preamble 43
3.2 Aerial Platform 44
3.3 Payloads 65
3.4 Ground Control Station 78
3.5 Summary 85

4 DESIGN VERIFICATION AND RESULTS 87

4.1 Overview 88
4.2 Laboratory tests 88
4.3 Field tests 96
4.4 Summary 119

5 SUMMARY AND RECOMMENDATIONS 121

5.1 Conclusion 121
5.2 Recommendations for Future Development 122

6 References 125

LIST OF TABLES

Table 1: Comparing different cameras 23
Table 2: Comparing analogue video transmitters 24
Table 3: Comparing different antennas 25
Table 4: Comparing mini-UAV constraints 34
Table 5: Field of view estimates at different heights for different cameras 37
Table 6: Summary of environmental requirements 41
Table 7: Comparing power gliders 48
Table 8: Autopilot comparisons 51
Table 9: Comparing brushless speed controllers 54
Table 10: Lead-acid battery characteristics 57
Table 11: Ni-Cd battery characteristics 58
Table 12: Ni-MH battery characteristics 58
Table 13: Li-Ion battery characteristics 59
Table 14: Li-Po battery characteristics 60
Table 15: Comparing primary batteries 60
Table 16: Summary of different battery types 61
Table 17: Comparing laptops 79
Table 18: Comparing RF serial data links 81
Table 19: Comparing power usage at different throttle settings 89
Table 20: Summary of flight tests performed to better the landings 105
Table 21: Summary of flight log data on payload with fixed day cameras 114
Table 22: Summary of endurance flight tests with panning camera payload 115
Table 23: Summary of endurance flight tests with different payloads 120

LIST OF FIGURES

Figure 1: Predator & Global Hawk 17
Figure 2: Photo (2001) of AeroVironment's Pointer UAV 18
Figure 3: Typical mini-UAV system components block diagram [27] 18
Figure 4: Examples of typical mini-UAV systems (Dragon Eye & Casper) 19
Figure 5: Aladin UAV day & night payload [15] 20
Figure 6: Casper-250 Camera Payload [16] 21
Figure 7: Radiation pattern of two half-wave dipole antennas 26
Figure 8: Radiation pattern for a Yagi antenna [40] 26
Figure 9: Radiation pattern for the PANL-0005 patch antenna 27
Figure 10: First aircraft design 47
Figure 11: Li-Po discharge characteristics of a FlightPower battery 62
Figure 12: Ground loops ([37], p12) 63
Figure 13: Battery connection modifications 64
Figure 14: Camera bracket with 2 board lens cameras 66
Figure 15: 2.4GHz Video RF link before and after modifications 67
Figure 16: Camera switch block diagram with a photo of the PCB 68
Figure 17: Camera payload with two fixed day cameras (260 g) 70
Figure 18: EPP foam, fibre-reinforced tape, plastic primer & paint used on payload. 71
Figure 19: Panning camera platform with colour and B/W camera (83 g) 72
Figure 20: Pod with panning camera platform (300 g) 72
Figure 21: Pan-Tilt platform with two fixed day cameras (85 g) 73
Figure 22: Pod with fixed colour cameras in pan-tilt platform 74
Figure 23: Indigo Omega FLIR camera 74
Figure 24: Night pod with Indigo Omega FLIR thermal camera 75
Figure 25: Payload connection on aircraft 75
Figure 26: Wiring block diagram inside aircraft for payloads 76
Figure 27: Servo breakout board with payload wiring 76
Figure 28: Wireless serial communications block diagram 80
Figure 29: Block diagram with photos of the GCS RS232 serial RF interface 82
Figure 30: Photo of GCS laptop with serial link 82
Figure 31: Block diagram of the aircraft's RS232 serial RF interface 83
Figure 32: 2.4 GHz Video receiver (Supplier P/N: E-RX2410) 84
Figure 33: Video receiving and display setup 85
Figure 34: Graph of engine power vs. throttle settings 90
Figure 35: Stationary range test area for data link 92
Figure 36: Aircraft side view for antenna placement 93

Figure 37: Modification to aircraft rudder for adding protection 97
Figure 38: Flight plan for endurance tests 98
Figure 39: Launching the aircraft 100
Figure 40: UAV used for benchmark flight tests 100
Figure 41: Screen capture of GCS software during benchmark flight tests 101
Figure 42: Micropilot landing circuit ([37], p83) 102
Figure 43: Landing circuit final leg 103
Figure 44: Wing centre piece with spoiler attached 107
Figure 45: Arial footage with engine noise 112
Figure 46: Aerial pictures of stationary cameras payload 113
Figure 47: Image captured from pan-tilt camera footage early morning 115
Figure 48: Image of the FLIR camera on a farm flying 90 m above ground 116
Figure 49: Centre of Gravity (CG) measuring jig 117
Figure 50: Aircraft Battery pack 128
Figure 51: Bench test for measuring the running motor power 129
Figure 52: Picture of Bench setup for battery tests 129
Figure 53: Battery Voltage & Current measurement with a throttle 130
Figure 54: Battery Voltage & Current measurement with a throttle 130
Figure 55: Battery Voltage & Current measurement with a throttle 131
Figure 56: Battery Voltage & Current measurement with throttle set to 75 % 131
Figure 57: Battery Voltage & Current measurement with throttle set to 90 % 132
Figure 58: Battery Voltage & Current measurement with a throttle 132
Figure 59: Ground voltage between battery and servo board 133
Figure 60: RC servo control pulses 134
Figure 61: Schematic circuit design for the payload camera & LED switch 135
Figure 62: Screenshot of Horizon software 136
Figure 63: Screenshot of autopilot flight parameters setup 137
Figure 64: Screenshot of Spoiler activation table 138
Figure 65: Photo of aircraft used for benchmark test (with spoiler on wing) 139
Figure 66: Screen shot of aircraft flight trail during benchmark test 140
Figure 67: Desired Altitude vs. Current Altitude over time 140
Figure 68: Desired speed, current speed and GPS speed plotted against 141
Figure 69: Throttle settings during altitude control 141
Figure 70: Current altitude vs. desired altitude during the descent of the 142
Figure 71: Spoiler activation during the landing descent. 142
Figure 72: Landing test flight 1 143
Figure 73: Landing test flight 2 143

Figure 74: Landing test flight 3 144
Figure 75: Landing test flight 4 144
Figure 76: Landing test flight 5 144
Figure 77: Landing test flight 6 *(Speed data not available)* 145
Figure 78: Landing test flight 7 145
Figure 79: Landing test flight 8 145
Figure 80: Landing test flight 9 146
Figure 81: Desired Roll vs. Current Roll and Aileron control 147
Figure 82: Desired Pitch vs. Current Pitch and elevator control 148
Figure 83: Log data for flight in winds > 30km/h at sea level 148
Figure 84: Wiring block diagram for payload with cameras that can pan side-to-side 149
Figure 85: Wiring block diagram for payload with cameras that can pan and tilt 150
Figure 86: Wiring diagram for payload with FLIR camera and LEDs 151

LIST OF ABBREVIATIONS

(H)	Height
(L)	Length
(W)	Width
2-D	Two Dimensional
3-D	Three Dimensional
A	Ampere
Ah	Ampere-hour
B/W	Black and White
Bps	Bits per second
C	Capacity (used to specify current ratings for batteries)
CCD	Charge-coupled device
CCT	Circuit
COTS	Commercial off the shelf
CSIR	Council of Scientific and Industrial Research
D	Diameter
dB	Decibel
dBi	Decibel isotropic
DPSS	Defence, Peace, Safety and Security (operational unit within the CSIR)
EO	Electro-Optical
EPP	Expanded polypropylene
F	Focal length (photography)
GCS	Ground Control Station
GHz	Giga-Hertz
I	Electrical Current
IEEE	Institute of Electrical & Electronics Engineers, Inc
IP	Internet Protocol
IR	Infra Red
ITAR	International Traffic in Arms Regulations
LED	Light Emitting Diode
LOS	Line of sight
Mb	Mega-byte
MHz	Mega-Hertz
miniDV	Miniature digital video
OEM	Original Equipment Manufacturing
P/N	Part Number
PCB	Printed Circuit Board
PCI	Peripheral Component Interconnect
PCMCIA	Personal Computer Memory Card International Association
p-p	Peak to Peak
PTZ	Pan Tilt Zoom
RAM	Random-Access Memory
RC	Radio Control
RF	Radio Frequency
RPV	Remote Piloted Vehicle
RS232	Recommended Standard 232, Computer serial interface, IEEE
SANDF	South African National Defence Force
TFT	Thin Film Transistor (Liquid Crystal Display, LCD technology)
TSO	Technology for Special Operations (operational unit within DPSS)
TTL	Transistor-Transistor Logic
TVL	Television (TV) Lines

UAS	Unmanned Aerial System
UAV	Unmanned Aerial Vehicle
USB	Universal Serial Bus
UV	Ultra Violet
V	Voltage
VAT	Value Added Tax
VDC	Voltage Direct Current
VID	Video
W	Watt
Wh	Watt-hour
XGA	eXtended Graphics Array (1024 by 768 pixels; 1.33:1 aspect ratio)

LIST OF TERMINOLOGIES

Rugged	Synonym for robust
V	Also implies VDC
CAM1	Camera 1
CAM2	Camera 2
Imax	Maximum Current
Imin	Minimum Current
Vmax	Maximum Voltage
Vmin	Minimum Voltage
Iavg	Average Current
Vavg	Average Voltage
Pavg	Average Power
dB	Output gain referenced to the source
dBi	Output gain referenced to an Isotropic source. An Isotropic source is the perfect omni-directional radiator, a true "Point Source", and does not exist in nature. It's useful for comparing antennas, as since it is a constant[1].

[1] http://www.dslreports.com/faq/14091 on 21 October 2009

1 INTRODUCTION

Chapter one describes the problem statement for unmanned aerial reconnaissance. A research study on existing methods and technologies of world wide trends was conducted to address the problem. A small fixed wing unmanned aerial vehicle (UAV) was identified to be the most suitable solution. The question of whether such a system should be procured off the shelf or designed and built is answered at the end of this chapter.

1.1 Preamble

Intelligence and information gathering has become increasingly important in modern military operations. Normally a well-trained military soldier will be required to get close to the enemy site that must be monitored. He must then gather and record information on everything he observes without revealing his presence. With the rapid growth in the electronic industry, lightweight surveillance equipment has become very sophisticated and is relatively cheap. This has made it possible to design and develop small airborne surveillance equipment that can be fitted into lightweight remotely controlled aircraft.

Applying these new technologies has resulted in unmanned vehicles becoming more attractive for obtaining information on the enemy. The most commonly used equipment for aerial reconnaissance is unmanned aerial vehicles (UAV). UAV's are flying platforms that do not require the use of a human pilot. The purpose of the UAV is to carry a specific payload for whatever task it is required to perform. The most commonly used payloads are camera equipment that is capable of transmitting aerial images back to the person controlling it. This means that the soldier does not need to get as close to the target as previously required to do. This makes it much safer to gather information. This chapter discusses the different types of UAV's available in the world today.

1.2 Existing UAV Technologies

There are many different technologies on unmanned vehicles in use today. All these types of technologies are designed for specific purposes. The different types can be divided into three main groups; land, maritime and aerial. This study will focus on the aerial type which is known as Unmanned Aerial Vehicles (UAV) or Unmanned Aerial Systems (UAS). The term UAV will be used throughout this dissertation.

Prior to 1980, these types of aircraft were known as Remotely Piloted Vehicles (RPV's). An aircraft without a pilot onboard was remotely controlled by an operator on the ground. As these aircraft became more advanced and started to fly totally autonomously, they became known as UAV's [6], p13. NATO Military Committee Air Standardisation Board (MCASB) defines UAV's as: "A powered aerial vehicle that does not carry a human operator, uses aerodynamic forces to provide vehicle lift, can fly autonomously or be piloted remotely, can be expendable or recoverable, and can carry a lethal or non-lethal payload" [3].

UAV systems are currently being applied for civil and military applications. The civil applications include traffic control, search and rescue, crop and pipeline surveying, power cables inspection, and many more [5], p7. For military use, the main applications for applying UAV systems are for reconnaissance, target acquisition, aerial surveillance or to act as a communications relay station. Some UAV's are also applied for armed combat and are called Unmanned Combat Arial Vehicles (UCAVs). The first published American UAV attack was on 4 November 2002 by the armed Predator UAV in Afghanistan [6], p9.

For each type of mission, a specific class of UAV system is required to perform that specific function. A variety of UAV's have been developed, ranging from small to large and from rotary wing to fixed wing systems. The different UAV's can be classified according to the weight, size, mission endurance or range. Currently there is no international standard for UAV classification. The larger class UAV's are considered to have a take-off weight of more than 200 kg [8], p9. Examples of these larger classes UAV's are the Predator and Global Hawk, shown in Figure 1, which are used by the United States Air Force (USAF). This class of UAV's is mainly used for aerial surveillance, but can also carry weapons and be used to attack specific targets.

Figure 1: Predator & Global Hawk[2]

Towards the end of the twentieth century, it became more popular to use the smaller UAV's for short range reconnaissance. This research work focused on the design and development of smaller and easily portable UAV's. The UAV's satisfying this criterion will fall into the mini-UAV or small-UAV class. A mini-UAV is defined as being hand-launchable, weighing less than 30 kg [5] p162, has a wingspan of 15 cm to 300 cm and can fly 30 km to 80 km [1]. A typical mini-UAV system will not require more than two persons to operate it.

Mini UAV's for military use have been in production since the 1980's. Dr. Paul MacCready's AeroVironment Company developed the Pointer UAV, with the prototype first flying in 1986 ([7], p27). The airframe of a high-performance model glider aircraft was used and fitted with an electric motor and propeller. A video camera and radio data link were also installed. Figure 2 is a photograph taken of this first hand-launched and backpack-carried UAV in 2001 when it reached a more mature status. It was difficult to keep track of this UAV because it was not equipped with any navigation devices, i.e. GPS. This limitation is no longer a factor. Mini-UAV's are nowadays equipped with GPS, small autopilots and light weight data links. This enables the portable UAV to sustain out-of-sight flights of more than 10 km in radius [4].

[2] Pictures from websites http://en.wikipedia.org/wiki/MQ-1_Predator & http://en.wikipedia.org/wiki/RQ-4_Global_Hawk

Figure 2: Photo (2001) of AeroVironment's Pointer UAV

Mini-UAV's are mostly used for reconnaissance, force protection, surveillance and target acquisition missions. Intelligence information is gathered in the form of video images of a specific area. Other possible missions would be to detect biological or chemical agents, act as a communications relay and supply small packages. The UAV can also be fitted with certain weapons with a lethal capability. [9]

Mini-UAV systems consist of at least one aircraft and one Ground Control Station (GCS). Figure 3 is a block diagram showing the main system components for a man-portable UAV system.

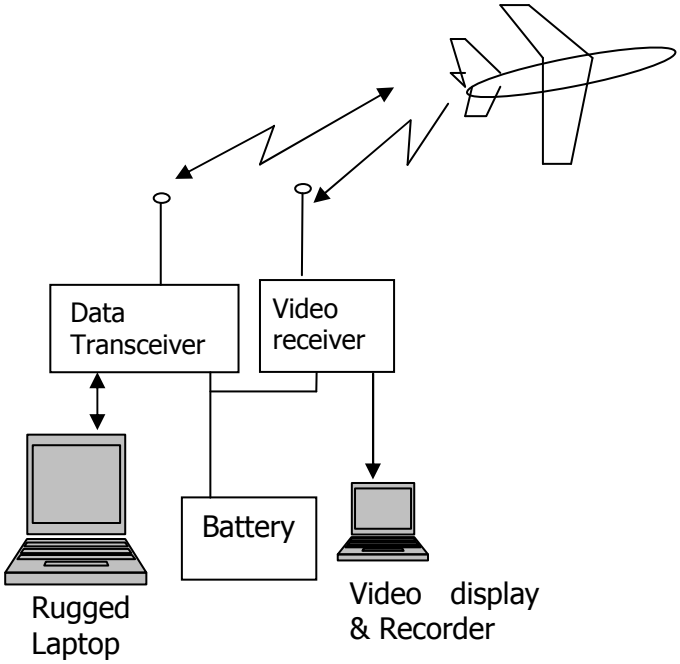

Figure 3: Typical mini-UAV system components block diagram [27]

A team of two people will usually be used to carry the system to the area that must be monitored. Transporting the UAV on foot will usually be restricted to a maximum carrying distance of 50 km. When the GCS has been correctly initialised, the aircraft will be launched either by hand or bungee. The operator will then control the flight path of the aircraft using the GCS. A GCS normally consists of a laptop computer and radio links, as well as a video display unit with a recording capability. Pictures of typical mini-UAV systems are shown in Figure 4.

Figure 4: Examples of typical mini-UAV systems (Dragon Eye[3] & Casper[4])

Apart from the aircraft itself, the most important part of the system is the quality and capability of the sensors on board that are needed to gather information. The sensor is the part of the system that provides the required intelligence information. The following paragraph provides details of the types of sensor technologies currently available and being used by the different systems.

1.3 Payload technologies for mini-UAV's

The size and weight of the mini-UAV systems are significant limiting factors because of the maximum payload that can be carried. The weight of the system equipment will directly influence the amount of fuel that the UAV can carry. This in turn will influence the mission endurance and range. However, range will generally be limited to line of sight (LOS) distance from the GCS to ensure remote control

[3] http://en.wikipedia.org/wiki/Dragon_Eye, 21 September 2009
[4] http://defense-update.com/products/c/casper200.htm, 21 September 2009

communication. In spite of these limitations, the UAV's still remain useful for a variety of military and non-military missions.

The most common sensor types used for reconnaissance work are cameras. Different types of cameras are available for different missions. Day cameras, low light cameras, infra red cameras and thermal imagers are popular for use as observations sensors. These cameras are configured differently by each manufacturer. Typically a payload would consist of a single type of sensor or a combination thereof.

The Aladin UAV from the German company, EMT, uses four colour video CCD cameras for daylight reconnaissance [15]. One camera is for pilot view and two are downward looking. The two downward looking cameras are fitted with a wide and a narrow angle view lens. The fourth camera is mounted on the side of the aircraft and used when flying in circles while the aircraft is banked. For night reconnaissance, a forward looking Infra Red (IR) thermal imaging video camera and an inclined forward looking colour video CCD daylight camera are used. These cameras are shown, as installed on the UAV, in Figure 5.

Figure 5: Aladin UAV day & night payload [15]

The Dragon Eye UAV, manufactured by a company in the USA, Aerovironment, has either dual forward and side-looking Electro-Optical (EO) cameras, forward and side-looking low light cameras or a side-looking IR camera [17]. These are three different configurations that are installed separately in the UAV by replacing the nose cone. The cameras are all fitted with fixed lenses.

The Casper-250 UAV from Becker Avionics [16] carries an Electro-Optical day sensor payload with a CCD camera as shown in Figure 6. This payload is a stabilised gimbal

ring assembly, with a 25 x zoom capability, which can rotate around 2 axes and pan and tilt. The camera can be controlled from the GCS while the aircraft is in the air. These gimbal ring stabilised cameras that can pan, tilt and zoom (PTZ) are much heavier than the smaller fixed cameras. However it is much faster and more effective to move the camera rather than the aircraft, making these cameras particularly useful.

Figure 6: Casper-250 Camera Payload [16]

The video images provided by the cameras must have the ability to be transmitted to the GCS. Different technologies that can provide this facility are available and will be discussed in the following chapter.

1.4 Wireless communications technologies

Wireless methods are required to control the aircraft from the GCS and also to view the video image in real time on the ground. Wireless technologies that are suited for this type of application are Radio Frequency (RF), for transmitting live video steaming, as well as digital data. Other technologies such as infra red (IR) and laser do not cover the required distance and are too directional to be used in this application. UAV manufacturers are reluctant to provide this technical information. This meant that extensive research was required to obtain and evaluate suitable equipment that was freely available.

Only RF technologies will be considered for this solution. One option for using RF is to transmit the video and data on separate links. A second option is to use one link for transmitting video and data simultaneously. Using two links will have the

implication of two RF modules with two antennas. This will add to the total mass, size and maybe[5] drag coefficient of the aircraft. If the option for one link is considered, a high bandwidth RF link will be required for transmitting the high resolution digital video images. Transmitting high resolution digital video images requires much more bandwidth than transmitting an analogue video signal with digital data on separate links.

The types of cameras that are suitable for installation in the UAV directly influence the choice of RF links. The cameras must be chosen before deciding on the type of RF link required. The cameras should, ideally, be inexpensive, small, light weight with low power consumption and be able to produce a clear image with as high as possible resolution. The research outcome on these types of cameras is shown in Table 1.

[5] The antennas can be built into the fuselage which will not add to drag, but only mass.

Table 1: Comparing different cameras[6]

Camera & Price	Size & Weight	Supply Voltage & Power consumption	Colour or Black & White Resolution (TV Lines)	Minimum lux & Focal length	Video output format	Pictures of cameras
Boardlens R1275	22 x 22 x 26mm 12g	12 V 840mW	Colour 580 TVL	2.0 (F2.0)	1.0V p-p composite at 75Ω	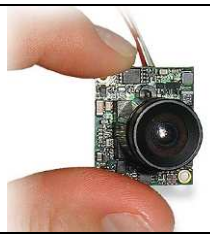
Mini Camera R1890	25 x 25 x 20.5mm 70g	12 V 960mW	Colour 480 TVL	0.8 (F2.0)	1.0V p-p composite at 75Ω	
Mini Camera R761	25 x 25 x 18.5mm 50g	12 V 1.2W	Black & White 420 TVL	0.05 (F2.0)	1.0V p-p composite at 75Ω	
SONY OEM Zoom camera R3662	39 x 42 x 62mm 95g	12 V 3.6W(max)	Colour 480 TVL	2.5 10x zoom & auto focus	1.0V p-p composite at 75 Ω	

Table 1 shows some of the small, light weight Custom off the Shelf (COTS) cameras that are readily available on the market. These cameras are ideally suited for this application. These cameras all produce a composite video output with a supply voltage of 12 V. In the video surveillance security environment, 12 V analogue video transmitters are commonly used. The CSIR has many years of operational experience with these types of transmitters which simplified a correct camera choice. According

[6] Information from http://www.eaglecctv.co.za/display_cat_2.htm, retrieved on 6 July 2009

to the specifications of these small cameras, the analogue video transmitter was considered to be the better option to start off with. The known transmitters that were considered for the UAV application are listed in Table 2.

Table 2: Comparing analogue video transmitters

Transmitter & Price	Size (mm)	Weight (g)	Output Power (W)	LOS Transmission range (km)	Frequency (GHz)	Picture
E-243000 R5250	120 x 55 x 38	200	5	10	2.4	
E-123000 R5250	120 x 55 x 38	200	5	10	1.2	

These video transmitters are available in two different frequencies (1.2 GHz and 2.4 GHz) with four selectable channels each. The choice in frequency depends on interference with other electronics as well as the requirement for covert operations. 2.4 GHz is an open frequency commercially available for general public use and available from many commercial outlets (Game etc.). The 1.2 GHz frequency band is used less often and was considered to be the better choice to begin with. Using this information, the second possibility of having only one wireless RF link, will only be considered if the first option does not meet the required specifications.

Various antennas with different gains are available for the RF links. Three different types of antennas were considered and are listed in Table 3:

- Omni directional.
- Yagi.
- Patch.

Table 3: Comparing different antennas

Antenna Type	Frequency	Gain	Size & weight	Picture
Omni[8]	2.4 GHz	6 dBi	195 mm (L) 14 mm (D) 29 g	
Omni Half wave dipole[7]	868 MHz	2 dBi	178 mm (L) 13 mm (D) 26 g	
Yagi[8] P/N: E-YA2409 P/N: E-YA2413	2.4 GHz	9 dBi 13 dBi	400 mm (L) 520 g 770 mm (L) 650 g	
Patch (Flat panel) P/N: PANL-A0005[9]	2.4 GHz	14 dBi	215 mm (L) 215 mm (W) 375 g	

Omni directional antennas, as the name indicates, have a radiation pattern that is 360° sideways around the antenna as shown in Figure 7. This implies that the

[7] Antenna information form supplier website http://www.rfdesign.co.za on 2009-09-11
[8] Antenna information from supplier website http://www.eaglecctv.co.za on 2009-09-11
[9] Datasheet for PANL-A0005 downloaded from the supplier website http://www.poyntingdirect.co.za/ on 27 Aug. 09

antenna can transmit and receive RF data from any horizontal direction should it be placed vertically.

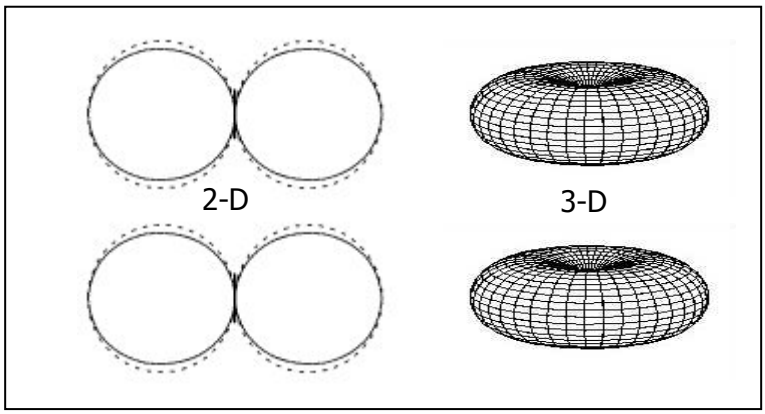

Figure 7: Radiation pattern of two half-wave dipole antennas[10]

Yagi antennas have more gain than Omni-antennas, but have directional radiation patterns. This implies that the antenna always needs to be pointed in the direction of the RF communications. Figure 8 shows the radiation pattern for a typical Yagi antenna.

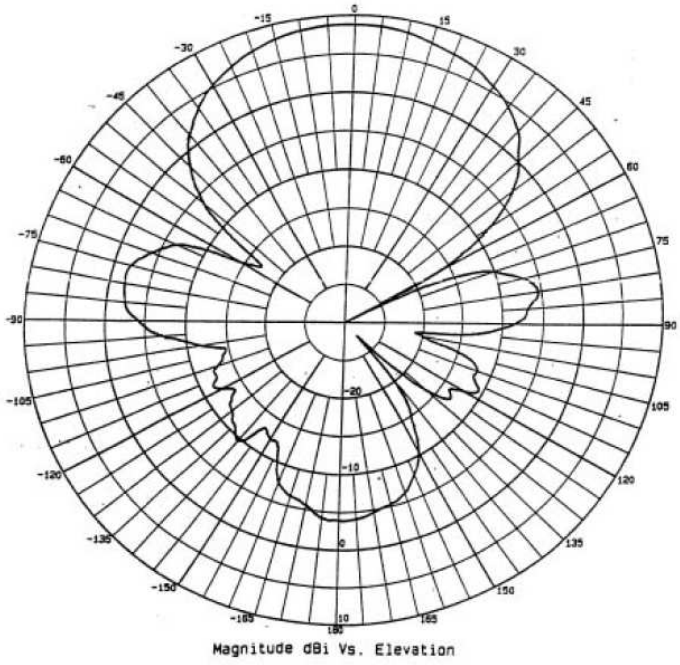

Figure 8: Radiation pattern for a Yagi antenna [40]

[10] Pictures from website: http://en.wikipedia.org/wiki/Dipole_antenna

Flat panel or patch antennas are also directional and have higher gains than the omni-directional antennas. Figure 9 shows the radiation pattern for the patch antenna listed in Table 3.

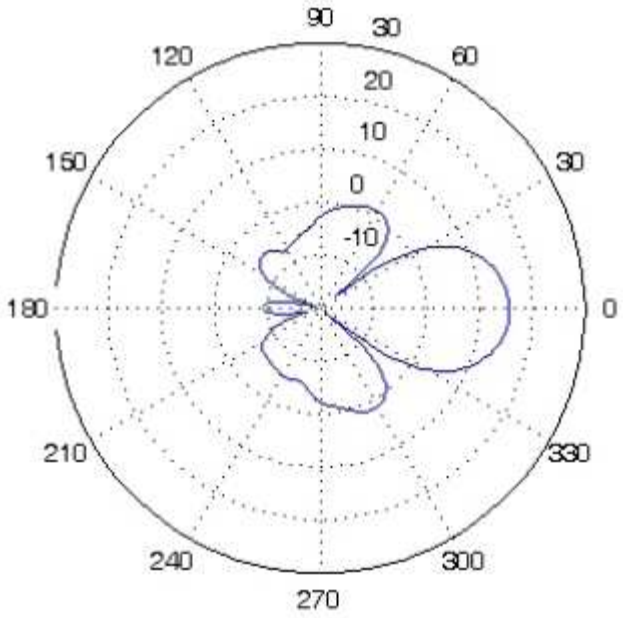

Figure 9: Radiation pattern for the PANL-0005 patch antenna[11]

The various characteristics of the different types of antennas were investigated. An omni-directional antenna was selected for the UAV and the patch antenna for the GCS. The omni-directional antenna will give better coverage to the aircraft as the aircraft orientation is changing continuously during flight. It has the added advantage of being smaller and lighter than the other antennas. The distance can be increased by using directional antennas. Due to the added complexity of keeping the antennas aligned, this option was not further investigated.

The antenna chosen for the GCS is based primarily on the highest gain antenna that will still be light and portable (Patch antenna). When the aircraft is far out (> 100m), the gain helps to achieve the further distance. The ±30 degree angle is big enough to maintain communication by pointing the antenna in the general direction of the aircraft. When the aircraft is close by, the high power of the transmitter is enough to still receive the image although the antenna might not be facing the aircraft. In some

[11] See manufacturer datasheet POYNTING - PANL-A0005.pdf from the website http://www.poyntingdirect.co.za , 2006-08-26

cases, the antenna direction must be changed to follow the aircraft when flying straight overhead.

1.5 Need for new development

There are many different types of portable UAV's available on the market. Why therefore is it necessary to develop a new model? This will depend on the answers to the following questions:

- How many UAV systems are required?
- What is the budget?
- What is the confidentiality of the project?
- Is it required to be flexible in adding new functionalities if new requirements arise with new technologies?
- What are the repairs and maintenance requirements?

The number of aircrafts and systems required, play an important role when determining which will be the best option: a new development or procurement of existing systems? Development costs are normally recovered by manufacturing and selling large quantities of a product. Therefore, taking only quantities and budget into consideration, the development route would be feasible if large quantities are required.

A few UAV suppliers were contacted to obtain some pricing structures for these systems. The prices for small man-portable UAV systems ranged from R2m to R3m. These prices include two to three aircrafts, one GCS, one spares kit, one day payload, one night payload and the necessary peripherals.

The confidentiality of the project is also very important. If a COTS system is chosen, any limitations and vulnerability of the UAV systems would be common knowledge. This would enable any potential enemy to take appropriate action and negate any advantages the UAV might provide. Developing a new system would give the military the benefit of being less vulnerable to counter actions during missions.

Developing a new system would have the added advantage of being able to alter and modernise the design at any stage. It is also normally not cost-effective to modify the design of other manufacturers' products.

Development of a new system takes two directions. The first would be the development of all components from scratch, starting at the drawing board. The second option would be to procure individual off the shelf components and integrate them to end up with a new product. The initial cost for a new development by making use of COTS items, was estimated to be in the order of R700,000 including all labour costs. Compared to R2m, this is much cheaper than purchasing a system off the shelf.

COTS items usually have also been laboratory tested, where most problems are identified and solved, before being placed on the open market. This benefit reduces the risk and development time. A good example is the autopilot system required to control the aircraft. This is a very complex system which would take a long time to develop, build and debug. The challenge to develop this system was considered too much of a risk and would further make the project too expensive.

The benefits of using COTS components in developing a new UAV system motivated the decision to follow this route. Therefore this paper will discuss in detail the procedures to follow when developing a prototype UAV using off the shelf components.

1.6 Purpose of this study

The SANDF is presently not equipped with any portable UAV's. A study was conducted in order to identify the specific requirements of the SANDF for a mini-UAV system. Technologically advanced systems, readily available for procurement in the market, were applied. The potential of each component and system capabilities had to meet the SANDF requirements for short range reconnaissance missions.

Furthermore, this study had to confirm that it was more advantageous to develop a UAV system, rather than purchasing an off the shelf unit.

1.7 Outline of this study

Chapter one looked at the broader view of aerial reconnaissance systems that are available on the market at the time of this study. The general availability of autonomous aerial vehicles was initially examined. Many options were identified with the final focus limited to the smaller types of UAV's. The different types of payloads and wireless communications' systems that are used on the smaller UAV systems were studied. The need to develop a new system, rather than purchase a system from an established manufacturer, was also explained.

Chapter two discusses the requirements for a small, light weight portable UAV system. The basic characteristics for small UAV systems are obtained from market research. These characteristics are used as a guideline to define realistic requirements that would typically be applicable for military use. The operational requirements would have to compliment the present component availability in order to deliver a workable solution at the end. After identifying the operational requirements, the physical requirements of the system are listed. These requirements define the physical dimensional constraints for each component of the system. Finally, the requirements for the different payloads and ground control station are stipulated.

Chapter three describes how to design a mini-UAV system for short range aerial reconnaissance using off the shelf components. The design of the aerial platform and components is first discussed. These components include the airframe, motor, propeller, speed controller, batteries, onboard computer, control systems, wireless communications and all the interfaces. The base station components were then designed which would be compatible with and able to control the aircraft.

Chapter four verifies that the design work is viable, of a high-quality and reliable. All laboratory and field testing is described. The test procedures and results are given in detail.

Chapter five summarizes the procedures followed during the mini-UAV system development. Conclusions and recommendations are given as well as suggestions for future work that can still be done to improve the UAV system.

2 REQUIREMENTS for a mini-UAV system

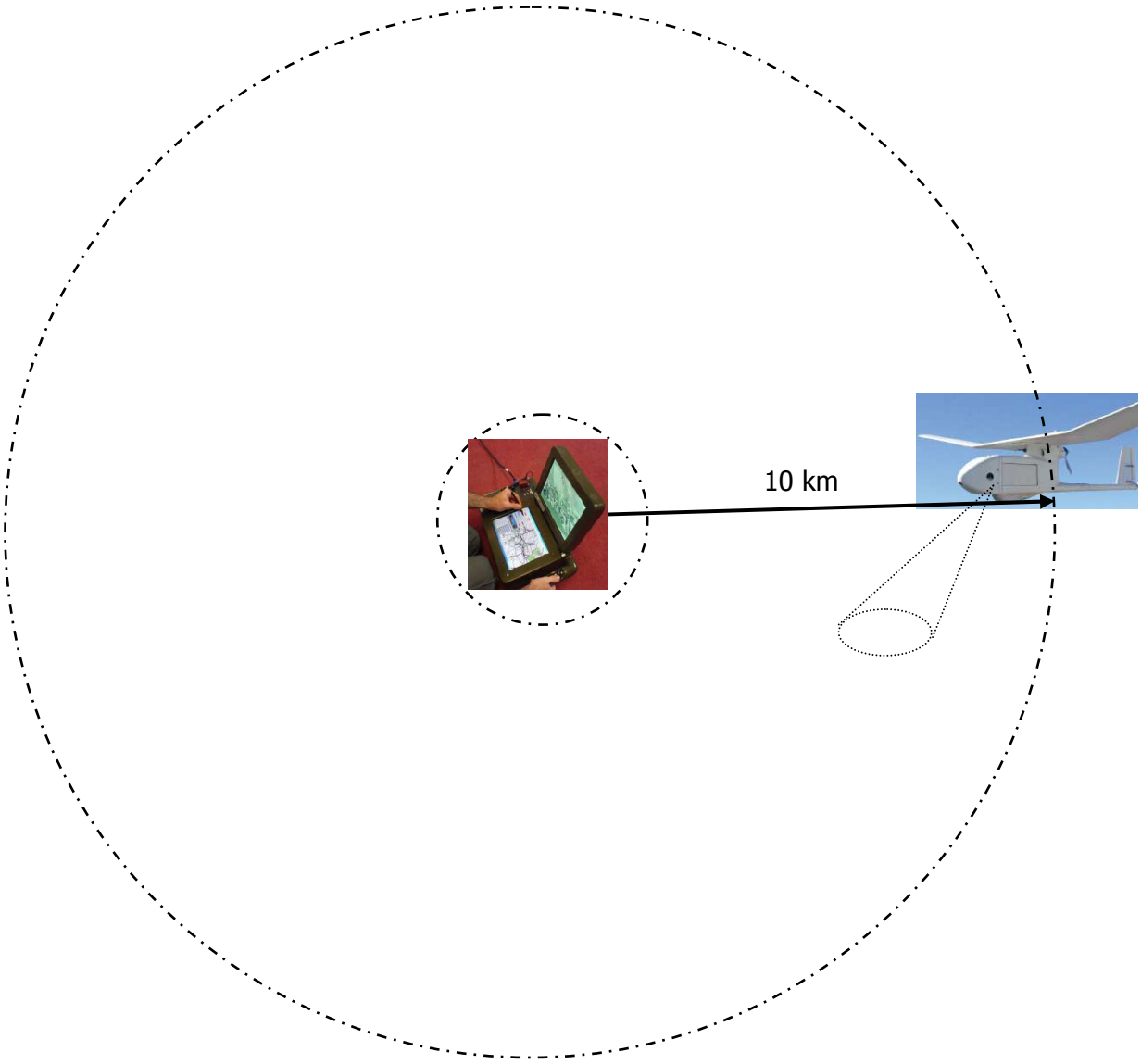

Chapter two describes the requirements for a reconnaissance aerial vehicle that can be carried and deployed by no more than two persons. The research outcome on available technologies at the time of the study was used as a guideline to formulate the requirements realistically. This chapter starts by listing the system requirements. The requirements of the system components that will be needed for the system as a whole are presented. These requirements are used as inputs to the development that follows.

2.1 Preamble

Data obtained from a few different mini-UAV systems was taken and used as inputs to specify the requirements. The requirements listed here were used as a guideline for constructing a model as a solution to the military's short range aerial reconnaissance requirements. This chapter describes the technologies for portable UAV systems being used by military institutions around the world. The characteristics, limitations and restrictions on these systems were examined so that the latest technological innovations could be identified for developing a prototype UAV.

Eight different areas of importance were identified for use as guidelines during the development phase. These are propulsion, wingspan, aircraft mass, flight endurance, range, payload mass, cruise speed and the method of launching and recovery of the aircraft. Examples of a few different existing UAV systems are listed in Table 4. In summary, the common factors amongst these mini-UAV systems are:

- Electronic brushless motor propulsion.
- Wingspan of 1.1 to 2.5 meters.
- Weight of 2.3 kg to 6 kg.
- Flight endurance of 45 to 90 minutes.
- Operational ranges of 5 km to 10 km from the base station.
- Payloads of 450 g to 850 g.
- Flying speeds of 21 km/h to 90 km/h.
- Launch by either hand, sling or bungee.
- Recovery by skid landings or deep stall landings.

This summary indicates the typical limitations for mini-UAV systems and was used to specify the various parameters required for the development.

Table 4: Comparing mini-UAV constraints

Mini-UAV	Pro-pulsion	Wing-span (m)	Weight[12] (kg)	Endurance (minutes)	LOS Range (km)	Payload[13] (kg)	Cruise speed (km/h)	Launch & Recovery type	Manufacturer	Date released	Reference
Dragon Eye	Electric	1.1	2.3	60	10	0.45	65	Bungee	AeroVironment, USA	2003	[17]
Skylark	Electric	2.4	4.0	90	10	0.5	37-75	Hand	Elbit, Israel	2004	[5], p.121; [10]
Desert Hawk	Electric	1.3	3.2	60	11	0.45	40-80	Bungee	Lockheed Martin, USA	2002	[11]; [12]
Raven	Electric	1.5	1.9	80	10	Not available	45-95	Hand	AeronVironment, USA	2004[14]	[13]
Merlin	Electric	1.6	6.0	60	7	0.80	55-75	Hand or sling	Sagem	Not available	[11]
Casper 250	Electric	2.5	4.8	90	10	0.85	21-80	Hand	SONIC Communications, Israel	Not available	[12]
ALADIN	Electric	1.5	3.0	45	>5	0.35	45-90	Hand	EMT, Germany	2003	[5]; [14]; [15]

[12] The weight is that of the aircraft, including the payload
[13] This is the weight for the daylight payload. Normally the payload for night usage can be up to double the weight.
[14] http://www.designation-systems.net/dusrm/app2/q-11.html, 22 September 2009

2.2 Operational Requirements

2.2.1 Background on operational requirements

The operational requirements must be specified so that the characteristics and limitations of the system can be defined. This will be the main discussion in this chapter and includes the aerial platform, the GCS and the payload. These requirements were originally captured in the User Requirement Statement, [27].

The setup time should take no longer than 15 minutes after arriving at the site from where the UAV will be launched. The equipment installed on the UAV should be able to provide real-time aerial video coverage of specified locations.

2.2.2 Aerial platform requirements

The aircraft must be able to:

- be launched by hand or bungee.
- land on rough terrains. No runway should be necessary to launch and recover the aircraft.
- take off and land in an area not larger than 50 x 100 meters surrounded by trees standing 30 m high.
- reach heights of 300 m above ground level.
- fly a radius of 10 km line of sight, (LOS), from the GCS under full control.
- fly for at least 60 minutes from take-off to landing with full payload.
- fly at speeds between 30 & 90 km/h.
- fly at very low noise levels so that it cannot be heard when it is flying 100 m or higher above ground level.
- be barely visible while airborne.

The physical requirements for an aerial platform that must comply with these performance characteristics are:

- a wingspan of less than 2.5 meters.
- the total weight, including payload, must not be more than 6 kg.
- the maximum dimension of any part must not exceed a length of 600 mm.

2.2.3 Observation requirements

The UAV should be able to transmit real-time images and the GCS should be able to receive these images during the entire time that the aircraft is airborne. These systems must be able to transmit these images during the day time, under low light conditions, as well as during the night. The night time conditions are considered to be cloudy with no moonlight. It is not a requirement that all three of these types of camera configurations have to be used at the same time. The specific camera type must be easily installed, depending on the actual light conditions prevailing at the time of launch.

The payload must include the cameras, video transmitter, camera controls and the enclosure that will be attached to the aircraft if needed. The aerial platform should be able to carry the payload with any camera configuration needed for day time, low light or night time. With full payload, the platform must still be able to maintain the required cruising speeds and maintain flight stability to capture real-time images. The payload should be placed at such a position that it will be quick and easy to install without requiring any special tools.

For day operation, the video must cater for a full colour image at no less than 20 frames per second. It should also have pan, tilt and zoom (PTZ) capabilities. The zoom capability should sufficient to allow facial recognition or reading of a motor vehicle number plate at a distance of 100m. If the PTZ functionality cannot be provided, there must be at least two fixed zoom settings that can be switched in flight. The wide field of view should ensure that humans, vehicles, roads and buildings can be easily recognizable. The narrow field of view shall be such that a person carrying a weapon can be recognised as well as the type of uniform, if any, that is being worn. The vehicle type must also be readily identifiable.

For night operation, the video image must include a low light and night observation capability. The low light camera must be able to identify camp fire sizes, car headlights and house lights, using a wide angle lens. The night observation camera must be able to zoom in for the identification of human presence and vehicle types (i.e. truck, car, motorcycle, etc).

A stabilised camera platform is required, to ensure a clear image reproduction. The video image must be displayed together with the GPS co-ordinates. A further requirement would be for the RF links to be encrypted.

Table 5 shows the estimated fields of view for the different camera payloads for day and night operation.

Table 5: Field of view estimates at different heights for different cameras

Height above ground	Day and low light image		Night image	
	Zoomed in	Zoomed out	Low light	IR / Thermal
100 m	9 m x 13 m	64 m x 85 m	29 m x 40 m	14 m x 20 m
200 m	19 m x 26 m	130 m x 175 m	60 m x 80 m	30 m x 40 m
300 m	28 m x 38 m	200 m x 270 m	90 m x 120 m	45 m x 60 m

The camera should be able to point at a chosen target, (i.e. GPS position), for as long as desired at any point in time during the operation.

It will be beneficial if video images can be recorded by the on board equipment installed in the UAV, in the event that the UAV operates out of the RF link range. The recorded image will be downloaded after the UAV has been recovered. It would be desirable that the recorder forms an integral part of the payload with the video transmitter. The video transmission provided by the UAV must be such that up to three video display terminals can be used to observe the transmitted signal from a separate location other than the GCS.

The option of equipping the UAV with an onboard RF beacon should be available. This will assist in recovery, if for some reason the UAV did not return to the launch site.

2.2.4 Ground Control Station (GCS)

The GCS must consist of a rugged laptop computer, a control panel or an acceptable games controller for manual flying, and a battery. If the laptop computer is unable to display and record the transmitted UAV images, a separate video display with recording must be provided. The GCS must be ergonomically packaged and provide for a minimum Ingress Protection (IP) rating of 65 (i.e. protected against dust and spraying water from all directions). All the display devices should be sunlight readable. The GCS must be able to control the UAV in autonomous, as well as remote piloted vehicle (RPV) mode. The option to have full manual control of the UAV is preferable for aircraft recovery in difficult landing areas.

The PTZ function of the onboard cameras must be controlled in real time from the GCS. The recording facility may be either analogue (Sony GVD tape recorder), or digital. The GCS should be able to operate continuously on battery power alone for at least 4 hours with all sub-systems fully activated. The GCS should be rechargeable from 110 VAC, 220 VAC, 12 VDC and 24 VDC power outlets in less than 12 hours. The ability to use solar panels for recharging or to extend the operating time of the GCS should also be available.

Extendable poles should be available as an option for operating in areas with high bushes and trees in order to raise the GCS antennas to a maximum of 10m. It would be advantageous if the GCS can be operated from within a moving ground vehicle while the UAV is in flight. A further benefit would be if control of the UAV could be transferred from one GCS to another.

2.2.5 Launch and recovery requirements

Hand launching would be the preferred means of getting the UAV airborne. A less preferable method would by a bungee launch. Making use of a runway is not considered as an option. The aircraft must be able to return to within a 15 m radius

from the point of launch, or at some other specified landing point, without being damaged. A preferred method of recovery would be to catch the UAV in a net with dimensions smaller than 5 m wide and 3 m high.

If a recovery net is not available, the aircraft must be able to land on a narrow strip less than 3 m wide and 50 m long and flanked by obstructions higher than 15 m. The direction of landing should be changeable in flight in cases of sudden changes in wind direction. This would give the advantage of always landing into the wind A further advantage would be for the UAV to be able to land on a ship, close to shore, without having to use a net. The design of the UAV should allow for recoverable water landings without damage to the aircraft or equipment.

2.3 Training requirements

Provision must be made for appropriate operator training and a detailed, easily understood, user manual should be issued. After the training, UAV operators should be able to:

- Unpack the system.
- Put the system components together.
- Prepare the flight mission.
- Launch the aircraft.
- Control the aircraft in flight.
- Recover the aircraft.
- Change and recharge batteries.
- Assess any possible damage on system to determine operability.
- Do minor repairs in the field, for example replacing wing tips.
- Package and transport the system.

2.4 Maintenance and support requirements

It should be possible to charge the batteries for the UAV and control station in the field, or while in storage, with the power source described in paragraph 2.2.4. The platform must be of modular design to enable repairs in the field. Spare parts should be supplied to make minor repairs in the field possible. The spares kit must be designed to minimise weight but maximise in-field reparability based on damage probability.

2.5 Environmental requirements

The UAV must be able to fly in coastal weather conditions with winds of 20 km/h to 35 km/h. This means that the UAV must be able to fly in light rain, IP level 55 (IP55), and it would be beneficial to have the ability to be submerged 1m in water, IP57. The UAV's functionality must cater for bush, desert and built-up areas. This requires that dust does not negatively influence operation, IP55. The UAV system must operate at altitudes from sea level to 4000 m, in temperature ranges from 0 ^{0}C to 50 ^{0}C. It is desirable for the UAV to be able to land in sea water during recovery. Table 6 summarises these environmental requirements.

Table 6: Summary of environmental requirements

Element	Requirement	Criteria
Wind	Less than 35 km/h	Must comply
Rain & Dust	IP level 55	Preferred
Water (Salt & Fresh)	IP57 (1 m submersible)	Beneficial
Altitude (min – max)	Sea level to 4000 m	Must comply
Mist / Fog	100 m visibility	Preferred
Humidity (min – max)	80 to 100%	Must comply – Preferred
Operating temperatures	0 to 50 ºC	Must comply
Storage and transport temperatures	-10 to 60 ºC	Must comply

2.6 Summary

These requirements should all be taken into consideration for the design and development of a mini-UAV system. The final design specifications must meet the "must comply" requirements of table 6. Preferred requirements are, to some extent, minimum design specifications. These requirements may be relaxed under certain operational conditions. The beneficial requirement is considered as a bonus to the design, but is not a crucial design specification. The following chapter will explain the development procedures for a mini-UAV system. COTS items, that comply with most of the requirements mentioned in this chapter, will mainly be used for the design.

3 DESIGN AND IMPLEMENTATION

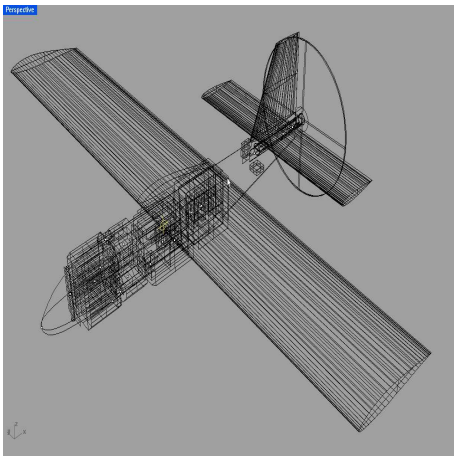

Chapter three describes how to develop a cost-effective mini-UAV system that can be used for short-range reconnaissance. The different components are discussed individually and in detail. Some components, bought off the shelf, can be used directly, while others require small modifications. Components that were not readily available needed to be developed. This chapter will provide information on all the building blocks required to develop and construct a mini-UAV system.

3.1 Preamble

Before the commencement of the UAV development program, a practical assessment was carried out to verify whether COTS technologies can be used to produce useful aerial images. A standard radio controlled (RC) hobby trainer aircraft, powered by a petrol engine, was set up with a small video camera and RF transmitter. The aircraft was flown manually and the recorded video image was analysed and presented to the customer. The outcome of this test flight confirmed that usable aerial video images can be generated to provide useful reconnaissance information.

The design stage of the UAV development project required that all the components should first be identified. From the research work discussed in chapter 1, the four main components that need to be addressed are:

- Airframe.
- Payload.
- Ground Control Station (GCS).
- Wireless communications.

At the start of the development, the airframe was designed and built with the help of aeronautical specialists. The availability of required system components was researched, identified and procured.

This chapter does not give all the details on this aircraft design, but explains in detail how each of the system components were identified, modified, designed and integrated. The initial airframe development appeared to be progressing satisfactorily. However, many flight tests led to the detection of some unacceptable instability problems in the airframe design. The design engineers attributed this problem to the type of material used in the construction. The aerodynamic design program is beyond the scope of this dissertation and will not be discussed in detail.

3.2 Aerial Platform

3.2.1 Introduction

The purpose of the aerial platform is to carry the payload that is required for aerial short range reconnaissance. Without a stable, easily manoeuvrable aerial platform, the payload cannot be successfully utilised to acquire the necessary reconnaissance information. The minimum components required for such an aerial platform are:

- Airframe (fuselage and wings).
- Propulsion (motor, propeller and speed controller).
- Energy source (fuel or batteries).
- Flight computer (autopilot with control system).

First of all, the correct airframe has to be chosen. This will determine which propulsion unit will be required. The choice of propulsion will determine what kind of energy source will be used. The combination of these three components will determine what type of flight computer is required. This chapter will discuss how to choose all these components, starting with the airframe.

3.2.2 Airframe

The size and type of airframe are determined by the requirements which were derived from the research conducted on mini-UAVs in chapter 2. From these requirements it was determined that the aerial platform should comply with the following criteria:

- Man-portable.
- Bungee or hand launched.
- Fly at least 300 m above ground level.
- A maximum wingspan of 2.5 m.
- Must not exceed a length of 1.3 m.
- A maximum height of 0.5 m.
- Must be able to carry a payload of at least 0.5 kg.
- Must not exceed a total mass of 5 kg, including the payload and fuel.

- Rugged, strong and durable.
- Low as possible noise levels.

The airframe can be either a prototype design and locally manufactured or purchased off the shelf. The design requirements for the aerial platform suggest an airframe of a typical hobby model airplane in size and weight. Model aircraft have been used by hobbyists for many years and hobby shops can supply a large variety of different models. These models are also inexpensive compared to the costs of designing, manufacturing and testing of a prototype model. The immediate advantage of purchasing hobby type airplanes is that they have already been flight tested. Spare parts are usually readily available and relatively cheap.

The requirements are very specific about the size, weight and performance characteristics of the required airframe. Mission scenarios that will be flown by the UAV will never require the aircraft to perform stunts or sharp turn manoeuvres. Airspeeds specified for the UAV are relatively low and do not require high performance, high speed airframes. Specific airframe requirements that must be taken into account are:

- Flight endurance and flight stability.
- Reliability, to ensure completion of planned mission.
- Large enough to house all the necessary components.
- Take enough fuel for a one hour flight.

These requirements eliminated many of the COTS models, leaving the power glider configuration as the most acceptable option. The power glider is designed for maximum endurance while using a minimum amount of power. Other advantages of the power glider configuration are:

- It does not have an undercarriage and therefore does not make use of a runway to take off or land. It is recovered by skid landings.
- It has high wing loading capacity which possibly allows it to carry a payload of 0.5 kg.
- The airframe can be removed from the wing, which makes the packaging more compact and portable.

Possible disadvantages of the glider type airframe can be:

- It is not robust enough to withstand landings on hard and rocky terrains.
- It does not have enough space inside the fuselage for carrying all the components.

Due to the unique take off and landing requirements, the aircraft available from hobby shops were not able to meet the specific requirements of this UAV project. To meet the requirements of the military, a prototype model UAV would have to be designed and developed. The development of a locally produced prototype model would ensure that the CSIR remained abreast with the rest of the world in this fast growing technological field.

Material for the airframe was based on previous manufacturing experience for the Desert Hawk UAV used by Lockheed Martin. The airframe was constructed from expanded polypropylene (EPP) foam, covered with fibre-reinforced tape. It was designed to get airborne using a bungee cord, with landing capabilities on rough terrains. The wing mountings were designed to easily break away from the fuselage. In this way minimum damage would be caused if the aircraft hit the ground wing first or fly into a bush or tree.

A pusher prop design was used, with blades that would fold away when the power train was not in use. This not only reduced the free flight drag, but also protected the propeller blades during landings. The cameras were mounted inside the aircraft and the video transmitter on top of the fuselage, to allow for airflow to keep it cool while in flight. The main wing was attached to the fuselage with Velcro tape and a 6 mm plastic bolt; the horizontal stabiliser with double sided tape and a 4 mm nut.

The data link antenna was mounted on top, close to the nose of the UAV, and the video transmitter inside the tail. This was the furthest possible mounting positions from each other. Batteries were placed in the nose to obtain the correct centre of gravity position due to the heavy motor mounted at the back end. The main wing consisted of three pieces to make it easier to package giving final aircraft dimensions of 1.0 m (L) x 1.7 m (W) x 0.34 m (H) and weighing 3 kg. Figure 10 shows photographs of the disassembled prototype UAV.

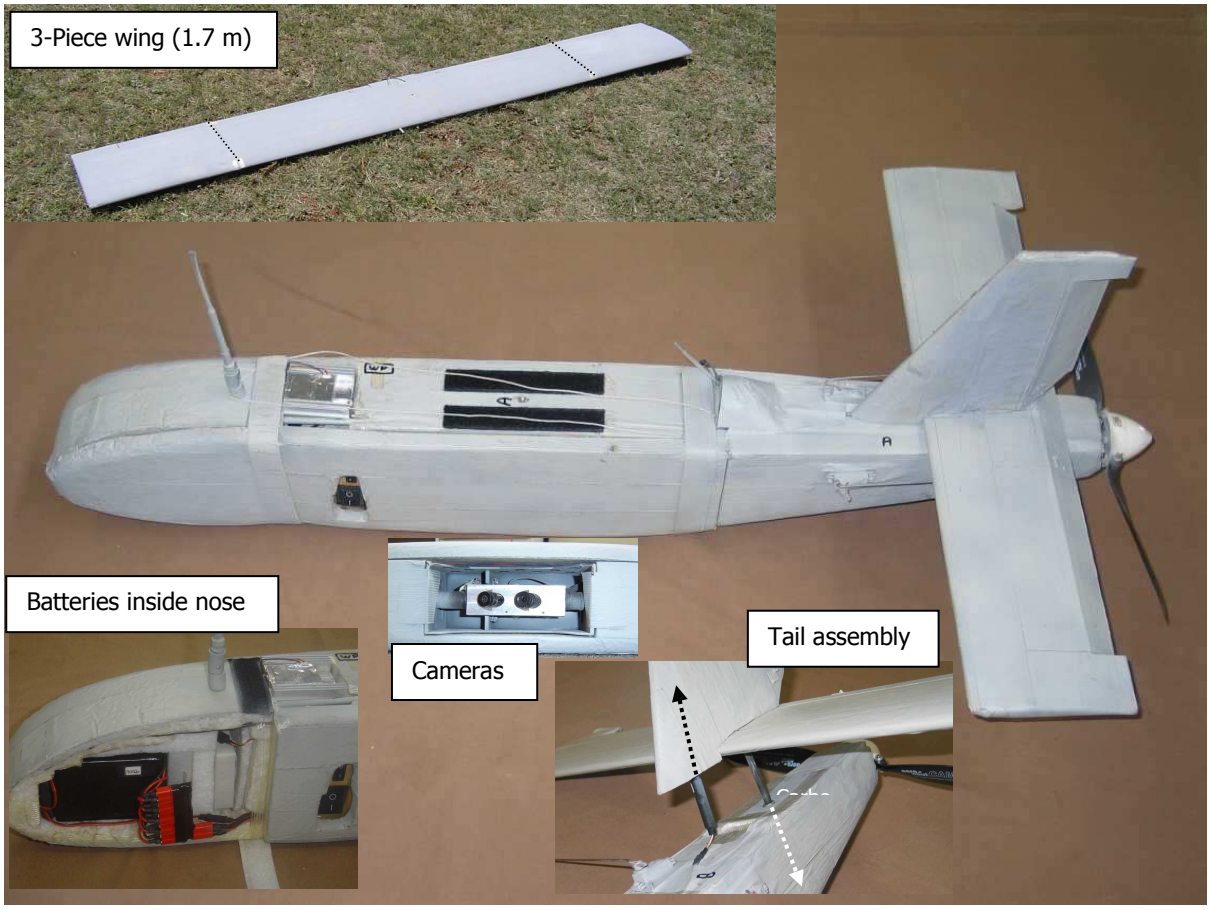

Figure 10: First aircraft design

The tasks performed to get to the point of a demonstration flight were:

- Design and construct the aircraft.
- Manual flight testing of the aircraft and adjustment of the trim settings.
- Integrate the flight computer into the aircraft mechanically and electronically.
- Programming the auto pilot for the specific airframe.
- Test flights with the autopilot in control.

The most time consuming task was to program the autopilot to fly the prototype autonomously. This task took the two engineers involved about three months of full time experimenting, to complete. After it was verified that this airframe design was not very stable, it was decided to search for and procure a model aircraft airframe.

The original concern, of not being able to take off and land on rough terrain, can be overcome by modifying the airframe, if needed. The space for housing components can also be increased by enlarging the fuselage or adding external containers.

Different power gliders, that fit these requirements, are available from hobby shops. Table 7 lists some of the different gliders that are available for procurement from international hobby shops.

Table 7: Comparing power gliders

Power Glider	Hobby Shop	Wing span	Flying Weight	Price[15]	Picture
Thunder Tiger E-Hawk 1500 Magenta[16]	Tower Hobbies	2-piece 1.520 m	0.6 kg (empty shell)	$120.00 (R1,080)	
Cumulus XXL Electric Sailplane[17]	Hobby-Lobby	3-piece 2.250 m	1.644 kg	$289.90 (R2,610)	
MP-Vision [24]	Micropilot	3-piece 2.450 m	2.72 kg	$9,500 (R85,500[18])	
Electra Pro[19]	Topmodel CZ	3-piece 2.550 m	2.1 kg	R3,000	

Micropilot's MP-Vision listed in Table 7, is a ready to fly, power glider that uses the Electra Pro airframe with built in control systems. This UAV from Micropilot is not a complete system as described in chapter 1, but is much cheaper. It also makes use of readily available spare parts which will ensure quick and cheap repairs.

[15] The exchange rate was taken as 9 ZAR to the USD where the price was not in local currency
[16] http://www3.towerhobbies.com/cgi-bin/wti0001p?&I=LXUYK6&P=ML#tech, 11 August 2009
[17] http://www.hobby-lobby.com/cumulus.htm?pSearchQueryId=136198, 11 August 2009
[18] This price includes the airframe, onboard control electronics, motor, speed controller and batteries.
[19] http://www.topmodelcz.cz/index.php?&desktop_back=eshop&action_back=&id_back=&desktop=eshop&action=zbozi_detail&id=724, 11 August 2009

Micropilot already configured the autopilot for this airframe. Based on experience, it is very time consuming to configure the autopilot for a different airframe. This solution will save significant time on the project. Procuring this UAV from Micropilot and adding the additional system components can be beneficial for this project. However, reliability and operational performance will have to be verified.

The shortcomings of Micropilot's MP-Vision compared to the project requirements are:

1. Flying time is only 55 minutes without any payload, compared to a minimum requirement of 60 minutes with payload.
2. Maximum of 4 km range, compared to minimum of 10 km.
3. Maximum payload of 450g, compared to 500g specified.
4. The airframe appears to be very robust, but this can only be verified after proper testing and evaluation.
5. The aircraft parts may be too long to be back packable, but this can also be verified once tested.
6. The system does not have a Ground Control Station (GCS).
7. The aircraft is not supplied with any observation payloads, but does come with a box that fits underneath the wing, that can be used to mount a camera in.

In spite of these shortcomings, this ready-to-fly UAV was procured. The shortcomings can be addressed as follows:

1. Extra batteries can be added, or the airframe can be modified to make it more efficient and remain airborne for one hour.
2. The flying range can be increased by exchanging the wireless RF links.
3. The payload can be constructed to be as light as possible and not exceed 450g.
4. The model can be made more robust if required, but this may reduce payload weight.
5. Aircraft parts can be modified to make them shorter for back packing.
6. Micropilot supplies the necessary GCS software needed to operate the UAV. The hardware can be procured and programmed as required.
7. CSIR can design and build its own remote control systems.

3.2.3 Flight computer (Autopilot)

For the first prototype aircraft, the correct flight computer had to be chosen. A flight computer, also known as the autopilot, is needed to fly the aircraft independently from time of launch to landing. This flight computer must comply with certain physical and operational requirements. The physical requirements are:

- Small in size.
- Light weight.
- Low power consumption.
- Correct interfaces for the aircraft controls.
- Durable to withstand rough landings.

The operational requirements are:

- Take off with a hand- or bungee launch, fly and land autonomously.
- Fly pre-programmed waypoints.
- Set flight height.
- Set flight speed.
- Change flight path during flight by moving the waypoints.
- Camera control during flight.

In addition to these requirements, the autopilot should also be inexpensive. Table 8 lists the size, weight and price of different flight computers that were available off the shelf at the time this project started. Most of the UAV manufacturers listed in Table 4 designed their own autopilots and cannot be procured separately from their systems, except for the CASPER-250. The CASPER UAV makes use of an off the shelf auto pilot designed and manufactured by Micropilot [16].

Table 8: Autopilot comparisons

Manufacturer	Product name	Size of PCB	Weight of PCB	Price (QTY 1) 2009
Micropilot [18]	MP2128g	10 x 4 cm	28 g	$6000 (USD)
Micropilot [18]	MP2028g	10 x 4 cm	28 g	$5500 (USD)
UNAV [19]	UNAV3500FW	10 x 5 cm	34 g	$5000 (USD)
UNAV [19]	PICOPILOT-NA	5 x 2.5 cm	18 g	$550 (USD)

The functions and features of the U-NAV and Micropilot autopilots are listed in Appendix F. Aeronautical specialists, who designed the first prototype airframe, were tasked to recommend an autopilot. They recommended the MP2028g autopilot from Micropilot. The MP2128g currently being used was not available at the time.

3.2.4 Propulsion

A wide variety of engines are readily available. Only engines used on smaller model aircraft which are more applicable to the present requirements will be considered. The different engine types to be considered are gasoline engines, electric motors and gas turbine engines.

Gasoline engines are the most commonly used model aircraft engines. The gasoline engine provides more than enough power to fly many different types of aircraft. One of the benefits of using a gasoline engine is that the aircraft can be refuelled immediately after a landing and be ready to fly again within a few minutes. The disadvantage of this type of engine is that it is messy and makes a lot of noise.

As the technology improved, electric propulsion was more commonly used by hobbyists. The reason for this is that the batteries became smaller, lighter, readily available and cheaper. As a result power gliders suddenly became very popular. A small electric motor, powered by a small light weight battery is used to get the glider to a safe altitude and the motor is then switched off. The propeller will fold back while

the aircraft, by means of remote control, glides in the wind and updrafts for as long as possible.

Gas turbines are used to power high speed jet-like aircraft and are very noisy. Due to the noise factor, this engine would not be considered for this application. It will not meet the user requirements in terms of noise and relatively fast flying speeds.

Of these three types of propulsion, the electric motor makes the least noise and is the cleanest and most reliable to work with. It is also much easier to start an electric motor than a gas engine. The logical choice would then be electric motor propulsion. This can be verified by all the small UAVs listed in Table 4 that use the same type of propulsion. Two types of electric motors are available to choose from: brushed and brushless motors.

Brushed electrical motors are cheaper to buy than brushless motors. On the other hand, brushed motors need some maintenance, since both the brushes and the commutator may require fairly regular maintenance. The most common maintenance is caused by carbon dust particles that form as a result of friction between the brushes and commutator. While the motor is rotating, the brushes also cause electrical noise that can interfere with the radio and other sensitive electronics.

Brushless motors are slightly more expensive and require a more complex speed control unit. However, they generate less electrical and audible noise and are more efficient than brushed motors. These motors also require less maintenance due to less wear and tare [25]. Brushless motors would therefore be the better choice. This is also verified in paragraph 2.1 by the research outcome on the type of propulsion being used by different UAV manufacturers. The brushless motor is therefore the logical choice to use for this project.

The size of the motor would be determined by the power required to launch the aircraft and keep it at the desired speed and altitude during flight. Aeronautical specialists were tasked to calculate and determine the power requirement suitable for this specific UAV. These calculations fall beyond the scope of this dissertation and are not shown. Only the final results will be given. Based on the characteristics and performance requirements of the UAV, the required power output of the engine, taking propeller efficiency into account, was calculated to be 500 W. Brushless motors are

about 90 % efficient and therefore a minimum engine power of 555 W was specified. A power output of 500 W is only needed during take-off and climbing to higher altitudes.

Brushless motors do not operate like normal brushed Direct Current (DC) electric motors. Three alternating currents need to be applied to the stator coils for the rotor to turn. With a DC power source, an electronic speed controller is required to pulse the 3 poles of the motor in order for it to turn. The required speed controller should be able to supply enough current to the motor when maximum power is needed. Thanks to the hobby market, these types of electronics have also reached an advanced state of development. High performance speed controllers in fairly small sizes at low cost are readily available.

Brushless motor speed controllers are rated in supply Voltage and output current. For a 555 W electric motor the supply voltage was calculated to be 12 V. By using the basic electric power equation (P = IV), the minimum current rating calculated for the speed controller is 46 A. To ensure satisfactory performance a speed controller with a current rating of 60 A or more was specified. Table 9 lists a few speed controllers that were considered.

Some of the speed controllers are equipped with an integrated Battery Eliminating Circuit (BEC) that provides 5 VDC to the control servos of the aircraft. As the name indicates, this will eliminate the need for a separate 5 V battery pack to power the servos. This implies less weight and one less battery to maintain. The SPIN66 speed controller has an onboard data logger that is a very helpful feature for development and testing. It logs temperature, run time, current, voltage, rpm and errors that occurred during operation.

Table 9: Comparing brushless speed controllers

Speed controller	Weight	Dimensions	Supply Voltage & Current rating	BEC[20] Voltage & Current	Price[21]	Picture
JETI SPIN66	70 g	50 x 25 x 13 mm	6 – 26 V, 70 A	5 V, 5 A	R1,700	
Phoenix 60[22]	58 g	60 x 26 x 12	12.6 V 60 A	5 V, 3 A	R1,260	
Schulze [23]future 12.46e	45 g	77 x 30 x 11	7.2 – 16.8 V 60 A	5 V, 3 A	R1,800	

3.2.5 Energy source

The batteries must be able to power the aircraft for at least one hour of flight time, including a short period required, using full power for take-off and climbing. There are many different battery types available on the market to choose from. Most hobby shops recommend Lithium Polymer (Li-Po) batteries. This was verified by comparing a few batteries.

The batteries to be considered must be able to deliver the required power, be light weight and compact enough for installation into the aircraft. For a battery to be able to deliver high power on demand, it must have a low internal resistance. The internal

[20] A Battery Eliminating Circuit (BEC) is a voltage regulator integrated in the speed controller to power the servos.
[21] The exchange rate was taken as 9 ZAR to the USD where the price was not in local currency
[22] The Phoenix 60 specification were found on the supplier website http://www.castlecreations.com/products/phoenix-60.html on 27 Aug. 09
[23] Schulze future 12.46e is also used in Micropilot's MP-Vision. The specifications were downloaded from the supplier website http://www.modelflight.com.au/schulze_electronic_brushless_speed_controllers_esc.htm on 27 Aug. 09

resistance for each battery type to be evaluated will give a good indication of the ability to produce the required power. In most cases the battery manufacturers will specify the internal resistance and maximum current ratings in their data sheets.

To take the cost factor into account, the batteries should be rechargeable and therefore re-usable. Primary (non-rechargeable) batteries are considered as an alternative option. These batteries may have a better power to weight ratio which would ensure longer flight endurance.

Rechargeable batteries that are commonly available and used commercially and by the Military are [26]:

- Lead Acid.
- Nickel-Cadmium (NiCd).
- Nickel Metal Hydride (NiMH).
- Lithium Ion (LiIon).
- Lithium Polymer (LiPo).

Primary batteries considered to be commonly used are:

- Alkaline.
- Lithium.
- Zinc-air.

The battery voltage should be sufficient to power the motor, control electronics and camera systems simultaneously. Due to the high current demand of the aircraft electronics, the battery should have as high as possible voltage. The lower the voltage, the larger the current required to deliver the system power requirements according to the direct current power equation:

$$P = I \times V \qquad (1)$$

Where:

P = Power (Watt).

I = Current (Ampere).

V = Voltage (Volts).

When choosing the speed controller, the supply voltage should also be considered. Speed controllers are available in different voltage ranges. The battery pack voltage must also be able to supply the rest of system electronics during high power demands from the speed controller. CCTV cameras and wireless transmitters are commonly designed to operate from 12 V sources. The physical size of the battery pack will be restricted by the available space in the fuselage.

One method to determine the battery pack size is to calculate the power consumption of the system and the available space in the aircraft. There are a lot of unknown variables in flight conditions that makes the power consumption of the aircraft very difficult, if not impossible, to calculate accurately. Another method will be to fit as many batteries into the aircraft as possible, considering size and weight. Test fly the aircraft with maximum weight until the battery is almost depleted, by monitoring the battery voltage in flight and record the flight time. Measure the remaining battery capacity by discharging the battery to its minimum allowed voltage level. The amount of battery capacity used (Ah) can be calculated from this and also from the average power used by the aircraft.

3.2.5.1 Rechargeable Lead-Acid Batteries

Lead-acid batteries are commonly used in vehicles and backup systems for household equipment. This type of battery is used due to its robustness, recharging capability and low internal resistance. Compared to other battery types, lead-acid batteries do not need sophisticated recharging electronics and can deliver high currents on demand. The important characteristics of 12 V lead-acid batteries from different manufacturers are listed in Table 10.

Table 10: Lead-acid battery characteristics

Manufacturer	Voltage & Capacity (Ah & Wh[24]) rating	Weight (Kg)	Volume (cm^3)	Energy density (Wh/kg)	Energy to size ratio (Wh/l)	Internal resistance (mOhm) & Maximum current rating (C[25])
Yuasa (NP7-12)[26]	12 V 7 Ah 84 Wh	2.59	957	32	87.7	25 mΩ 6 C
Power Kingdom[27] (PS7-12)	12 V 7 Ah 84 Wh	2.12	932	39	90.1	25 mΩ 15 C

The advantages of lead-acid batteries are that they do not need sophisticated chargers, have high output current ratings, and are relatively cheap and easily available. The disadvantages are that these batteries are big and heavy and therefore not suitable for flying. This battery may be considered to power the ground control station electronics.

3.2.5.2 Rechargeable Nickel-Cadmium (Ni-Cd) Batteries

Ni-Cd batteries are commonly used by hobbyists and are available in 1.2 V cells in different sizes. Table 11 shows the typical Ni-Cd battery characteristics of two different manufacturers that will be applicable to this project. The internal resistance seems low, therefore this battery might be considered as an option.

[24] Wh is calculated by multiplying the rated Voltage with the capacity (V x Ah)
[25] C is the capacity of the battery, i.e. A battery with a 7 Ah capacity that have a current rating of 6 C, can deliver 42 A.
[26] Battery manufacturer specifications can be found at *www.aetes.com/**YUASA**/pdf/**YUASA_NP7-12**.pdf*
[27] Battery manufacturer specifications can be found at http://www.home-ups.co.za

Table 11: Ni-Cd battery characteristics

Manufacturer	Voltage & Capacity (Ah) rating	Weight (g)	Volume (cm^3)	Energy density (Wh/kg)	Energy to size ratio (Wh/l)	Internal resistance (mOhm) & maximum discharge current rating (C)
SAFT (VRE-C) [29]	1.2 V 2.5 Ah	75	24.88	40.0	121	5 mΩ 4.8 C
UNIROSS, Std. range (C-cell) [30]	1.2 V 2.68 Ah	70	26.55	42.8	121	8 mΩ 3 C

3.2.5.3 Rechargeable Nickel Metal Hydride (Ni-MH) Batteries

Just as Ni-Cd, Ni-MH batteries are also used by hobbyists in radio controlled toys. Ni-MH batteries are available in 1.2 V cells in different sizes. Table 12 shows the typical Ni-MH battery characteristics that are applicable to our application of two different manufacturers. This battery has more or less the same internal resistance as the Ni-Cd, but offers almost double the energy density. This would also be an option to consider.

Table 12: Ni-MH battery characteristics

Manufacturer	Voltage & Capacity (Ah) rating	Weight (g)	Volume (cm^3)	Energy density (Wh/kg)	Energy to size ratio (Wh/l)	Internal resistance (mOhm) & maximum continuous discharge current rating (C)
SAFT (VRE-C) [29]	1.2 V 3.5 Ah	59	16.23	71.18	259	4 mΩ 11C
UNIROSS, (UH-SC3000C) [30]	1.2 V 3.0 Ah	58	17.86	62.07	202	5 mΩ 5 C

3.2.5.4 Rechargeable Lithium Ion (Li-Ion) Batteries

Li-Ion batteries are most commonly found in laptop computers and cell phones because of their high energy density. These batteries are not subject to memory effects which cause problems with the Ni-Cd and Ni-MH batteries. Table 13 shows the Li-Ion battery characteristics from two different manufacturers.

Table 13: Li-Ion battery characteristics

Manufacturer & Product	**Voltage & Capacity (Ah & Wh) rating**	**Weight (g)**	**Volume (cm^3)**	**Energy density (Wh/kg)**	**Energy to size ratio (Wh/l)**	**Maximum continuous discharge current rating (C)**
SAFT, VL 25500-125 [29]	3.6 V 2.0 Ah 7.2 Wh	59	22.89	122.03	314	0.5
UNIROSS, ULC-1865-2200 [30]	3.6 V 2.2 Ah 7.92 Wh	46	17.04	172.17	465	0.5

3.2.5.5 Rechargeable Lithium Polymer (Li-Po) Batteries

Li-Po batteries are mostly used by hobbyists in RC model aircrafts. The reason for this is the high power density and maximum current characteristics of this type of battery. Table 14 shows the battery characteristics from two different Li-Po battery manufacturers.

Table 14: Li-Po battery characteristics

Manufacturer & Product	Voltage (3 Cells) & Capacity (Ah & Wh) rating	Weight (g)	Volume (cm^3)	Energy density (Wh/kg)	Energy to size ratio (Wh/l)	Maximum continuous discharge current rating (C)
FLIGHT POWER (EVO20-2500) [31]	11.1 V 2.5 Ah 27.75 Wh	184	100.97	150.81	275	20 C
DUALSKY (XP22003SL) [32]	11.1 V 2.2 Ah 24.42 Wh	167	69.30	146.22	352	16 C

3.2.5.6 Primary Batteries

Various primary batteries (alkaline, lithium and zink-air) are listed in table 15.

Table 15: Comparing primary batteries

Primary Battery	Energy density (Wh/kg)	Energy to size ratio (Wh/l)	Maximum continuous discharge current rating (C)	Internal Resistance (mOhm)
Alkaline Manganese primary (Duracell) [34]	163	398	Not specified	136 mΩ (for D-cell)
Lithium Manganese primary (Duracell) [34]	230	550	Not specified	Not specified
Lithium Thionyl Chloride primary battery (SAFT LSH 20) [29]	468	861	0.35	Not Specified
Zink-Air Button Cells (Duracell) [34]	442	1673	Not specified	3000

3.2.5.7 Summary of the different battery types

After comparing these battery characteristics, the best choice for use in small portable UAV's appears to be the rechargeable Li-Po type. The battery with the best performance for this project was taken from each type and compared in Table 16.

Table 16: Summary of different battery types

Manufacturer & Product	**Energy density (Wh/kg)**	**Energy to size ratio (Wh/l)**	**Maximum continuous discharge current rating (C)**
Lead-Acid	39	90	15
Ni-Cd	40	121	4.8
Ni-MH	71	259	11
Li-Ion	172	465	0.5
Li-Po	**146**	**352**	**16**
Primary Alkaline Manganese	163	398	1.5[28]
Primary Lithium Thionyl Chloride	468	861	0.35
Primary Zink-Air	442	1673	0.07[28]

It can be seen that the rechargeable Li-Po battery has a high energy density and the highest maximum current rating. Although the Li-Ion battery has a higher energy density, it will not be able to deliver the required amount of power due to the very low current rating. The Ni-Cd and Ni-MH may also be able to deliver the required power, but would be too big and heavy compared to the Li-Po batteries. The overall

[28] Calculated with the specified internal resistance at the point where the battery voltage drops by 20%

characteristic of the Li-Po battery makes this battery the most suitable option for powering the UAV.

Li-Po batteries vary in size, weight and maximum current ratings depending on the specific manufacturer. The highest energy to size ratio, with a high enough current rating is preferable for this application. Batteries can be connected in parallel to reduce the internal resistance, which implies higher current ratings.

Considering this option for the other battery types is only applicable for the Li-Ion type due to its high energy density. But due to the low current rating, too many batteries have to be placed in parallel to achieve this.

The typical Li-Po battery discharge characteristics from FlightPower are shown in Figure 11. Note that these graphs are shown for one cell (3.7 V nominal) only. For a 12 V system, three cells will be required that will have a nominal voltage of 11.1 V (12.6 V fully charged with no load).

In the graph it is noted that the battery voltage drops rapidly from about 3.5 V, with a constant current load of 5 times its current rating (C). In the most extreme case where a current load of 30 C is applied to the battery, the voltage drops rapidly from 3.2 V. With 3 battery cells in series, the low level voltage will then be between 9.6 V, (3 x 3.2), and 10.5 V (3 x 3.5), depending on the load.

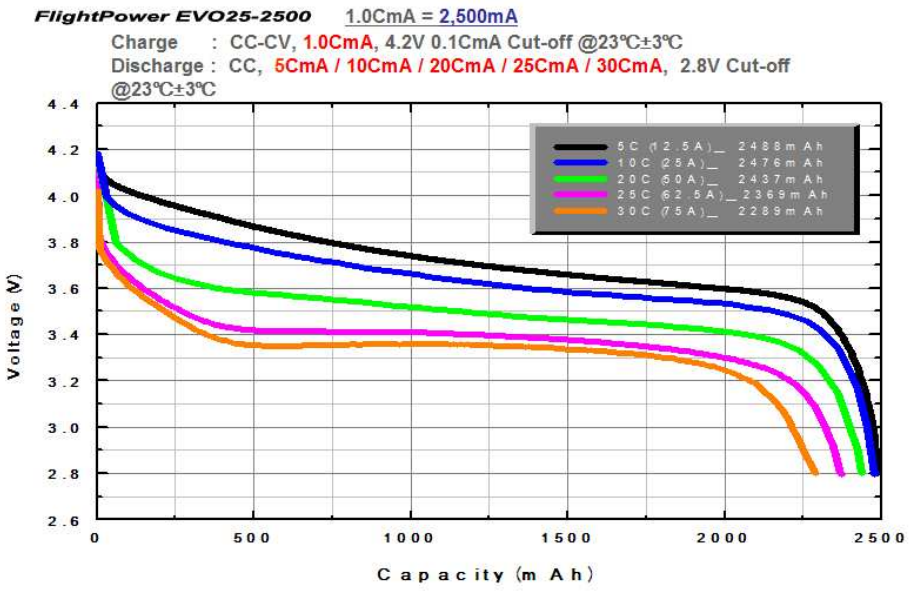

Figure 11: Li-Po discharge characteristics of a FlightPower battery

3.2.5.8 Power supply wiring

Special care must be taken when connecting the power supply to the different electronic components inside the aircraft. The autopilot manual from Micropilot indicates how to connect the electronic boards to avoid ground loops ([37], p12).

Figure 12 shows how some of the current drawn by the speed controller can flow through the servo board and autopilot. The electronic speed controller draws a high AC current that can induce electrical noise on the ground wires. This can influence the operation of the autopilot, or even damage it. The video image produced by the cameras can also be adversely affected. Unfortunately these ground loops cannot always be avoided, especially if the servos are powered from the speed controller's BEC circuit. Micropilot makes some suggestions in the autopilot manual ([37], p12, 13) on how to avoid ground loops. The autopilot can be powered by a separate battery, or a small (10 Ω) resistor can be placed on the ground side of the RC connector.

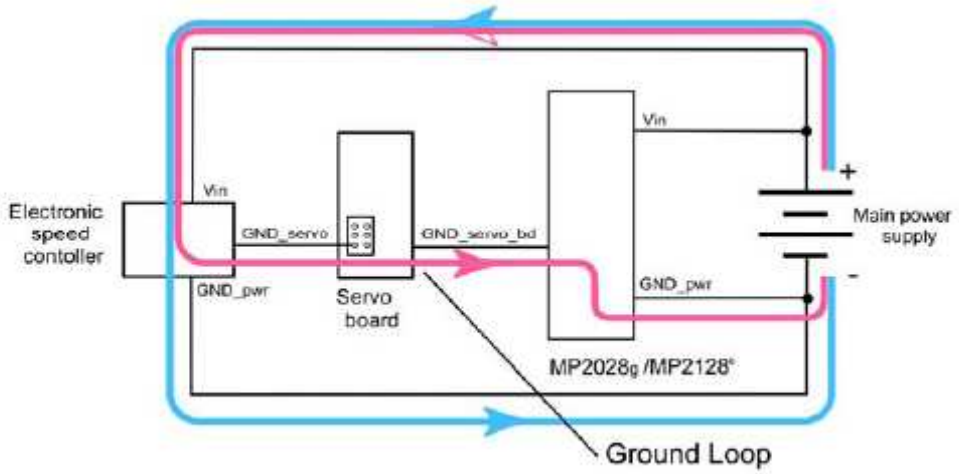

Figure 12: Ground loops ([37], p12)

The electrical noise on the ground wires is caused by the voltage drop, created by the high AC currents drawn by the speed controller. Appendix A shows the measurements of these currents. Figure 59 shows the noise that is generated between the battery ground and the servo board ground while the motor is running at full power.

The battery pack connector of the procured Micropilot UAV was modified so that the payload can also be powered from the aircraft's battery pack, as shown in Figure 13.

Four batteries are connected in parallel using the four connectors. The choice of four batteries is mainly driven by the space that is available inside the fuselage.

It is always a good idea to install only fully charged batteries and to keep the battery packs together and not swop different batteries around. Should batteries at different charge levels be connected together, the more charged ones will discharge into the less charged ones. This can damage the batteries due to the unregulated high currents that can be induced.

Connecting newer batteries to older ones can also cause problems during discharge. By the time the older batteries are depleted, the newer batteries may still be able to provide power. This can cause the older batteries to discharge beyond the operating voltage levels and the newer batteries to supply currents above their current ratings. This can damage the batteries beyond repair.

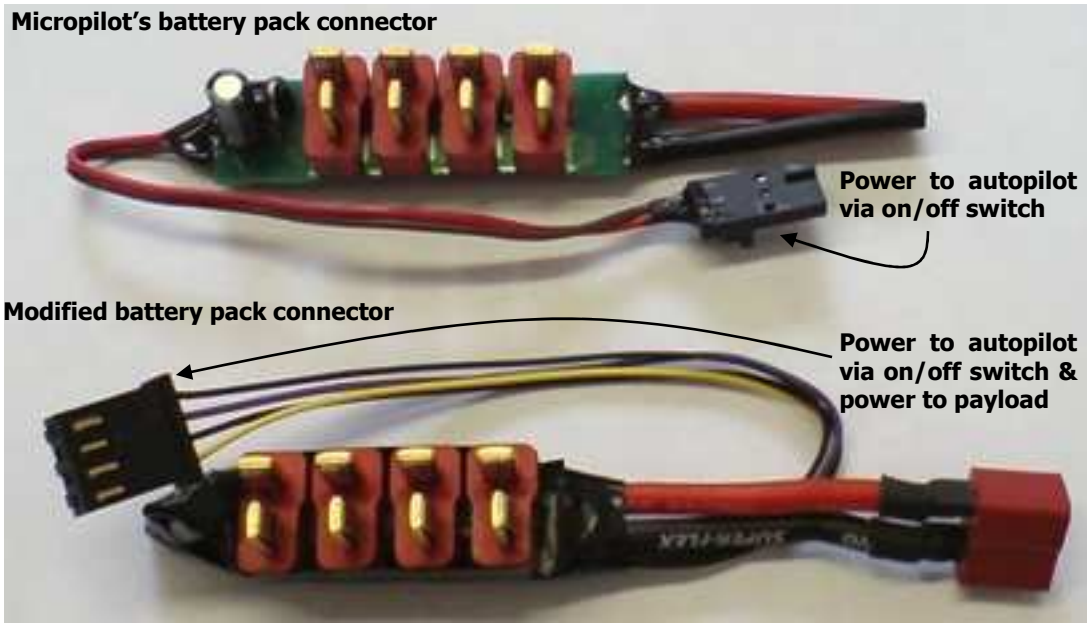

Figure 13: Battery connection modifications

3.3 Payloads

3.3.1 Overview

The main purpose of the unmanned aircraft is to gather reconnaissance information. This would mainly consist of pictures in the form of still photos or real time video streaming. The types of sensors required would be still cameras and video cameras. The camera image must then be transmitted back to the Ground Control Station (GCS) for the image to be viewed in real time. To achieve this, the payload must consist of at least one camera and a video transmitter.

3.3.2 Cameras

The cameras and video transmitter combination should be inexpensive, small, light weight and have low power consumption. In spite of all these limitations, it should still be able to produce a clear image.

Table 1 lists a few video cameras that were found to comply with the abovementioned criteria. According to the research outcome in chapter 1.3, the common type of observation sensors used on small UAV's are video cameras with fixed or zoom lenses. Table 1 shows that the cameras with fixed lenses are available in much smaller and lighter packages than the cameras with zoom lenses.

Some UAV manufacturers (Lockheed Martin, and MNT) make use of two or more fixed lens cameras with different focal lengths. By switching between the cameras, different fixed zoom settings are achieved. Using two fixed lens cameras for this project would ensure a payload that is light, small and inexpensive. The first payload was developed to have the two fixed lens cameras stationary relative to the airframe. One camera is fitted with a wide view lens while the second camera has a narrow field lens. The wide-field lens is used for general surveillance. Switching to the narrow field lens camera is possible when greater detail is required over the surveillance area.

The boardlens colour camera was chosen from Table 1. A special bracket was made to house the two cameras. Light weight materials such as aluminium (2.8 g/cm^3, [35])

and poly black stone plastic (1.140 g/cm^3) were chosen to construct this bracket. Figure 14 is a picture of this specially constructed bracket. The final weight of the bracket with the two cameras is 52 g.

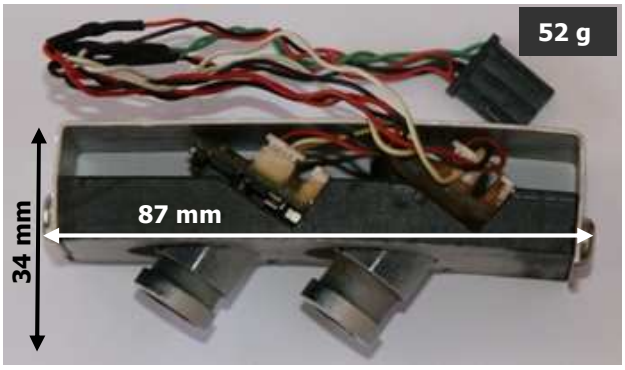

Figure 14: Camera bracket with 2 board lens cameras

The cameras in the first camera bracket prototype pointed vertically downward (90^O relative to the aircraft). The initial flight tests, discussed in chapter 4, showed that the video image produced at this camera angle setting passed by too fast while the aircraft was in flight. This was corrected by tilting the cameras 35^O forward.

3.3.3 Payload video transmitter

The cameras are required to display real video images at the Ground Control Station (GCS). The cameras listed in Table 1 produce a composite video output and require a supply voltage of 12 V. In the video surveillance security environment, analogue video transmitters are commonly used. The CSIR has accumulated a large amount of working experience with these types of transmitters making it easier to obtain the best solution. The tested- and proven-to-work transmitters that were considered for the UAV application are listed in Table 2.

During the testing and verification it was found that the 1.2 GHz transmitter, that initially showed to be the better choice, interfered with the data link. The 2.4 GHz transmitter, on the other hand, tested satisfactory with no interference. The video link was taken out of the housing and modified, using different connectors, to make it smaller and lighter. This is shown in Figure 15. The total weight of the video transmitter before modification is 173 g. After the modifications, the weight comes

down to 93 g. The original size of 64 mm x 64 mm x 35 mm is also reduced to 59 mm x 55 mm x 24 mm.

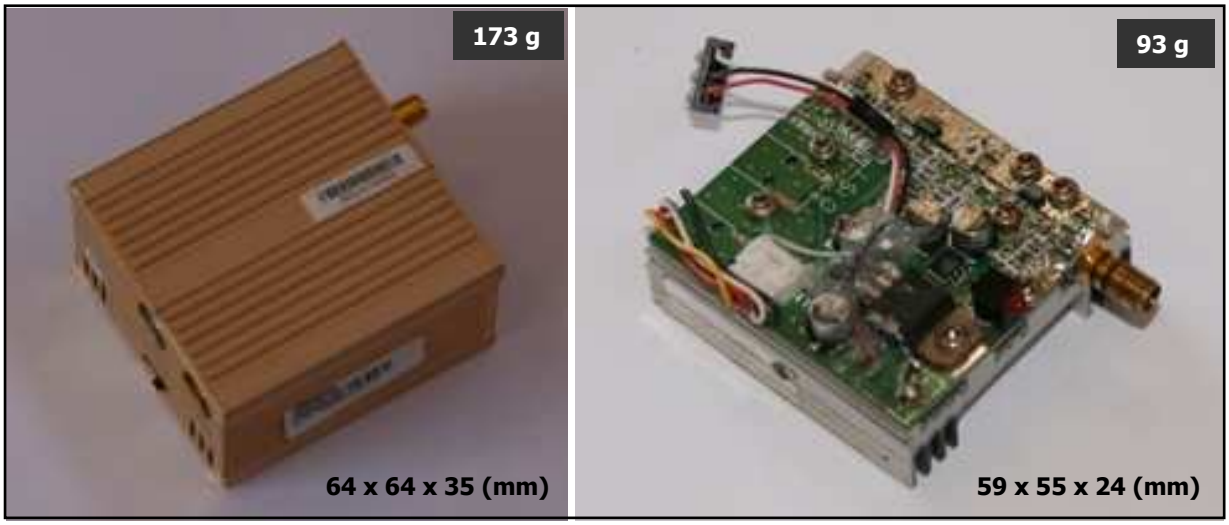

Figure 15: 2.4GHz Video RF link before and after modifications

The omni-directional antenna listed in Table 3 was chosen for the video transmitter on the aircraft, due to the high gain. The patch antenna was chosen for the receiving end on the ground, also because of the high gain. Directional antennas have more gain than omni-directional antennas and therefore are used on the ground to get a longer range. The YAGI antenna was tested, but proved that when using this, a lot of time and effort is required to get the direction and orientation correct. The patch antenna produced the same video quality and proved to be a great deal more user friendly.

3.3.4 Switching between the cameras

The restriction on the video transmitter is that only one video image can be transmitted at any given time. The available video splitting products that will be required to combine the two camera images into one are too big and heavy for the aircraft. The only solution was to add a camera switch functionality that could be controlled from the ground.

To do this, a small electronic circuit had to be designed. Figure 16 shows the block diagram and a photograph of the actual unit. The cameras are powered from the same battery pack that powers the motor and electronics inside the aircraft. The wiring was

carefully installed to prevent introducing any ground loops, as shown in Figure 12. Electrical noise generated by the speed controller does not affect the camera image. The total weight of the camera switch PCB is 11 g.

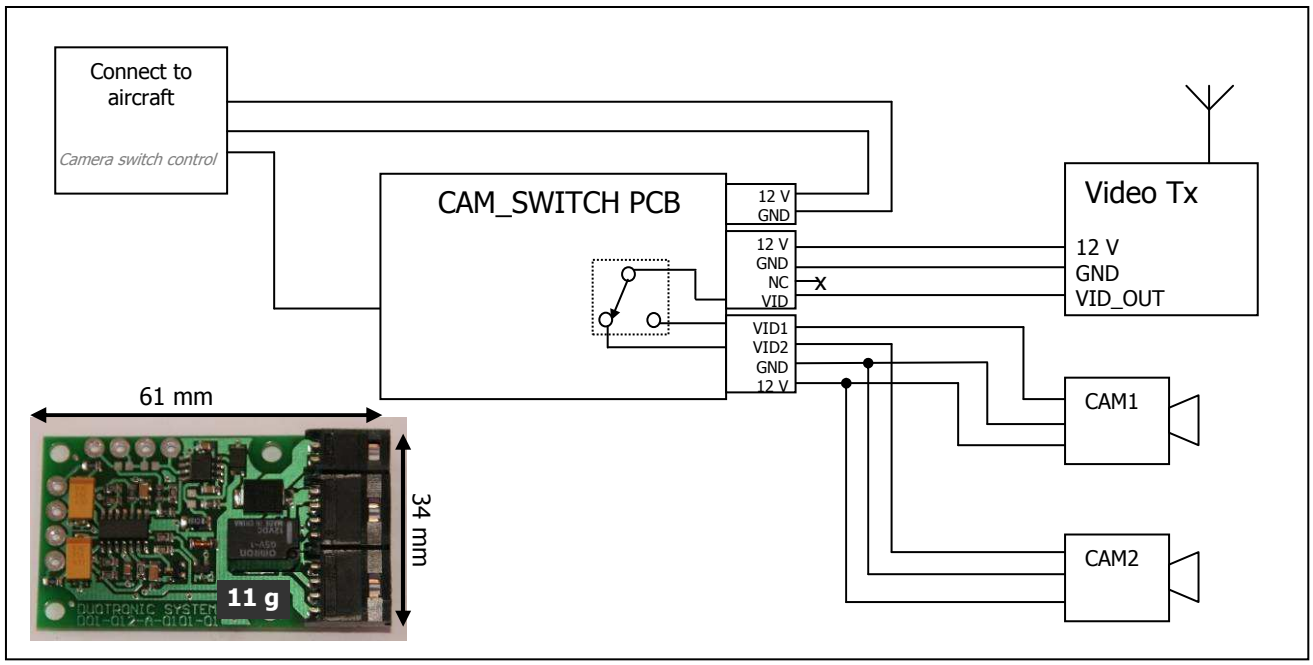

Figure 16: Camera switch block diagram with a photo of the PCB

In order to save battery power, the first design was to be able to switch the power between the two cameras. This meant that only one camera was powered at a time. However, during testing, it was seen that the time for the camera to produce an image after being powered on, took too long. The design was changed so that both cameras are powered on simultaneously, while only the video signal is switched. This camera switch design and schematic circuit is shown in Appendix B.

The cameras and transmitter, together with the camera switch, was built into a housing that fits underneath the aircraft. The housing was constructed from the same material used for the first aircraft. This material was proven to be light weight, strong, durable and easy to repair. The design requirements for this housing were:

- It must be as light as possible.
- Because the unit is installed underneath the fuselage, it must be able to withstand the impact and protect the aircraft during landings.

- It must be as small as possible and aerodynamically shaped to minimise the drag.
- The cameras and electronics must be protected.
- The video transmitter must have sufficient airflow for cooling purposes.

3.3.5 Pods

The payloads were designed and built to fit underneath the fuselage so that they could easily be changed around. These payloads consisted of different aerodynamically shaped pods, fitted with cameras and a video transmitter. Four payloads were designed and configured with different camera setups:

- Two stationary day cameras with different lenses.
- One day and one low light camera with different lenses on a pan platform.
- Two day cameras with different lenses on a pan and tilt platform.
- One Infra Red (IR) camera.

3.3.5.1 Day pod with two fixed cameras

Taking all the above requirements into account and with the experience gained from the first aircraft, a camera payload was constructed, and is shown in Figure 17. The payload weighs 260 g, which is less than the specification of a 500 g maximum allowable payload. The dimensions of the payload are 330 mm (L) x 70 mm (W) x 55 mm (H), excluding the antenna.

Figure 17: Camera payload with two fixed day cameras (260 g)

This payload is attached underneath the fuselage of the aircraft using Velcro and elastic bands. The video transmitter is mounted on the back and kept open to allow for sufficient cooling air flow. The camera switch PCB is mounted next to the cameras, inside the foam housing. The connector mounted on the side of the pod connects to the aircraft. The electric power for the payload and camera switch control is supplied through the connector.

The antenna hangs down below the aircraft while airborne and simply folds back when the aircraft reaches ground level during the landing. RF transmission patterns of the dipole omni-directional antenna require that the antenna must be perpendicular to the receiving side, in order to increase range. Therefore the antenna must be able to hang downwards while the UAV is airborne, to obtain maximum transmission range.

EPP foam is a light weight material, (0.022 g/cm^3), used to construct the payload housing, (pod), but is not strong enough to withstand the landings on its own. After the foam is cut and sanded to form an aerodynamic profile, it is covered with fibre-reinforced tape (125 g/m^2). Although it was not wind tunnel tested, the sanded profile should ensure that the aerodynamic drag coefficient is kept as small as possible. This is a very strong and durable combination. However, after a few weeks of being exposed to direct sunlight, the tape became brittle and pealed off.

This problem was overcome by spray painting the fibre tape to protect it from the lethal UV rays from the sun. However, the spray paint on the tape came off too easily. A number of different plastic primer sprays were tested, until one was found to make the paint stick to the tape. A light colour, non-reflective, matt paint, was chosen that is not easy to see from the ground. Figure 18 shows the materials used to construct the payload.

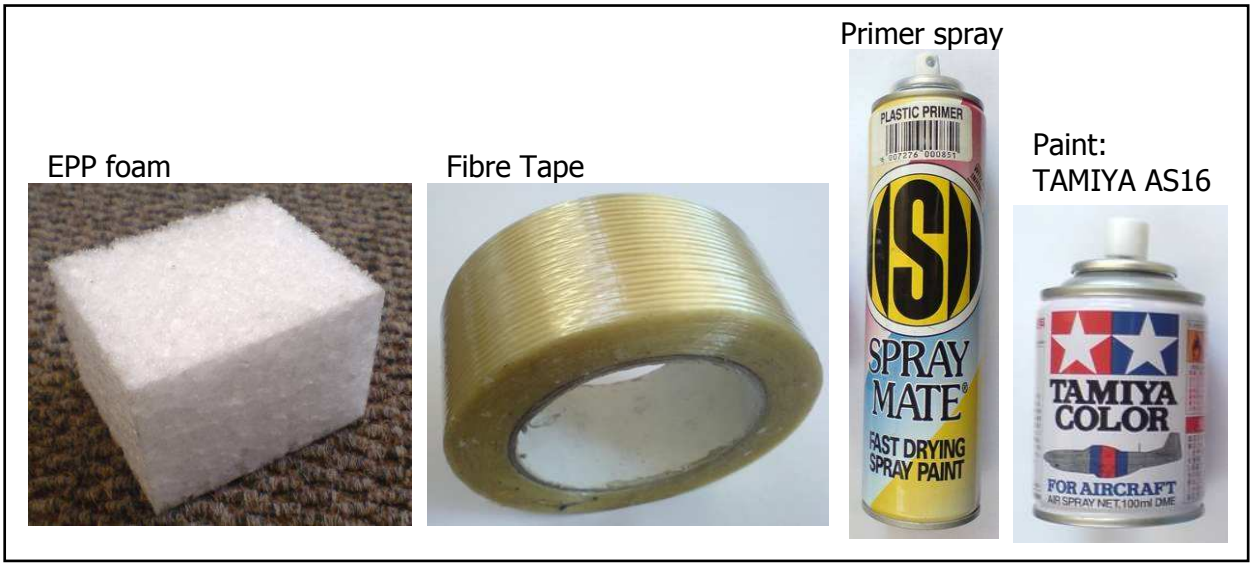

Figure 18: EPP foam, fibre-reinforced tape, plastic primer & paint used on payload.

3.3.5.2 Day pod with two cameras panning sideways

After the pod with the two fixed day cameras was built and successfully tested, the designing and testing of a few other payloads could begin. It was soon evident that controlling the camera movements by manoeuvring the aircraft was not quick enough. Also, when the aircraft banks to the left or right, it was seen that the cameras must be panned sideways to counter for the aircraft orientation.

A second payload was designed, built and tested similarly to the previous payload, but with the capability to tilt. This payload was equipped with one colour and one black and white (B/W) camera listed in Table 1. The tilting platform with the two cameras is shown in Figure 19. The wiring diagram is shown in Figure 84. A servo is mounted at the rear end of the camera to control the pan movement up to 55 degrees either side of the aircraft longitudinal axis. This servo is controlled by the autopilot via the wireless link from the GCS.

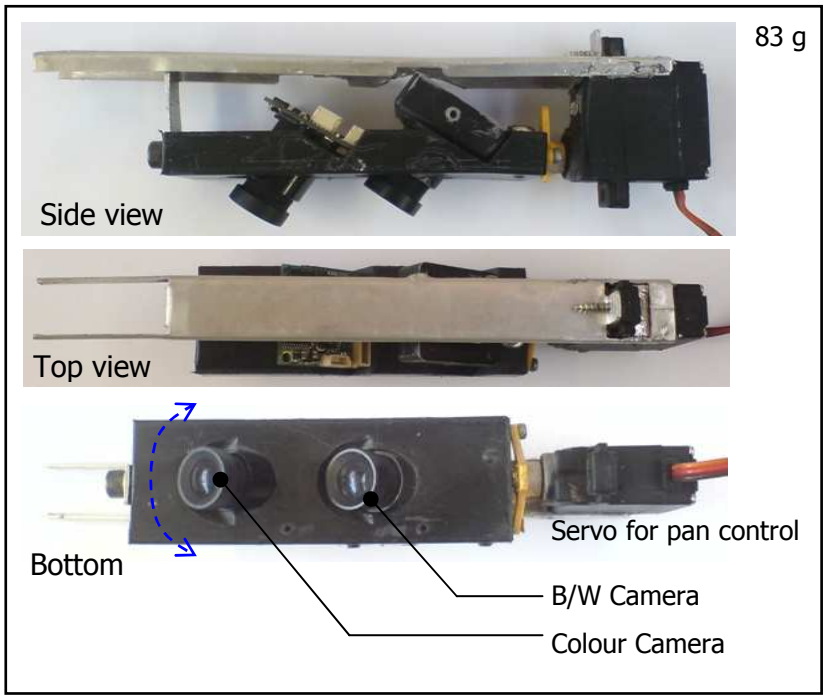

Figure 19: Panning camera platform with colour and B/W camera (83 g)

The platform was built into a pod with dimensions of 340 mm (L) x 80 mm (W) x 75 mm (H) excluding the antenna, and shown in Figure 20. To allow for camera movement, the pod is slightly bigger and heavier than the pod with the stationary cameras. However, the weight of 300 g is still less than the specified 500 g. The performance difference due to the size and weight difference was measured during the test flights in chapter 4.

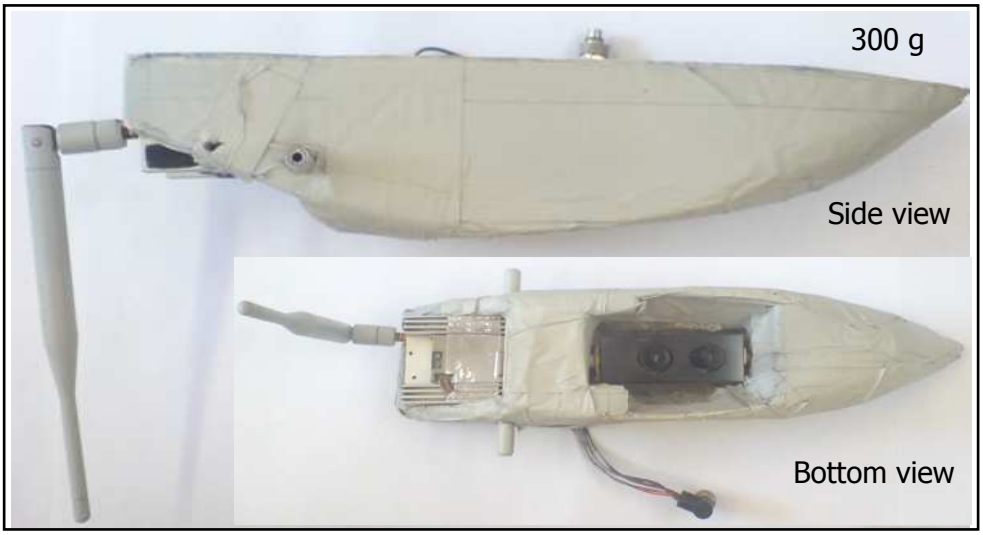

Figure 20: Pod with panning camera platform (300 g)

3.3.5.3 Day pod with two pan-tilt cameras

Test flying the day pod fitted with panning cameras, showed that controlling of camera movement from the GCS was possible. The idea arose to use the same concept and develop an entire camera platform that can pan and tilt. The two cameras were fixed inside separate brackets that could tilt together by means of an additional second servo. This platform was also constructed from light weight materials and weighed 85g as seen in Figure 21. The wiring diagram is shown in Figure 85. The front servo connects to the camera brackets by means of a control arm. The servo movement either pulls the cameras forward or pushes them rearwards. The panning functionality works similar to the previous design.

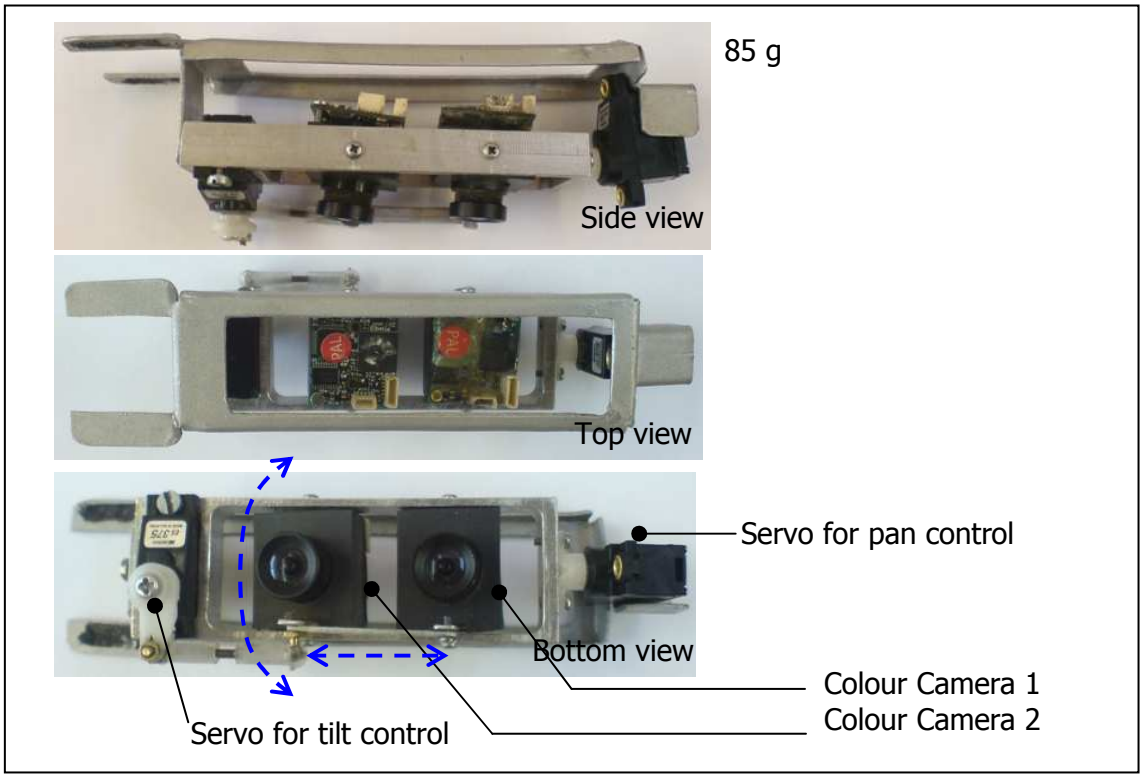

Figure 21: Pan-Tilt platform with two fixed day cameras (85 g)

This pan-tilt platform with the two cameras was built into a foam housing. The total weight of this pod was 310g with dimensions of 340 mm (L) x 80 mm (W) x 75 mm (H). Figure 22 shows the pod before it was spray painted.

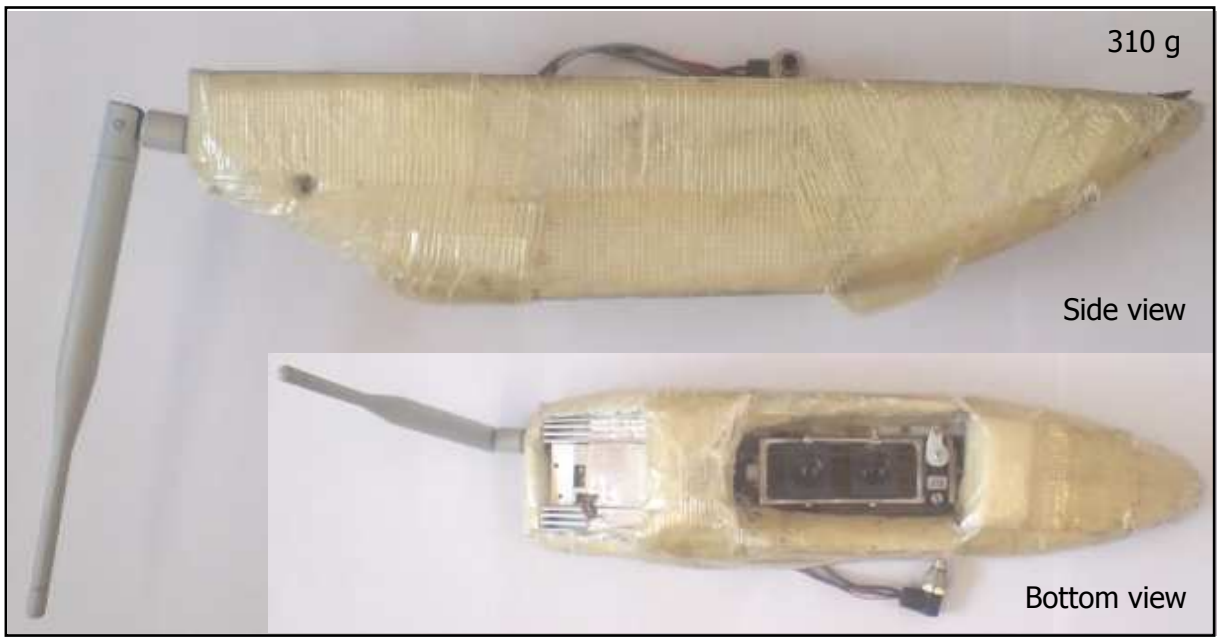

Figure 22: Pod with fixed colour cameras in pan-tilt platform

3.3.5.4 Night pod with thermal imaging camera

At the time of this project, only one night vision camera was found suitable. IR or thermal imaging cameras that were small and light enough just started to become available. They were however, still under International Traffic in Arms Regulations (ITAR) control due to the sensitive nature of the product. The Indigo Omega IR camera was available and imported after the necessary paperwork and guarantees were furnished. This camera weighs 120 g with dimensions of 35 mm (W) x 37 mm (H) x 65 mm (L) (with the lens) and is shown in Figure 23.

Figure 23: Indigo Omega FLIR camera

This camera was built into a foam-and-tape housing together with the necessary electronic components and video transmitter shown in Figure 24. The wiring diagram is shown in Figure 86. The total weight of this night pod was 309 g with the dimensions of 50 mm (W) x 90 mm (H) x 300 (L) mm (without antenna). Light emitting diodes (LEDs) that can be switched on or off by the GCS, were added to the payload. When the aircraft is flying over a target, the lights are switched off and when it is close to the GCS, it is turned on to make the aircraft visible for the landing.

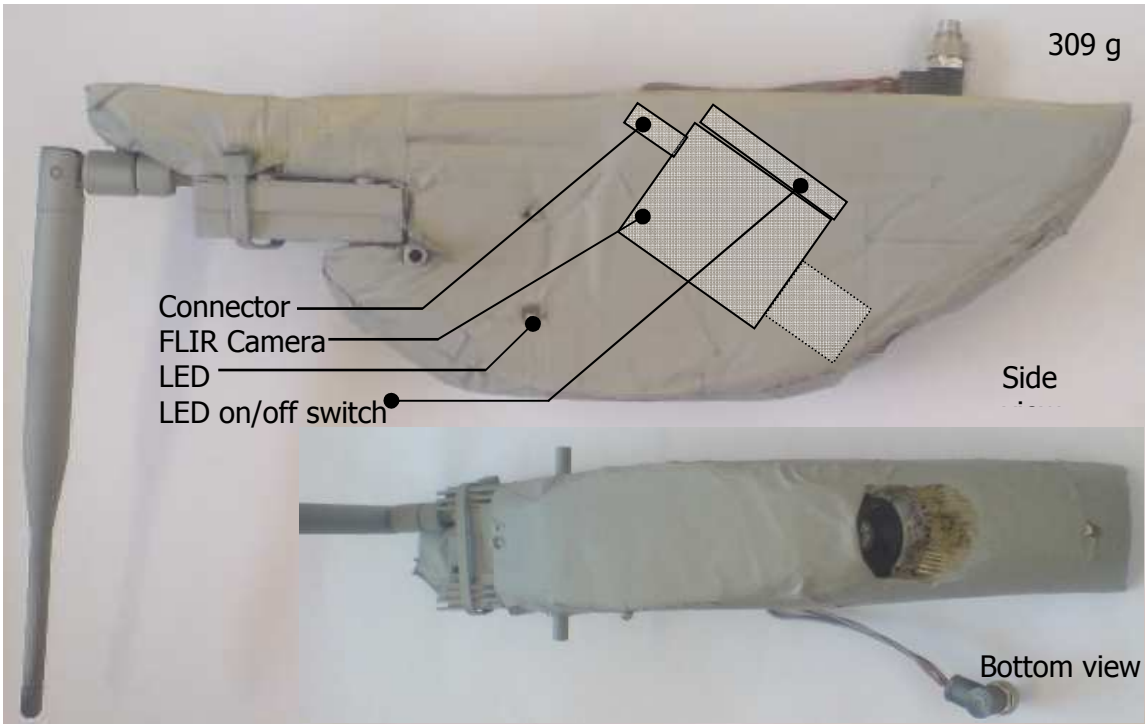

Figure 24: Night pod with Indigo Omega FLIR thermal camera

Modifications were made to the aircraft so that the payloads can easily be installed to the airframe. A female socket was placed on the fuselage (shown in Figure 25), that the pod, fitted with the necessary male plug, could be easily connected.

Figure 25: Payload connection on aircraft

The wiring block diagram for the payload connection on the aircraft is shown in Figure 26. The servo breakout board inside the aircraft is where the servos are connected and controlled by the autopilot. Eight servo connections are used for the aircraft controls (ailerons, rudder, elevator, throttle, flaps and spoiler) and three are used for controlling the payloads (camera switch or LEDs on/off, camera pan and tilt). The payload servos are also powered by the BEC on the speed controller via the servo breakout board. The ground connection of the servo breakout board is not connected to the payload. This is to avoid creating more ground loops.

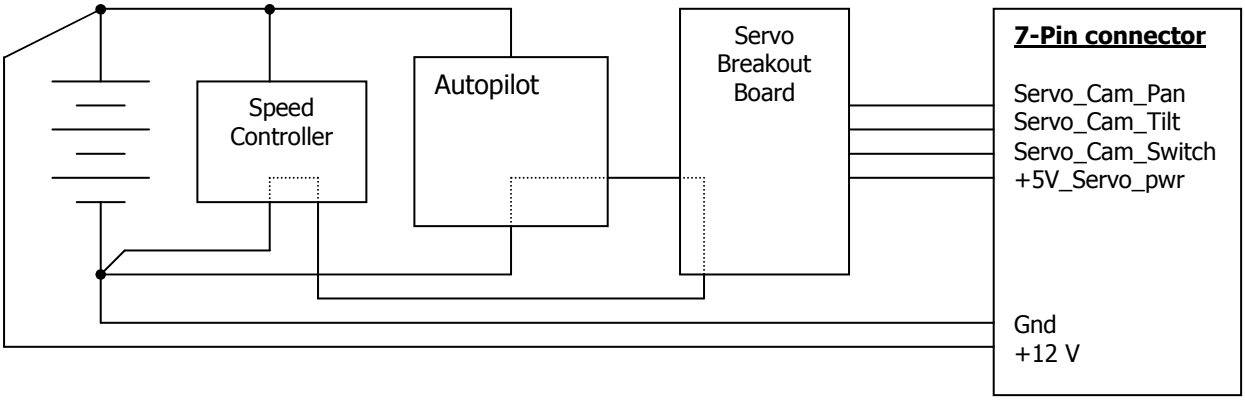

Figure 26: Wiring block diagram inside aircraft for payloads

A photo of the payload connections to the servo breakout board is shown in Figure 27.

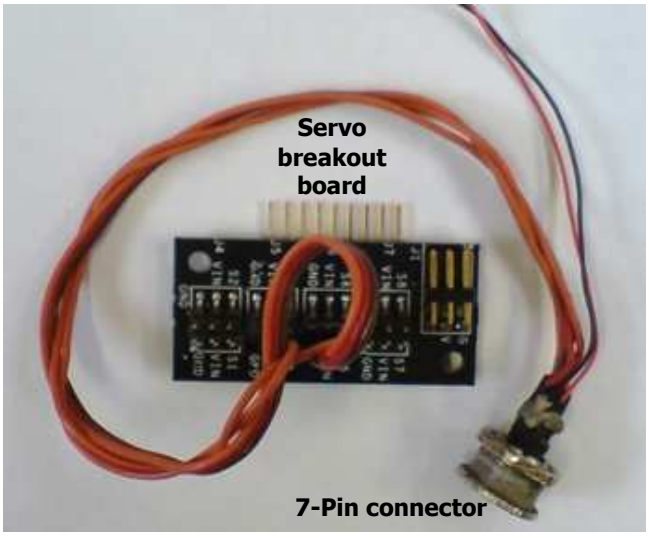

Figure 27: Servo breakout board with payload wiring

Chapter 4 contains the results and performance outcome of the four different pods that are used on the Micropilot MP-Vision aircraft.

3.3.5.5 Predicted payload influence on performance

The payload influences the performance of the aircraft in several ways. One is that the power usage of the payload reduces the available power needed to fly the aircraft. The electrical power consumed by the payload is calculated by adding up all the different power requirements of the payload.

- Two day cameras: 840 mW each (Table 1).
- FLIR camera: 1.5 W (according to the brochure).
- Video transmitter: 12 W (Measured 1 A and 12 V).
- Camera switch: 480 mW (Measured 40 mA and 12 V).
- Servo average: 290 mW (10 mA in rest; 250 mA while moving; 58 mA average with 20 % movement @ 5 V).

The day camera payload total power consumption is 14.74 W and the night payload with the FLIR camera consumes 13.98 W in total. For the aircraft to be able to fly for 55 minutes (specified by Micropilot) with a 8400 mAh, 11.1 V battery pack [18], the average power usage of the aircraft is calculated to be 102 W. Thus, the 14.74 W of the payload consumes almost 15 % of the aircraft's power usage.

The second aspect of the payload that has an influence on the performance of the aircraft is the weight. The payloads weigh between 260 g and 310 g. This is 9.3 % to 11.1 % of the aircraft weight of 2.8 kg (with batteries, but without the payload).

Thirdly, the payloads increase the aerodynamic drag of the aircraft. The increase in drag was not calculated, but rather field tested. Total payload influence on the aircraft's performance was evaluated during range and endurance flight tests. These results are discussed in chapter 4.

3.4 Ground Control Station

3.4.1 Overview

Micropilot does not supply a base station with the MP-Vision UAV, but does supply the software needed to control the aircraft. Before putting together a ground control station we needed to know what building blocks are needed. From the research in chapter 1, the minimum required components for a functional GCS are:

- Laptop computer.
    - Hardware
    - Software
- Wireless data link.
- Video components.
    - Video RF receiver
    - Video display
    - Video recorder

This chapter will describe how to choose, develop, integrate and configure all the GCS components.

3.4.2 Laptop computer

The laptop computer is required to install the software which will control the aircraft and payload. This software is normally supplied with the procurement of the autopilot. The software from Micropilot, which is called Horizon, was supplied with the MP2028g autopilot and MP-Vision UAV which was fitted with an autopilot. The software is supplied with a manual explaining how to install and configure the autopilot, as well as how to operate the software. The suppliers also specify the minimum requirements of the computer used to run this software package. Micropilot's minimum requirements for the computer are ([38], p3):

- Pentium II, 500 MHz

- 256 Mb of RAM.
- Windows 2000 or XP, (XP recommended).
- RS232 serial port.

To display the transmitted video data on the computer, the minimum requirements will be:

- Pentium III, 1GHz.
- 512 Mb of RAM.
- Windows media video source device. Ether USB, PCI, Fire-wire (IEEE 1394) or PCMCIA.

Because the laptop will be used out in the field, a more rugged type laptop will be required that will meet or exceed the minimum requirements specified by Micropilot. Some of the rugged-type notebooks available at the time of this study are listed in Table 17. The cheapest one that met the requirements was selected which is the Dolch NotePAC.

Table 17: Comparing laptops

Manufacturer & Model	IP rating	Processor, RAM	Com Ports of interest	Operating System	Screen	Price[29]	Picture
Dolch NotePAC[30]	54	Pentium 4 1.6 GHz, 480 Mb	1 x RS232 2 x USB	Windows XP	14.1" XGA TFT Sunlight readable	R44,000	
Kontron Revolution[31]	54	Pentium III-M 1.4 GHz, 512 Mb	1 x RS232 2 x USB	Windows XP	12.1" XGA TFT Daylight readable	R51,000	

[29] This price includes VAT and was quoted in 2005
[30] Technical data from datasheet "NotePAC TechSpec_int.pdf"
[31] Technical data from datasheet "ReVolution_Datasheet_EMEA.pdf"

The rugged notebook was procured and loaded with Windows XP operating system and the latest Horizon software version received from Micropilot.

3.4.3 Wireless communications

The RF data link is a wireless serial communication between the GCS and the aircraft. This link is very important for controlling the aircraft during flight. It is used to monitor the aircraft's position and status during the flight. It is also used to send in-flight commands to the aircraft.

Micropilot specifies a serial RS232 communications link between the autopilot and the GCS ([37], p15). The serial communications must be configured with the following settings:

- Baud rate of 9600 bps (19200 or 57600 baud may also be used).
- No parity.
- 1 Stop bit.
- No flow control.

The physical connections and wiring are detailed in the user manual [37], p15. Figure 28 shows a block diagram of the wireless communications setup between the GCS and the autopilot in the aircraft.

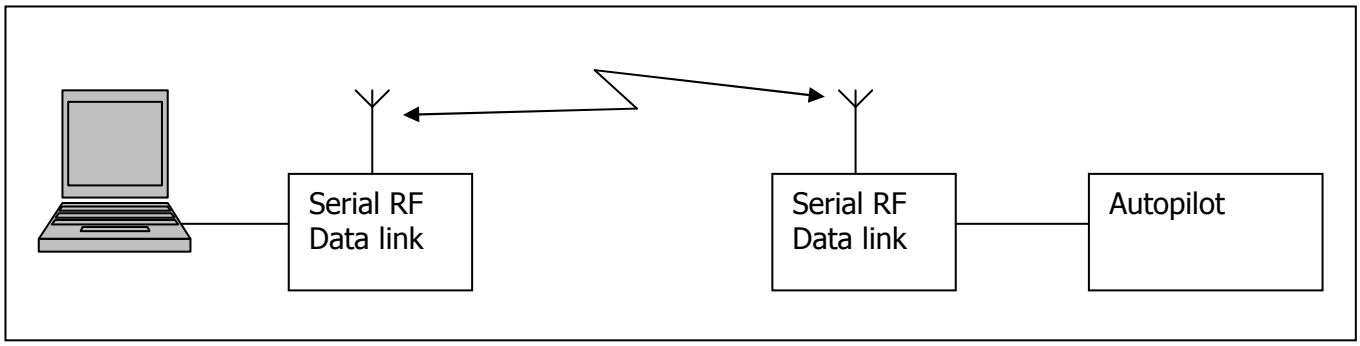

Figure 28: Wireless serial communications block diagram

According to the requirements, the serial data link needed for this application must comply with the following:

- Be as small and light weight as possible.
- Have low power consumption.
- Provide for serial RS232 communications with a minimum data rate of 9600 baud.
- Be able to provide a reliable communications link with a line of sight (LOS) range of more than 10 km.

Different RF serial data links, that appeared to be suitable to comply with the requirements, are compared in Table 18. The Aerocom AC4486-250M product is the smallest and lightest serial link that can be implemented on the aircraft. As this is a serial transceiver, meaning it can send and receive data, it is also used on the GCS side. The test results for this link can be found in chapter 4.

Table 18: Comparing RF serial data links

RF data link	RF frequency & Serial data rate	Dimensions	Weight	Transmit Power	Specified range with dipole antennae (LOS)	Picture
XStream-PKG-R	900 MHz or 2.4 GHz < 57600 bps	7.90 x 13.90 x 3.80 cm	200 g	140 mW	11 km (900 MHz) 5 KM (2.4 GHz)	
Aerocomm AC4486-250M [39]	869 MHz < 57600 bps	(49 x 42 x 5 mm)	< 21 g	250 mW	15 km (868 MHz only)	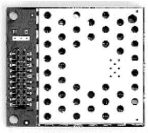

As this is a relatively cheap commercially available serial link, no data encryption is available. As soon as the concept is proven to work, this link can be replaced with an encrypted link if available. The AC4868-250M link is an OEM product that requires the correct interface in order to be applied correctly. The supplier of this OEM module also supplies a RS232 adapter board where the AC4868-250M can be connected. The block diagram for this connection is shown in Figure 29.

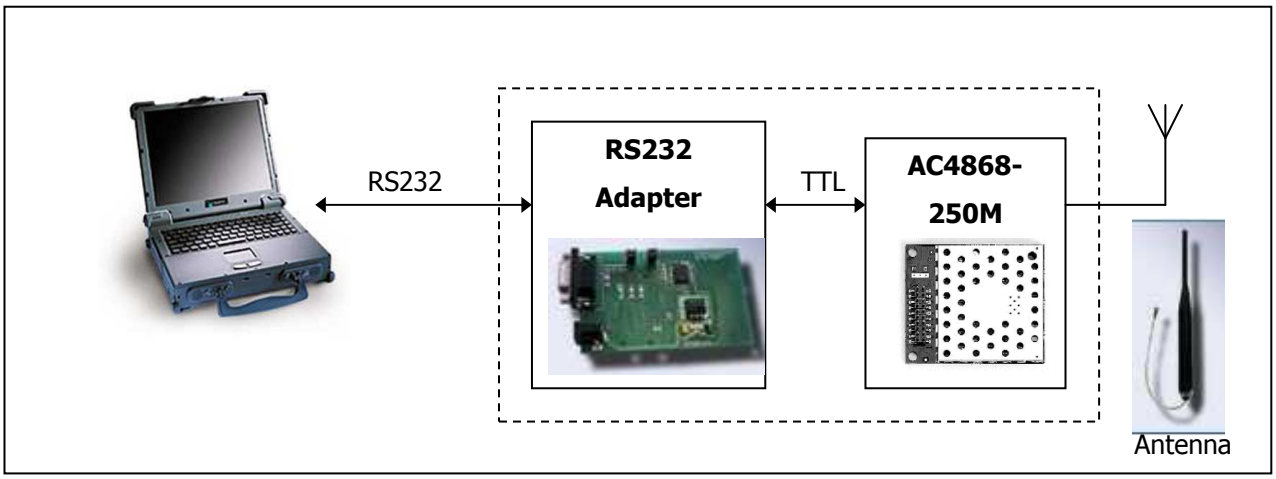

Figure 29: Block diagram with photos of the GCS RS232 serial RF interface

The RF serial link and RS232 adapter boards are built into an enclosure that connects to the laptop. The RF serial link is powered by a 12 V, 1.2 Ah Lead-acid battery which connects to the laptop with a standard RS232 serial extension cable. The laptop with the serial link and battery is shown in Figure 30.

Figure 30: Photo of GCS laptop with serial link

This custom off the shelf RS232 adapter is too big and does not fit into the aircraft. A smaller RS232 adapter was developed and built with a total weight of 11 g and dimensions of 58 (L) x 42 (W) x 10 (H) mm. The RF link, together with the R232 adapter weighs 25 g. The antenna recommended by the supplier for the AC4868-250M link is an 868 MHz half wave dipole antenna with a gain of 2 dBi. See Figure 31.

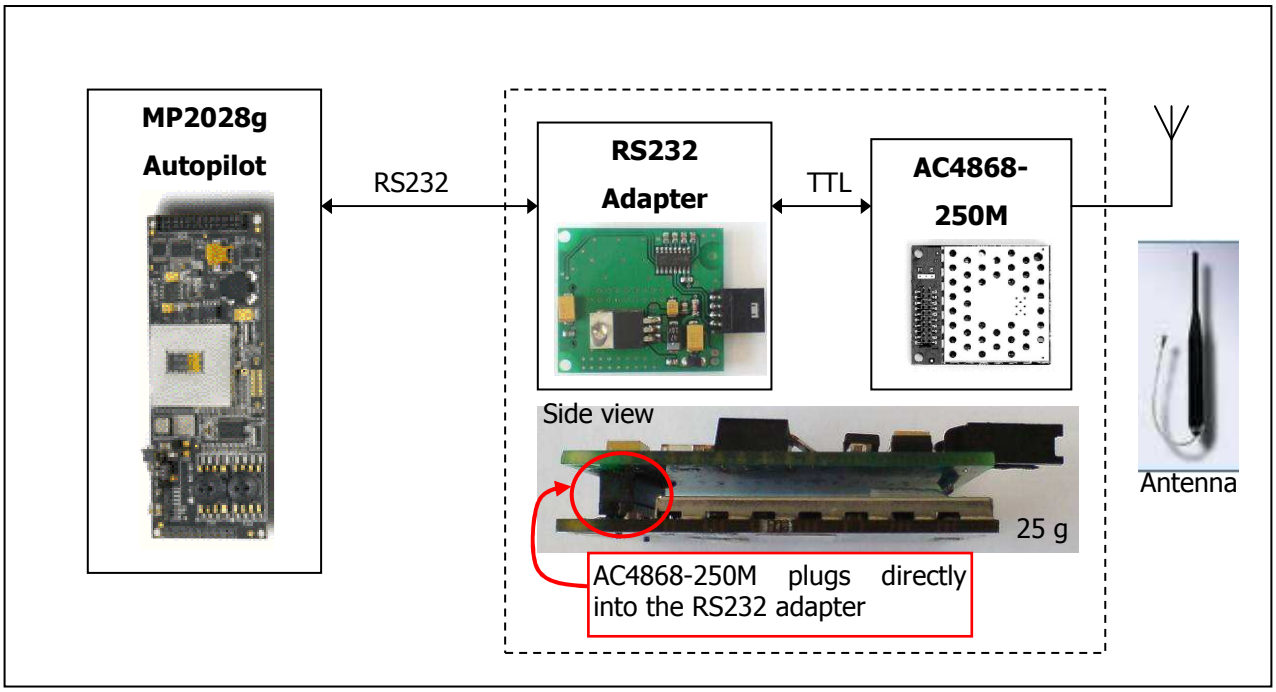

Figure 31: Block diagram of the aircraft's RS232 serial RF interface

Modifications were made to the aircraft in order to use the new RS232 data link. The connector plug between the autopilot and the data link was changed and the antenna replaced. The placement position of the data link inside the aircraft was moved from the battery compartment to where the autopilot is positioned (due to space restrictions). Enough space was available on top of the autopilot. By placing the RF data link on top of the autopilot created the possibility of Electro Magnetic Interference (EMI). This concern was eliminated by monitoring the autopilot behaviour and GPS reception after switching the aircraft on. Many test flights afterwards also verified that this was no concern.

3.4.4 Video

The video image transmitted from the aircraft camera payload must be displayed and recorded at the GCS. The camera payload uses a 2.4 GHz analogue RF transmitter for transmitting the video image in real time (paragraph 3.3.3). A 2.4 GHz video receiver is used for receiving the transmitted video image. As the video transmitters and receivers are designed and supplied in pairs, different video receivers were not evaluated. The receiver that was recommended for the selected transmitter was procured and is shown in Figure 32.

Figure 32: 2.4 GHz Video receiver (Supplier[32] P/N: E-RX2410)

The output of this receiver is a standard 1 V peak to peak (p-p) composite video output with a RCA connector. The received image can be displayed on the laptop or on a separate display device. It was found to be preferable if the video image is displayed on a separate display device. This way it is quicker to switch between aircraft control and observing the video displayed. For this application the SONY GV-D1000 display device was chosen, as the CSIR already has experience in using this. This video display device also has the required recording capability. Figure 33 shows a block diagram with photos of how the video receiving components are connected.

[32] http://www.eaglecctv.co.za/display_product_1594.htm, 2009-09-07

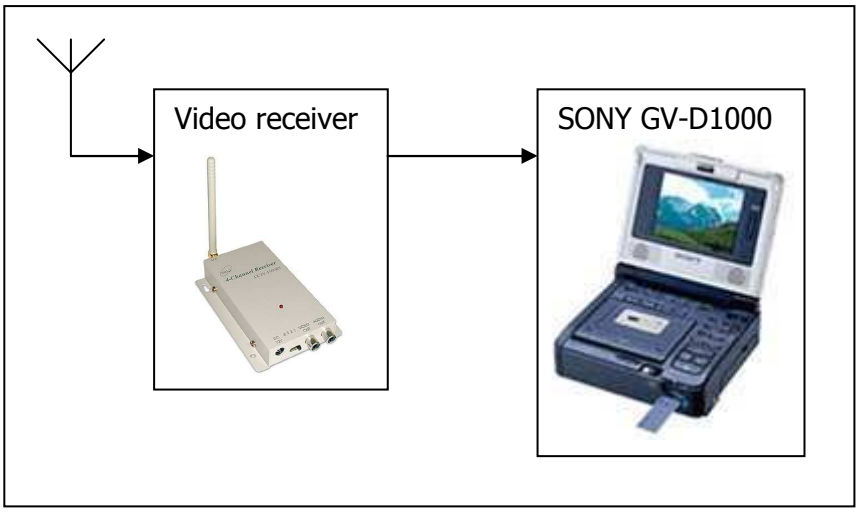

Figure 33: Video receiving and display setup

3.5 Summary

The development commenced with the design and manufacturing of a custom airframe. All the other components needed were identified by a literature study and procured to be tested. During the testing and evaluation, it was found that the airframe could not be configured to fly reliably. The Micropilot UAV was purchased because it provided a stable aerial platform that can be used to carry different payloads. The Micropilot UAV did not initially meet all the performance requirements. A few modifications were made so that range and endurance requirements could be met. These necessary modifications were transferred from the first prototype. The main change was the RF data link to enable the aircraft to be controlled within a LOS range of at least 10 km from the GCS.

Different payloads were constructed to enable the aircraft to conduct the required aerial reconnaissance missions. The payloads were designed to cater for day, low light and night observation. Three different payloads for day observation were designed. The first design was made to test the concept. This design led to two more designs which were built with the camera pan and tilt functions. The payloads were also designed to have a minimum influence on the aircraft performance.

The aircraft systems were modified so that the payloads could be powered from the main battery and be controlled via the autopilot. The GCS components were procured

and integrated to control and monitor the aircraft as well as the payloads. The GCS also displayed and recorded the live video image transmitted from the aircraft while in flight.

The next chapter describes all the tests and verifications that were done on the system components that were modified, designed and integrated.

4 DESIGN VERIFICATION AND RESULTS

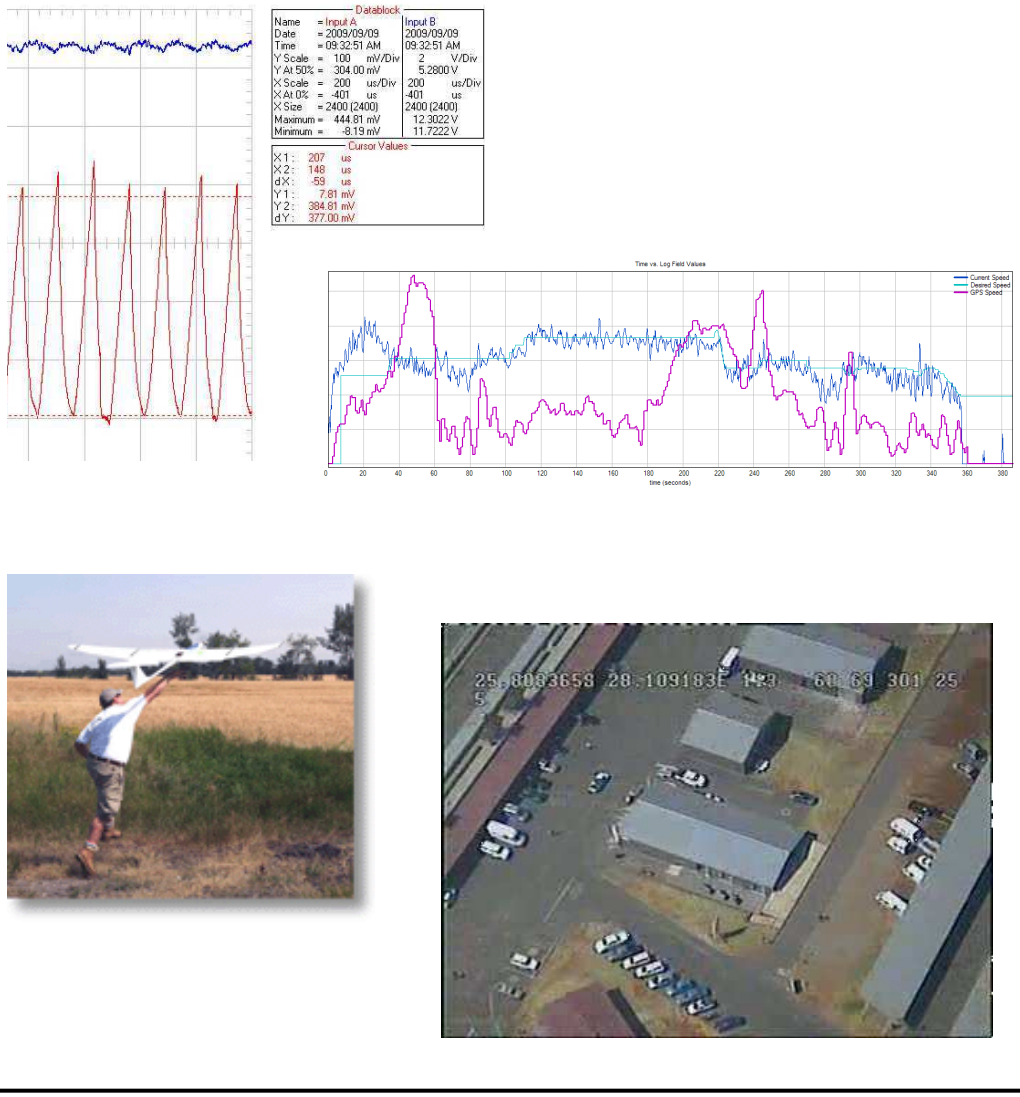

This chapter describes how the UAV system and components were tested and what the results of the tests were. It begins with the laboratory tests to verify the performance of each component. The system is then tested in the field to verify how the aircraft, payloads and complete system perform. The results are captured and analysed.

4.1 Overview

The test procedure was to first complete the laboratory tests under controlled environmental conditions on each individual system component. As the components were integrated, the interface compatibilities were tested and verified. After completion of the laboratory tests, the components and sub-systems were subjected to external field tests.

The final test phase was to perform test flights with the complete system. The first test flight was performed on the aircraft without any modifications. This was used as a benchmark to determine the effect of the modifications on the system performance. The aircraft was modified and further test flights were conducted with and without the payloads.

4.2 Laboratory tests

4.2.1 Battery tests

Battery tests were performed to measure the power consumption of the motor at different power settings. During the initial test flights, these settings were recorded during take-off, straight and level flight, climbing, descent and landing. The GCS software will display the current throttle setting of the motor while the aircraft is in flight. Instead of displaying the motor revolutions, the throttle setting is displayed as a percentage of maximum power available from 0 % to 100 %.

The aircraft was fixed to a bench in the laboratory while the throttle was controlled by the Horizon software. The test setup and measurements are detailed in Appendix A. Table 19 summarises the measured average supply voltage and current drawn by the speed controller. The scope meter readings are shown in Figure 53 to Figure 58. The scope meter displayed the average current and average voltage during the measurements that were used in Table 19.

The speed controller does not draw DC current from the battery when powering the brushless motor. A 7.8 kHz AC current is measured when the speed controller drives the brushless motor.

Table 19: Comparing power usage at different throttle settings

Throttle setting	Vavg (V)	Iavg (A)	Pavg (W)
15 %	12.5	1.9	24
30 %	12.5	8.5	106
45 %	12.3	17.2	211
60 %	12.1	30.9	373
75 %	11.9	46.3	550
90 %	11.9	46.4	552
100 %	11.9	46.5	553

From the summary of Table 19 it can be seen that the maximum continuous power consumption of the motor was 553 W and occurred at 100% throttle setting. The power difference between 75 % and 100 % throttle is very small. It is therefore assumed that the aircraft reaches full power at a throttle setting of 75 % and more.

It is also noticed that the fully charged battery voltage of 12.6 V decreases to between 12.5 V and 11.9 V with throttle settings between 15 % and 100 %. This is useful information for monitoring the battery voltage during flight. This implies that the battery voltage will always show less voltage at higher throttle settings. For example, when the aircraft is climbing or banking it uses higher throttle settings at which the battery voltage indicator will show a lower voltage. This is a result of the higher currents supplied by the battery and the internal battery resistance which cause a voltage drop.

Figure 34 shows the graph of the battery power drawn from the speed controller versus different throttle settings. From this graph it is visible that the curve is the

steepest between 30 % and 75 %. This implies that power consumption increases more rapidly as a result of applying more throttle above 30 %. The ideal would be to keep the throttle setting below 30 % while the aircraft is flying. This might be achieved with further tests, evaluations and changes.

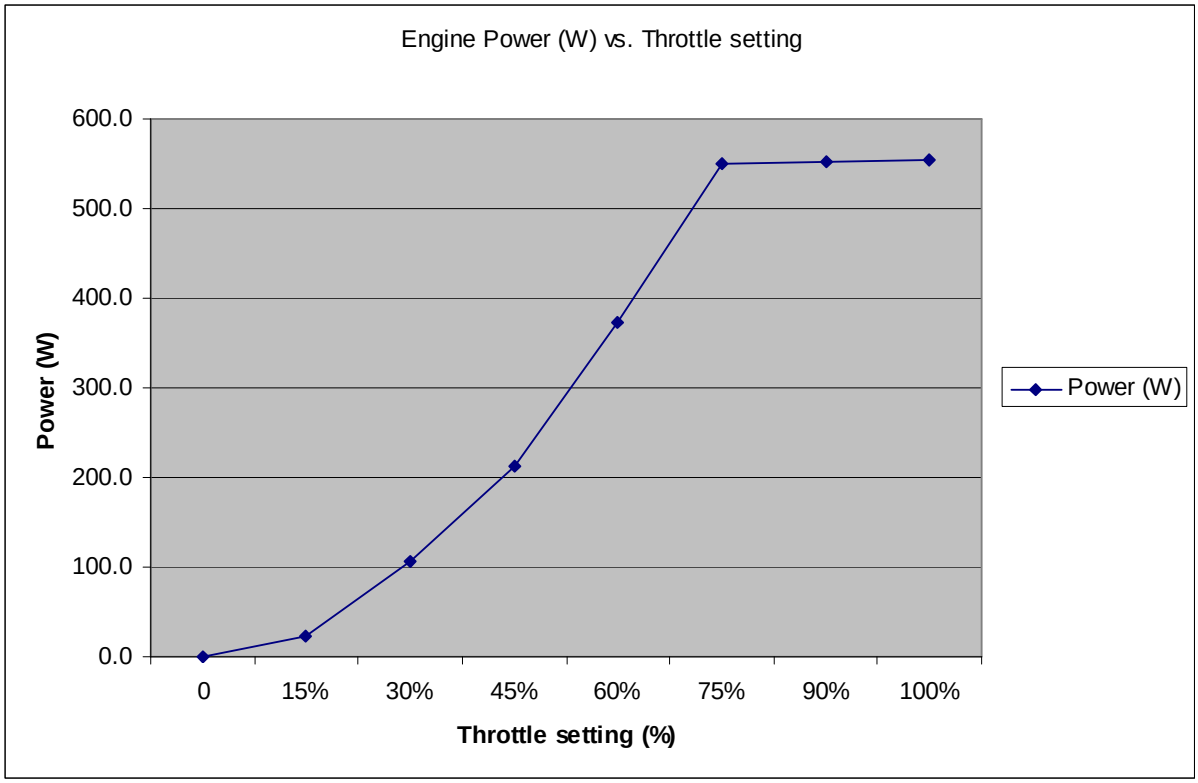

Figure 34: Graph of engine power vs. throttle settings

In the recorded scope meter readings (Figure 53 to Figure 58) it can be seen that during the peak currents, the supply voltage drops to the lowest point. This measurement is used to calculate the internal battery resistance of 16 mΩ for the four batteries connected in parallel. It is also noted that the peak currents are much higher than the average measured currents. With a throttle setting of 100 %, the average current is 46.5 A which peaks at 60 A.

These high currents must be taken into account when designing the wiring of the aircraft. The wires from the battery to the speed controller must be as short as possible with as much copper as possible, without adding to much weight. This would ensure a low resistance which will reduce the voltage drop between the battery and speed controller. This will also decrease the power loss across the wires.

In order to keep the aircraft airborne for one hour with a 8.4 Ah battery pack, the aim would be to keep the average current usage below 8.4 A. According to the battery tests, this is equivalent to about 30 % average throttle for the duration of the flight. Flights can also be planned to minimise climb and sharp turns, to maximise the flight endurance.

4.2.2 Wireless communications

The MP-Vision UAV required some modifications to increase the aircraft's controllability range from the GCS. The wireless data link and antenna was replaced with newly designed equipment described in paragraph 3.4.3. The antenna was mounted in the tail of the aircraft, rather than placing it on the outside. The aim was to minimise drag. An external antenna would add to the wind resistance. The steps followed to test the communications between the GCS and the aircraft were:

1. Verify connectivity with direct cable connection.
2. Verify connectivity within close range (10 m) for the new installed wireless link.
3. Verify system compatibility.
4. Verify communications range with aircraft stationary on the ground.
5. Verify possible interference with video transmitter (camera payload added).
6. Implement changes and add modification where needed.

The autopilot manual ([37], Chapter 3, p19) indicates how to set up and test the communication system. After verifying the direct cable connection and the new RS232 link with the AC4868-250M modem, a static range test was performed. The aircraft was taken to the CSIR tower while the GCS was moved away from the aircraft by car, on a road where the tower was in line of sight for most of the time.

Figure 35 shows a Google map of the road that was used. A maximum distance of 15 km was achieved, which was limited by the LOS coverage available on the road. This implied the possibility of the link to be adequate for even further distances than 15 km. In spite of the LOS limitation, the data link was shown to be capable of good communications over more than 10 km.

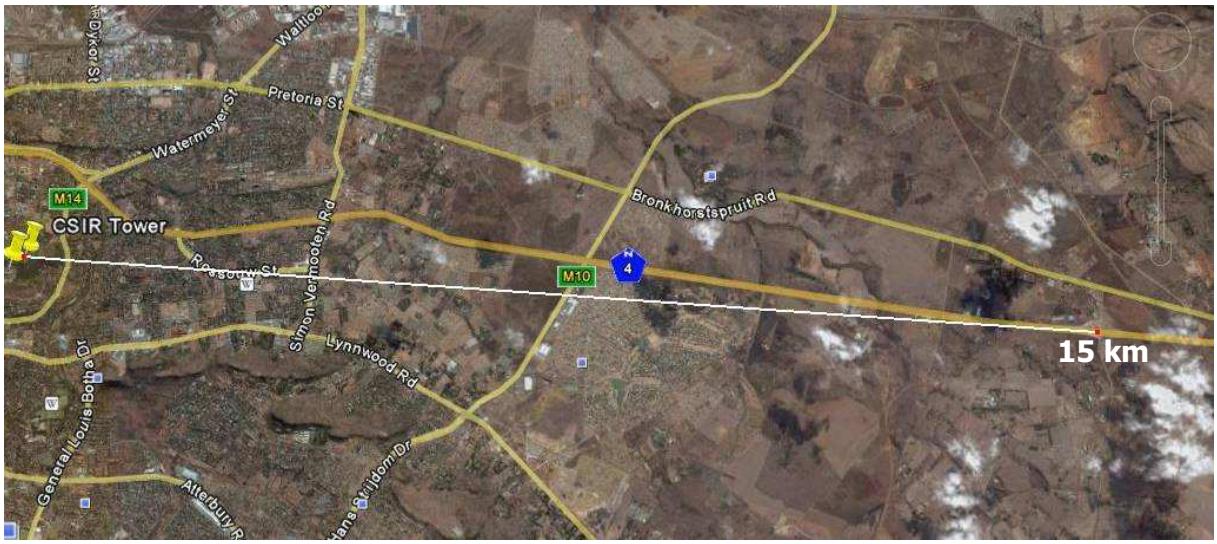

Figure 35: Stationary range test area for data link

The same test was repeated with the camera payload installed underneath the fuselage. The video signal, as well as the data link was still operational at a distance of 15 km. However, the radio link interfered with the video signal. Every time data was transmitted from the aircraft to the GCS, the video image was distorted.

The main challenge, when placing multiple antennas on a small aircraft, is that they remain too close together and easily interfere with each other. After examining the radiation pattern of a dipole antenna, as shown in Figure 7, the antennas were placed over one another. This is directly applicable to the data link and video transmitter dipole antennas on the UAV.

Figure 36 shows a side view of the antenna placement on the aircraft that produces a good data link, as well as a good video image, over a LOS distance of 15 km. Radiation patterns are sketched to show the reason why the antenna in the tail interfered with the video image. The antenna sticking out on top of the aircraft increases the drag, but is an acceptable penalty to ensure a good quality picture. Aerodynamically designed antennas may be considered in the future.

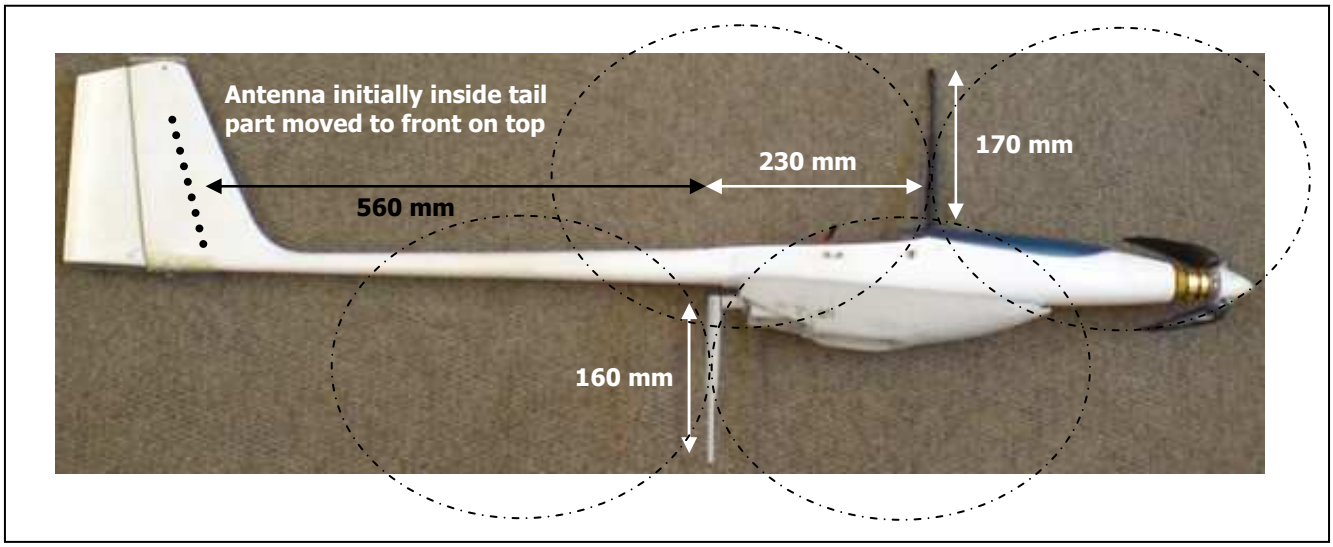

Figure 36: Aircraft side view for antenna placement

The 1.2 GHz video RF link was also tested, but the data link interfered with the video image, even after the antennas were placed over each other as shown in Figure 36. The video image experienced too much distortion, which meant that unfortunately only the 2.4 GHz could be used. The next step was to perform the actual test flights with this configuration, to verify the operational range while ensuring satisfactory video images and data link quality.

4.2.3 Installation verification

After the communications between the aircraft and GCS had been tested, the operation of the installed components inside the aircraft had to be verified. It would be easy to assume that the installation by Micropilot would be correct, but their operation was also verified after making a few changes. The modifications that required confirmation that they would not adversely influence the rest of the system were:

- Wireless RS232 serial link (Figure 31).
- Battery connections (Figure 13).
- Payload connections (Figure 25).

The wings were attached and the batteries, GPS antenna and pilot tube were connected to the aircraft in a ready-for-a-flight configuration. The aircraft was placed

on the ground outside the building in order to obtain GPS signals. The GCS and aircraft were switched on. The offset positions and movement of all the control surfaces on the aircraft were set and tested as described in the autopilot manual [37], Chapter 4, p26.

After switching the aircraft on, the autopilot went through an initialisation phase to check all its sensors. It then waited for GPS lock. If it is not a cold start for the GPS lock, it normally takes about 45 seconds for the GPS to lock on to the satellites. A cold start is when the GPS module gets power for the first time or if it moved more than 500 km from the last shut down. The autopilot has a backup battery for the GPS module to store the last GPS information when powered down. This ensures that the GPS gets a lock-on much quicker. After a cold start, the time required for the GPS to get a lock-on can take anything from 5 minutes to 15 minutes.

After the system verifies a GPS lock-on, the control surfaces of the aircraft will react to any change of position. This is an indication that the aircraft is ready to fly. For example, when the aircraft is rolled from side to side, the ailerons respond to try and bring the aircraft into the correct flight position. The same applies for the rudder and elevator movement. This method is applied every time before a flight to verify that the control surfaces are operating correctly. If no GPS lock was received, the autopilot will not allow the aircraft to be able to fly.

Payload and motor connections were done by visual inspection. The camera image should be displayed on the screen if all connections have been done correctly. Switching between cameras from the GCS should display a change in image seen on the display unit. The camera movements can also be verified by moving the slider buttons on the GCS Horizon software.

The motor functionality can be tested by giving the take-off command while holding the aircraft in the air and staying clear of the propeller. The propeller will spin at maximum revolutions. Care must be taken when selecting full power as the aircraft could easily be pulled out of the person's grasp.

If all these checks were successful, the aircraft was considered to be ready to fly.

4.2.4 Payload tests

Before flight tests were performed on the payloads, static laboratory tests were carried out to verify that it met the design criteria. Each payload was verified that:

- Cameras and video transmitter operate within the voltage range of 10.0 V to 12.6 V.
- Cameras produce a pure image without any interference when connected to the aircraft.
- Correct focus is set for a distance of 100 m and greater.
- GCS switching operates correctly between the cameras (day pods only).
- GCS control of pan and tilt operation of the cameras is correct (pan & tilt payloads only).
- Wireless links operate over a LOS distance of 10 km.

The cameras were connected to the laboratory power supply with the voltage set to 12.6 V. This is equivalent to the voltage of the fully charged battery pack when no load is connected. The camera image was displayed on the SONY GV-D1000 video walkman. The supply voltage on the bench power supply was gradually reduced to 10 V. The camera image was observed to remain the same over this voltage range.

After verification that the cameras can operate within the supplied voltage range, the next step was to ensure that the video transmitter showed the same properties. A similar setup was used as with the camera voltage tests. For this test, the direct wire connection between the camera and the video display was replaced with the wireless transmitter and receiver combination. The test results indicated that the cameras and video transmitter are able to perform satisfactory within the same voltage range.

The Horizon software has the capability to add, configure and control different payloads. Up to 24 servo controls can be connected to the autopilot and controlled by the GCS software ([37], p14). Horizon was configured to drive one of these servo outputs with a button, in order to switch between the two cameras. The first payload was connected to the aircraft and tested. When the button was pressed, the camera image switched. Screenshots of the Horizon software interface are given in Appendix C.

The second payload is able to pan and switch between the cameras. The same camera switch was used as for the first payload. A slider icon, for panning the camera, was added on the Horizon software. See Figure 62.

The third payload is able to pan, tilt and switch between the cameras and was tested in the same manner. Horizon was configured to pan and tilt the cameras with two separate slider icons and the same camera switch button. The results showed that the cameras can be controlled with the Horizon software. Figure 62 shows the Horizon user interface configuration.

4.3 Field tests

4.3.1 Overview

The field tests were conducted at a hobby airfield 1460 m above sea level (according to Google Earth) with enough space to perform flights of more than 1 km. Range testing was done away from built-up areas where 10 km flights could be conducted safely. The test data in this document was performed in the early summer time around Pretoria (September – October 2009). Two separate battery packs were used during the tests so that one could be charged while the other one is in use. One of the tests that were performed near Port Elizabeth is used to indicate how the aircraft performs in rough windy conditions at sea level.

4.3.2 UAV benchmark

After the MP-Vision UAV was purchased, a test flight was conducted to evaluate the aircraft performance before any alterations were carried out. Visual observations indicated that the aircraft was sufficiently stable in flight to warrant further modifications. The data link, however, was only satisfactory over a range of 2 km and less. During the landing the rudder of the aircraft broke with minor damage. After repairing the rudder, a modification was added to protect the rudder for future landings. Figure 37 shows the protective steel wire that was glued onto the fuselage.

The steel wire will take the impact during the landing in order to protect the rudder from any damage. This modification proved to be a successful solution. After many flights, the rudder did not get damaged again.

Figure 37: Modification to aircraft rudder for adding protection

After implementing all the necessary modifications to the aircraft, a benchmark was established by evaluating the system without any payloads attached. During the test flight, the following performance characteristics were assessed:

1. Take-off (with fully charged batteries).
2. Flight stability.
3. Flight height above ground level.
4. Flight endurance.
5. Recovery (landing).

All the necessary preparations were carried out before the first test flight was conducted. The preparations included all the post-installation and pre-flight checks documented in the user manual, ([37], p33-41).

The aircraft can be programmed to fly specific GPS coordinates or relative waypoints from the launch point. The relative waypoints are the North and East distances in meters from the take-off point. The flight plan used for testing the flight endurance of the aircraft was written as follows.

1. Take off (marked X in Figure 38).
2. Climb to an altitude of 300 m from ground level.
3. Fly to the point 1000 m north and 1000 m west of the launch point (Waypoint 1).

4. Fly to the point 1000 m north and 1000 m east of the launch point (Waypoint 3) on a straight path.
5. Fly to the point 1000 m south and 1000 m west of the launch point (Waypoint 4).
6. Fly to the point 500 m north and 1000 m west of the launch point (Waypoint 1) on a straight path.
7. Fly to the point 500 m south and 1000 m east of the launch point (Waypoint 2).
8. Continue to fly the waypoints (4 to 7).

Figure 38 shows the flight trial of the aircraft after it has flown the 4 waypoints several times. The take-off point is marked with "X". This is also the point where the aircraft landed.

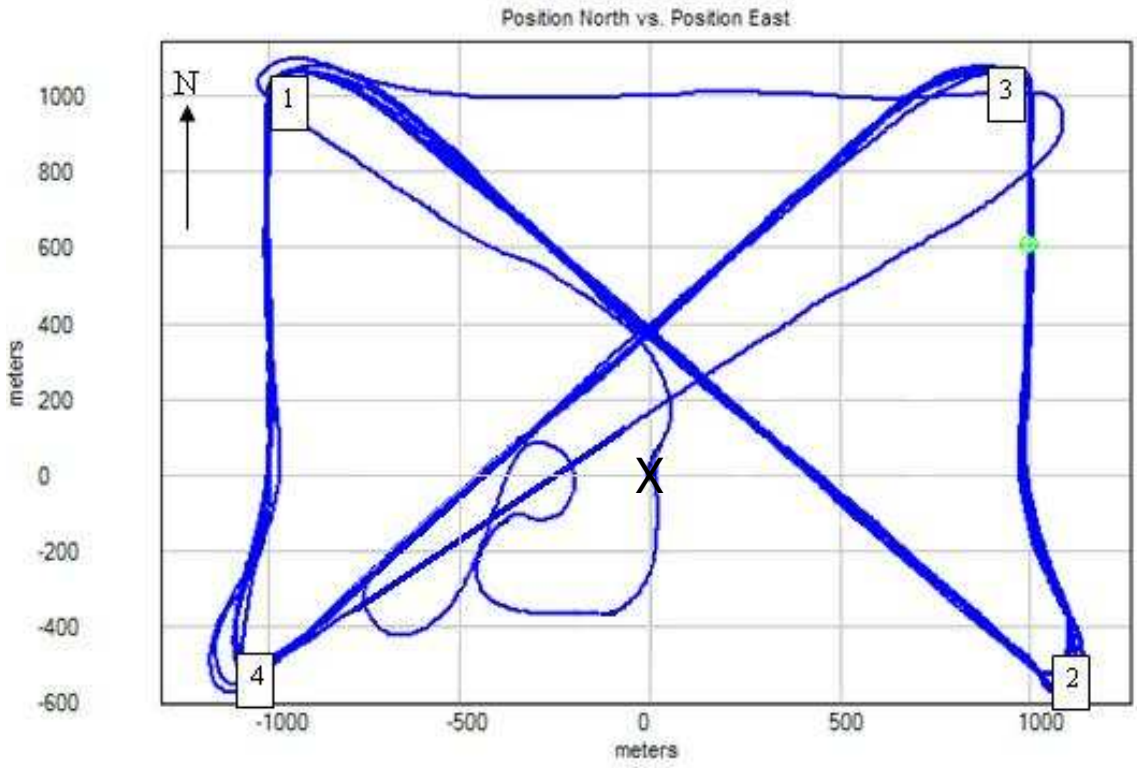

Figure 38: Flight plan for endurance tests

The battery voltage on the Horizon software (see Figure 41) was monitored continuously during the flight. It is important to know at what voltage the batteries are no longer able to supply sufficient power to drive the various on-board components.

The batteries supplied by Micropilot were not available locally and alternative replacement batteries were sourced to fit into the aircraft.

The batteries supplied by Micropilot consist of four 2100 mAh three cell Li-Po batteries and are shown in Figure 50. Each battery capacity is 2100 mAh, giving a total battery capacity of 8400 mAh with a total weight of 581 g. The replacement battery pack consists of four 2200 mAh batteries and weighs 660 g. Although this battery pack weighs 79 g more in total, it also has 400 mAh more capacity. A counter balance weight of 38 g was added on the rear end of the aircraft to compensate for the heavier batteries in the nose. See Figure 40. This was done to keep the centre of gravity the same.

The minimum operating voltage can be determined by the discharge characteristics of a Li-Po battery. Figure 11 is used to predict this minimum battery voltage and it was found to be approximately 10.6 V. At this voltage the batteries should still have sufficient power left to land the aircraft safely. Between the battery and autopilot is a diode to protect the autopilot from reverse voltage polarity. This means that the actual battery voltage is 0.7 V higher than measured by the autopilot and shown by the GCS display. The GCS software was set to give a low battery warning when the autopilot measured battery voltage reaches 9.9 V.

During the endurance test flights, the land command was executed as soon as the battery warning came on. After the aircraft landed, the log file was downloaded and analysed. The batteries were taken out of the aircraft and discharged at 1 C (8800 mA) to a cut-off voltage of 9 V (3 V per cell). The remaining battery capacity was recorded to calculate the percentage of battery capacity left after the flight.

Before launching the aircraft, the prevailing weather conditions were recorded. The aircraft was hand launched by holding it in the air with one hand while running and throwing it; almost like throwing a spear. The picture in Figure 39 [18] gives an indication of how this is done.

Figure 39: Launching the aircraft

After the test flight, the aircraft landed close (30 m) to the take-off point. Aeronautical engineers were tasked to assist with the first test flights. They verified that the aircraft performance appeared to be stable and satisfactory. Figure 40 is a photograph of the aircraft that was used for the benchmark tests.

Figure 40: UAV used for benchmark flight tests

The tests were performed during the morning hours. The total weight of the aircraft was 2.845 kg with the counter balance weight. A wind of 16 km/h was measured at the time the aircraft was launched. The aircraft was airborne for 58 minutes when the battery warning came on, after which the landing command was activated. The aircraft overshot the landing point by about 500 m due to landing downwind. After the flight, the batteries were discharged to 9.0 V at a rate of 1 C. The remaining

battery capacity was 350 mAh, which was 4 % of the total capacity. These measurements confirmed that the aircraft should be positioned close to the landing point by the time the low battery warning is anticipated.

The aircraft was stable in flight and navigated accurately during the entire flight. A screen capture of the GCS software was recorded to verify the accuracy of the navigation system. This is shown in Figure 41. A flight trail is provided to indicate where the aircraft had flown. It is clear from the straight flight trail that the aircraft navigated very accurately between the two northern waypoints. Although it is not shown in this figure, the navigation between the other waypoints was just as accurate for the total duration of the flight.

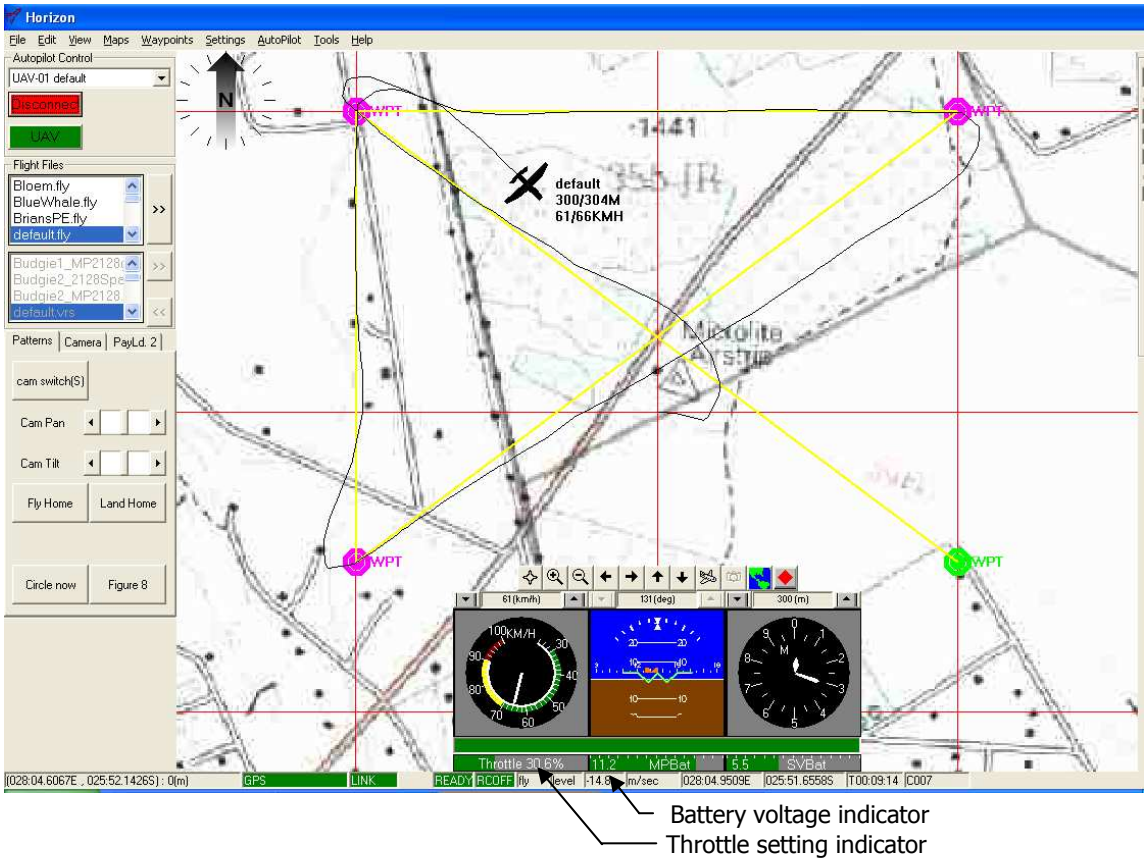

Figure 41: Screen capture of GCS software during benchmark flight tests

Analysing the flight log data indicated that the aircraft also maintained altitude and airspeed. The aircraft never went more than 5 % below the desired altitude, but went as high as 20 % above, due to the thermal updrafts. The highest airspeed was 35 % above the desired 61 km/h and the lowest was measured to be 18 % below.

This is still within the safe flying speeds. According to Micropilot, the stall speed of the aircraft is around 28 km/h. The aircraft should always fly faster than this for it not to loose control in flight.

The requirements are that the aircraft should be airborne for at least 60 minutes, with a full payload. This endurance test was done without the payload, which implies that the aircraft would be unlikely to meet the 60 minutes requirement. From the outcome of these tests a benchmark was set of the UAV performance with no payload. At this stage, the major performance deficiencies, discussed in paragraph 2.2.2, were identified as the short endurance time and robustness on landings.

4.3.3 Aircraft recovery enhancements

After the benchmark had been set for the aircraft, the inaccuracy of the landing position was investigated. Further test flights were conducted to analyse the problem and to find a possible solution. The autopilot controls the aircraft to descend to a pre-set circuit altitude and then to follow the set flight path as shown in Figure 42.

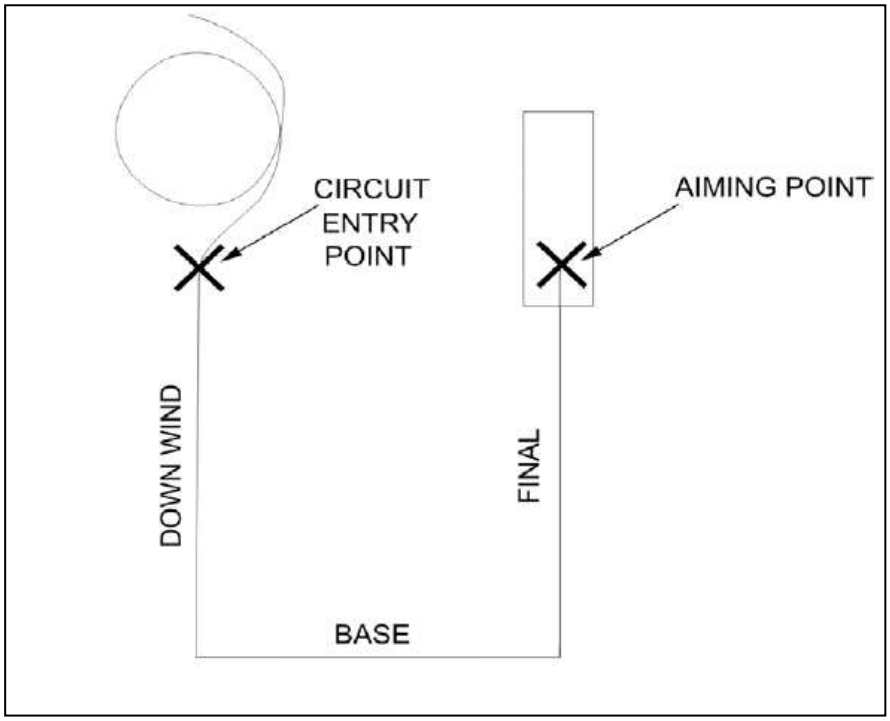

Figure 42: Micropilot landing circuit ([37], p83)

During the final leg of the landing circuit, the autopilot controls the aircraft to follow a set glide path. This glide path is determined by the circuit altitude above ground

level and final leg length, as shown in Figure 43. These parameters are programmed during the setup of the aircraft. When the aircraft is below the glide path, more power is automatically applied to regain the desired glide path. When the aircraft is above the glide path, the autopilot reduces the aircraft's power to descend at a greater vertical rate, while maintaining the desired airspeed.

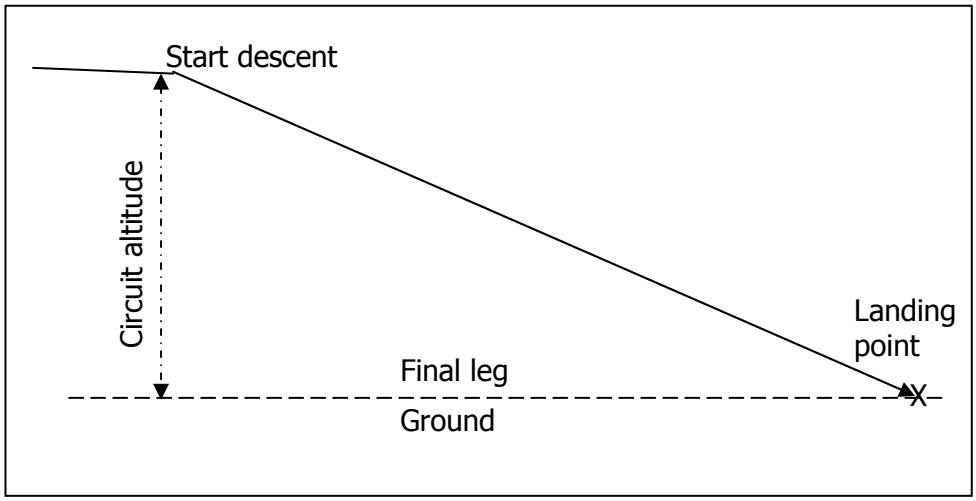

Figure 43: Landing circuit final leg

Different test flights indicated that the aircraft's landing point varies according to the wind conditions. Strong winds greater that 20 km/h caused the aircraft to land short of the landing point. Distances of up to 100 m were recorded during the test flights. No wind or light winds from behind caused the aircraft to overshoot the landing point. Ideally, the aircraft should land at a point as close as possible to the launch position. The landing glide path must also be as steep as possible in order to avoid surrounding high obstacles, for example trees. This implies that the landing circuit must have a short as possible final leg with a high as possible circuit altitude.

The autopilot flight parameters which have an influence on the landing accuracy are (Figure 63 shows a screen shot of the Horizon software where these can be set):

- Circuit altitude.
- Circuit final leg length.
- Circuit base leg length.
- Aim point offset.

- Approach throttle setting.
- Approach speed.
- Waypoint diameter (setting of how close to a waypoint the aircraft must pass to be valid).
- Reduce speed altitude (setting the altitude where the aircraft must start to reduce speed during the landing).
- Final reduce speed (set the speed the aircraft reduces by from the reduce speed altitude to ground.).
- Landing flap deflection.

While the aircraft is operational, it records various flight parameters onto non-volatile memory (flight log) that can be downloaded after the flight. Micropilot also provides a flight log viewer with the software that can be used to analyse the recorded data from each flight. The desired altitude is compared to the actual measured altitude that indicates how the aircraft maintained the glide path on the final leg. The actual height is measured by a static air density pressure sensor. Different flight parameters were tested. However the landing was still not accurate every time, but did improve. The flight parameters that were changed, as well as the results in landing accuracy are listed in Table 20. The parameters that were changed are highlighted in **bold**.

Table 20: Summary of flight tests performed to better the landings

CCT ALT	CCT FINAL LENGHT	APPROACH THROTTLE	LANDING FLAPS DEFLECTION	WAYPOINT DIAMETER	WIND SPEED[33]	AIMPOINT MISSED[34]	Follow glide slope	Appendix D Figure
60 m	**300 m**	30 %	65 %	14 m	+ 14 km/h	- 110 m[35]	Under	Figure 72
60 m	**400 m**	30 %	65 %	14 m	+ 15 km/h	- 100 m	Under	Figure 73
60 m	**200 m**	30 %	65 %	14 m	+ 10 km/h	+ 100 m	Above	Figure 74
60 m	200 m	**50 %**	**85 %**	14 m	+ 5 km/h	+ 60 m	Above	Figure 75
60 m	200 m	50 %	**100 %**	14 m	+ 2 km/h	+ 80 m	Above	Figure 76
60 m	200 m	**30 %**	100 %	14 m	+ 5 km/h	+ 18 m[36]	Under / Above	Figure 77
90 m	**300 m**	30 %	100 %	14 m	+ 8 km/h	+ 30 m	Under / Above	Figure 78
60 m	300 m	30 %	100 %	**5 m**	+ 5 km/h	+ 130 m	Under / Above	Figure 79
60 m	**200 m**	30 %	100 %	5 m	+ 5 km/h	+ 15 m	Under / Above	Figure 80

[33] + indicates a head wind, - indicates a tail wind
[34] + indicates that the aim point was overshot, - indicates that the aircraft landed short
[35] Average of 5 flights (-50 m (See Figure 72), + 60m, -550 m, -20 m, +10 m)
[36] Average of 4 flights (+20 m, +30 m, +15 m, +8 m)

The aircraft landed about 100 m short in the first test. Analysis of the altitude data indicated that the engine power was reduced to 0 % when the aircraft reached an altitude of 15 m above ground level during the landing. Micropilot pointed out that the autopilot is hard coded and cannot be changed in software to stop the propeller from spinning at this altitude, as a safety precaution. However, it is possible to change certain parameters when the UAV is more than 15 m above the ground, to improve the landing position accuracy.

For the second test, the final leg was lengthened from 300 m to 400 m to make the glide path less steep. This did not improve the landing accuracy and the aircraft landed short again. The final leg was then reduced to 200 m, which caused the aircraft to overshoot the landing point. The altitude, speed and throttle data of these three flights were analysed.

It became apparent that when the aircraft is below the glide slope, it does not apply enough power to regain altitude. Hence, the approach throttle setting was changed from 30 % to 50 %. During the next test the head wind was less and the aircraft overshot the landing. It was not certain if the overshoot was caused by the lower approach headwind or the increase in approach throttle setting. The assumption was that it was caused by the change in wind. This assumption was confirmed with the flight tests that followed.

Table 20 also indicates the tests and the parameters that were changed in sequence. The results of how the aircraft followed the glide path and how far it landed from the launch point are also shown. These tests were unable to achieve the desired landing within the required limits, but they did result in getting a closer position than the first tests.

Another solution had to be found in order to prevent the aircraft from overshooting the landing point. The aircraft is a glider and, with the available control surfaces, it cannot descend rapidly enough without exceeding the maximum permissible airspeed. One way would be to reduce the glide slope by increasing the final leg. This would imply that a large flat terrain with no high surrounding obstacles would be needed to recover the aircraft. A minimum glide slope ratio of 5:1 was specified as sufficient. This would enable the aircraft to land in areas surrounded by 10 m high obstacles within a 50 m radius from the landing point. A glide slope of 5:1 means that for every 5 m of forward

travel, the aircraft must be able to descend at least 1 m. A 60 m circuit altitude with a 300m final leg complies with this glide slope ratio.

In order to achieve this, a spoiler was designed and placed on the wing to assist the aircraft in following the required glide slope angle. Figure 44 shows the spoiler in the deployed position. The spoiler system consists of a 575 x 30 x 1.6 mm aluminium plate and a servo with control arm. The spoiler position is set by a servo control that will pull or push the aluminium plate upwards or downwards.

When the spoiler is in the upright position, it increases the drag allowing the aircraft to descend at a higher rate without exceeding the max airspeed. The disadvantage of this solution is that it adds another 69 g to the total mass of the aircraft. Adding extra weight can increase the stall speed and cause the aircraft to land harder due to the extra kinetic energy.

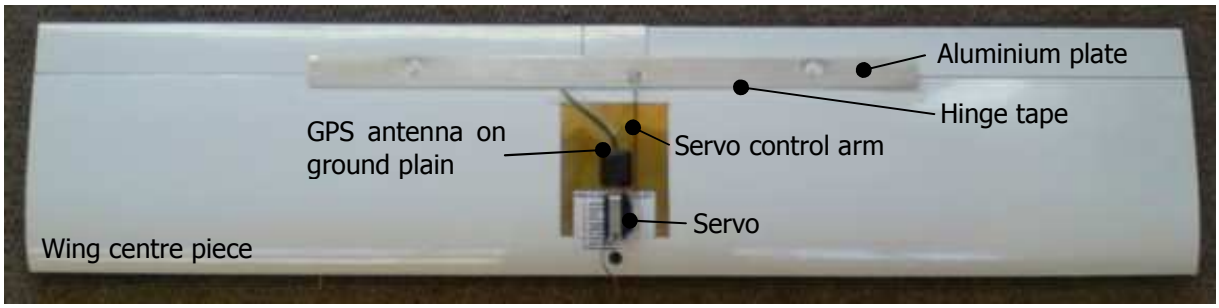

Figure 44: Wing centre piece with spoiler attached

The MP2128g autopilot supplied with the UAV has the capability of controlling the servos according to pre-defined parameters which is set up in a table. Figure 64 in Appendix C shows how the table, that is used to control the spoiler function, is defined. This table will only allow activation of the spoiler during the approach phase of the landing sequence.

Figure 71 in Appendix D taken from the flight log data, shows how the spoiler deflects as a result of any deviation from the desired glide path. As soon as the autopilot detects that the aircraft is above the glide path, the spoiler is pulled upwards. The amount that the spoiler is pulled up is determined by the height difference between the aircraft altitude and glide path altitude. Flight tests verified that the aircraft follows the glide path much more accurately when using the spoiler.

Other factors that have a direct effect on the navigational accuracy during landing are the GPS positioning and air pressure. The aircraft relies on the GPS for horizontal navigation, which is on average[37] only accurate within 15 m. This can add up to a total of 30 m difference between the launch and landing point. For vertical height measurement, only the static air pressure sensor is used. The air pressure can change while the aircraft is in flight, which leads to inaccurate height measurements by the static pressure sensor. For every meter that the aircraft measures the altitude from the ground incorrectly, the aircraft can miss the landing point by 5 m, due to the glide ratio during the landing.

During the landing, the height must be accurate within a few meters when the aircraft is close to the ground. An acoustic sensor that can be used for measuring altitude more accurately close to the ground is made available from Micropilot. Micropilot specifies that the sensor needs to be placed underneath the wing, which implies a negative influence on the wing's aerodynamic probabilities. The sensor electronics does not fit in the aircraft and also adds another 61 g to the total mass of the aircraft. It was decided not to implement this sensor, but the option to evaluate it at a later stage will be considered.

4.3.4 Flight stability tests

A flight endurance test was done after adding the spoiler to the aircraft. The flight data was analysed for verification of the flight performance. Flight performance tests included the verification of the preset parameter accuracy and the ability of the aircraft to correctly navigate to way points. The autopilot controls the aircraft's performance by controlling the following:

- Airspeed; by measuring the dynamic air pressure from the pitot tube and adjusting the elevator control surface.
- Altitude; by measuring the static air pressure inside the aircraft and adjusting the throttle settings.
- Roll; by adjusting the aileron position.
- Pitch; by making changes to the elevator control surface.

[37] GPS information found at http://www.garmin.co.za/gps_explained.php on 1 October 2009

- Yaw; by making changes to the rudder control surface.

The Micropilot autopilot controls the aircraft by means of proportional, integral, and differential (PID) feedback loops [37]. Each of the P, I and D terms are user adjustable to configure the autopilot correctly for the aircraft being used. With the first prototype, all these control loops had to be configured correctly to ensure aircraft stability. Setting these feedback loop gains are explained in detail in the Micropilot's autopilot manual [37] and therefore will not be discussed here. This could not be configured accurately enough and was one of the reasons why the first prototype could not fly reliably. The UAV from Micropilot had these control loops already correctly set up and configured.

The aircraft control stability can be verified by observing how the aircraft flies straight and levels, turns and climbs. The flight log of the aircraft was then also analysed to verify that the aircraft maintains airspeed, altitude, pitch, roll and yaw. The data analysis for pitch, roll and yaw shown in Appendix D.3, verifies that the autopilot was able to control the aircraft within acceptable limits.

Flight stability also includes the aircraft's ability to navigate pre-programmed waypoints. The waypoints are plotted on the map in the Horizon software. The aircraft plots a flight trail that can be used to verify the navigation accuracy to a given waypoint. The aircraft can be programmed to follow a straight path between two waypoints. After reaching a waypoint, this will cause the aircraft to turn onto and follow the line between the waypoint it just passed, and the next one.

The aircraft can also be programmed to fly between waypoints without following a straight path. After reaching a waypoint, the aircraft will fly to the next waypoint without turning onto the line between the two waypoints. This was verified by loading waypoints into the on board computer and capturing the flight path on the Horizon software, as shown in Figure 66.

The endurance and flight stability tests were performed during the afternoon with a steady surface wind speed of between 8 km/h and 10 km/h. The ambient temperature on the ground was 32 ºC. Aircraft flight time was 60 minutes, before the battery

warning came on. After the landing, the battery capacity was measured to be 415 mAh or 5 % of the total remaining capacity.

The average throttle usage for the entire duration of the flight was calculated from the log data to be 31 %. Appendix D.1 shows the graphs of how the aircraft maintained speed and altitude. In Figure 67 it is noticed that the altitude varied by 55 m above the desired altitude from time to time. This was attributed to possible up-drafts which caused the aircraft altitude to increase faster than the autopilot could respond. The assumption of up-drafts is based on the fact that the throttle position was zero during these altitude increases. This is shown in Figure 69.

This test indicated that by adding the spoiler to the aircraft, the performance was not influenced much, if any. The flight duration and flight stability appear to be similar, but the landing accuracy is improved, in the sense that it landed much closer to the launch point.

The system was also tested near sea level at Port Elizabeth in strong and gusty wind conditions. The surface wind speed was measured above 30 km/h, with gusts of up to 45 km/h on that day. The launch was easy and the aircraft climbed almost vertically due to the high wind speed. Figure 83 in Appendix D shows how the aircraft maintained air speed. By taking the difference in GPS ground speed and aircraft airspeed, the wind speeds was calculated to be up to 60 km/h at an altitude of 150 m above the ground. From the graph it can be seen that the aircraft maintained its airspeed of 61 km/h within 19 km/h under these conditions.

On landing, the GPS ground speed was measured at approximately 5 km/h. This implied that the head wind was about 5 km/h slower that the aircraft's speed. The aircraft could not navigate properly with such a low ground speed and landed about 50 m short to the right of the landing point. During the flight, the airspeed was manually increased from 61 km/h to 74 km/h from the GCS, resulting in more accurate navigation.

The maximum allowed airspeed is set at 111 km/h by Micropilot. During all the time of flying the aircraft, there was never any need to fly at this speed and the accuracy of the setting will be confirmed in the near future.

4.3.5 Test flights with payloads

4.3.5.1 Introduction

All the endurance flight tests for the different payloads were performed on the same day. Weather conditions were cloudy, 90 % overcast, with temperatures varying from 22 ºC to 26 ºC. The wind was measured between 5 km/h and 20 km/h throughout the day, but overall calm at any given time. The density altitude fluctuated between 1400 m (measured 10am) and 1422 m (3pm). A Skywatch GEOS Nº11 hand-held weather station was used for measuring the weather conditions.

4.3.5.2 Stationary cameras payload

The cameras in the first payload were facing straight down. These flight tests were done with the very first aircraft (Figure 10). The image moved too fast to be used in real time. The principle of how to solve this problem was based on the following observations:

While driving a car and looking out the side window straight at the passing bushes or buildings, one struggles to get a fix on the picture. But if one looks out the same window with one's eyes focused more in the direction in which the car is travelling, the image becomes clearer. The solution with the cameras was to tilt them slightly (35 degrees) forward. This proved to be a perfectly practical solution to the problem.

Another problem found with the camera image on the first aircraft was the electric interference from the DC motor on the video image. This was due to the wiring of the power distribution on the aircraft. Figure 45 shows a snapshot of an image taken with engine noise. The wiring was corrected and the image was cleared of noise

interference. The solution was to move the wires, supplying the cameras with power, away from the speed controller to be connected directly at the battery terminals.

Figure 45: Arial footage with engine noise

The two cameras were fitted with a 4 mm and a 16 mm lens to give the wide and narrow fields of view required. Figure 46 shows snapshots taken from the recorded live video of how the aerial image appears with the 4 mm and the 16 mm lenses. Notice how the picture zooms in when switching between the cameras. These images were taken with the aircraft flying at 300 m above ground level. The first aircraft had a text overlay that was used to indicate GPS position, heading, ground speed, airspeed and altitude on the video. This can be seen in Figure 46. It is not yet implemented on the payloads used with Micropilot's UAV, but is being considered for implementation.

The image quality of the cameras and video transmitter combination was considered as satisfactory for use in aerial reconnaissance. It was decided to adopt this solution initially, but to build other payloads that can pan and tilt the cameras.

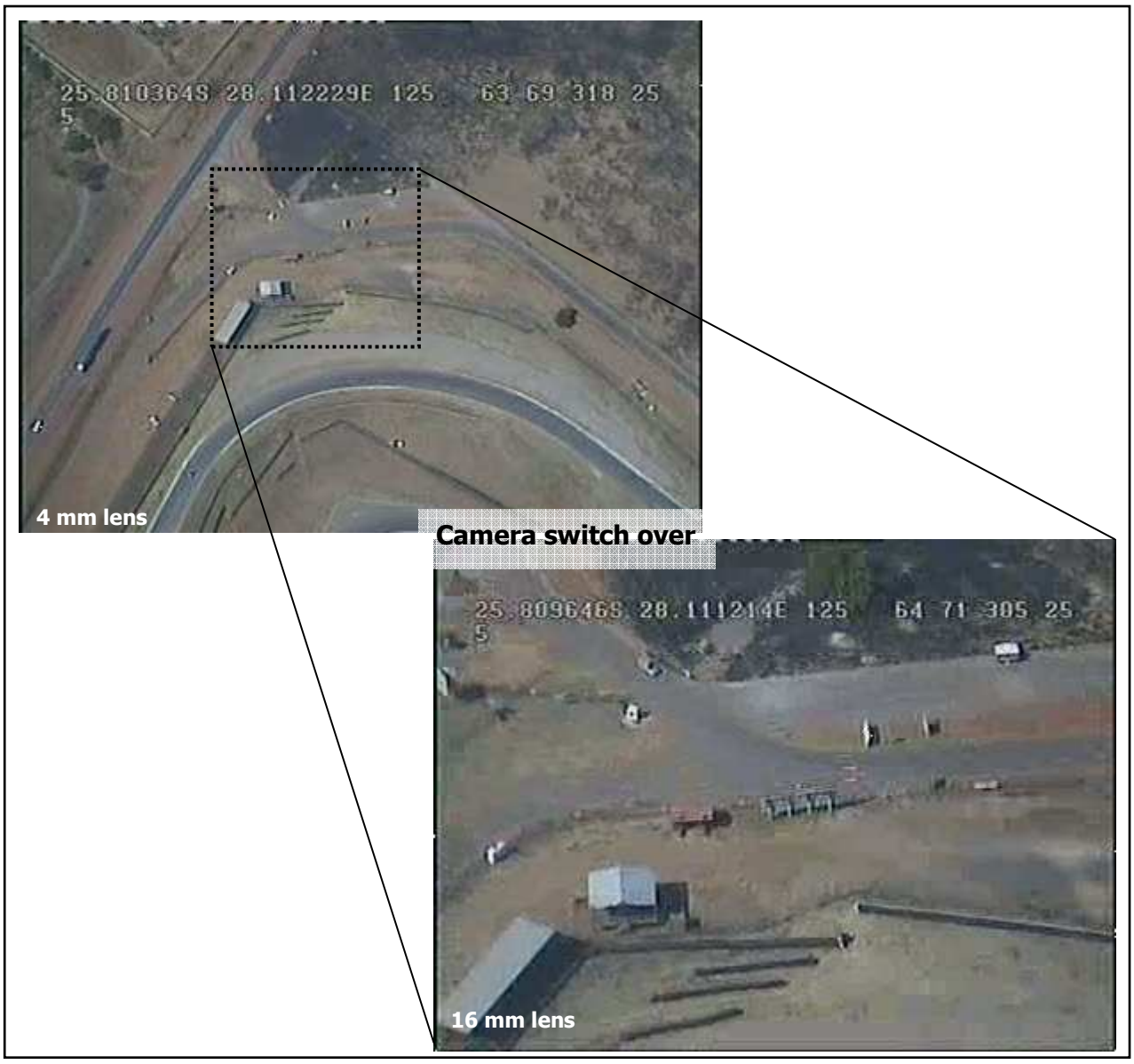

Figure 46: Aerial pictures of stationary cameras payload

The wider view lens gives a much more stable image than the narrow view one and is useful for producing a better image of what is below the aircraft. The camera switch over is rapid and the narrow field of view camera was positioned such that it zooms to the centre of the wide view. This makes it relatively easy to zoom into a specific area. The cameras underneath the aircraft are open and gather a lot of dust during the landings. The lenses must be wiped clean each time before a new flight.

The effect of adding the payload on the aircraft's performance was also tested. The payload was attached underneath the aircraft and switched on. The same flight test as the first endurance test was performed. The aircraft was airborne for 44 minutes

before the battery warning came on. This test was performed in the early afternoon. The ambient temperature was 23 ºC with a wind of between 10 km/h to 13 km/h during take-off and landing. Table 21 summarises the outcome of the endurance flight test for the day payload with stationary cameras. The time to climb to the flight altitude of 300 m was also recorded. This will be compared with the other payloads to give an indication of the size and weight effect on the aircraft's ability to climb.

Table 21: Summary of flight log data on payload with fixed day cameras

Payload dimensions (mm)	Payload mass (g)	Average Throttle (%)	Flight time (min)	Time to climb to 300 m (sec)
330 x 70 x 55	260	38.43	44	53

4.3.5.3 Panning cameras payload

There are a few differences between the panning and stationary cameras' payloads. The panning camera payload has a low light camera as the second camera and weighs 40 g more and is a bit bigger than the stationary camera. The performance of the aircraft with this payload would be expected to be a bit less than the results from the tests conducted with the lighter payload.

An endurance test flight was performed with this payload on the same day as the other payloads. This test was performed just over an hour after the first test flight. This time the wind was 7 km/h and the temperature 25 ºC. The aircraft was airborne for 38 minutes before the battery warning was displayed.

During the flight, the cameras were moved to the left and right by means of the slider icon on the Horizon software. The panning function of this payload was verified to be very effective. Especially when the aircraft was turning, the cameras could be adjusted to face downwards, instead of facing at an angle to the horizon. Figure 45

shows what this looks like when the aircraft is turning. Table 22 gives a summary of the flight endurance test with the panning camera payload.

Table 22: Summary of endurance flight tests with panning camera payload

Payload dimensions (mm)	Payload mass (g)	Average Throttle (%)	Flight time (min)	Time to climb to 300 m (sec)
340 x 80 x 75	300	41.64	38	58

4.3.5.4 Pan-tilt cameras payload

The pan-tilt camera payload is the same size and shape as the panning camera payload and weighs only 10g more. The endurance test was not repeated for this payload as it is very similar. Figure 47 shows an image of a farm house that was captured from the day camera with the 4 mm lens of the pan-tilt camera payload.

Figure 47: Image captured from pan-tilt camera footage early morning

The pan and tilt function makes the payload a lot more useful by allowing the user to scan the area under observation more easily. The slider icon on the Horizon software was found to be a bit difficult and slow to use when rapid camera movements are

required. A game pad (joystick) was added to the GCS computer for controlling the camera movements in flight via the Horizon software. This was tested and found to be much easier to operate than the slider icons.

4.3.5.5 FLIR camera payload

For the night pod, the same endurance test was performed to determine the flight time with a fully charged battery pack. The total flight time was 34 minutes before the battery warning was displayed. The wind speed was measured at 12 km/h during take-off and an ambient temperature of 22 ºC. Figure 48 shows an image of the aerial footage taken during another flight at night time with no moon and no clouds, while the aircraft was flying 90 m above ground. This was out of town on a farm with no ambient light. The heat signatures of a building and people can clearly be seen on this image.

This camera only provides for a fixed lens and is too big, heavy and expensive to add a second one with a different lens. The zoom function with this camera can only be controlled by changing the flight height of the aircraft above the area of observation.

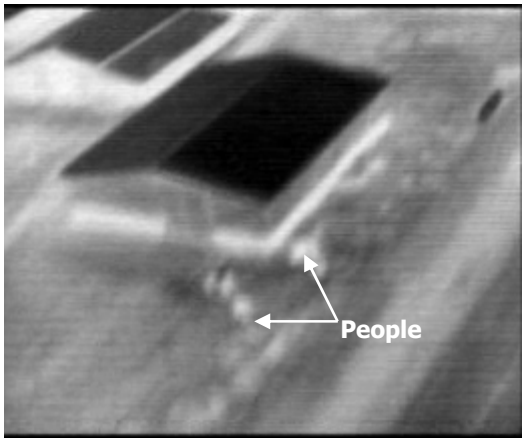

Figure 48: Image of the FLIR camera on a farm flying 90 m above ground

When the aircraft returned, the LED lights on the payload were switched on and the aircraft was clearly visible during the landing. This trial showed that night flying was

feasible and that the thermal imaging camera can produce images that can be used to identify objects.

4.3.5.6 Launch tests

The hand-launched take-off worked very well until the payloads were added. Sometimes the aircraft would not enter into a climb mode after release from the launching hand. Initially, the aircraft descended, almost touching the ground, before starting to gain height. Some changes were implemented by means of trial and error before the main influencing factor, centre of gravity shift, was identified.

The payloads were not always attached at exactly the same position on the aircraft and therefore the centre of gravity (CG) was different each time. According to Micropilot, the CG of the aircraft must be as close as possible to 75 mm aft of the leading edge of the wing. The correct positioning of the payloads was made possible by making use of a hand-made CG jig, as shown in Figure 49. The aircraft is balanced on its wings while measuring the distance from the leading edge of the wing to the balancing point.

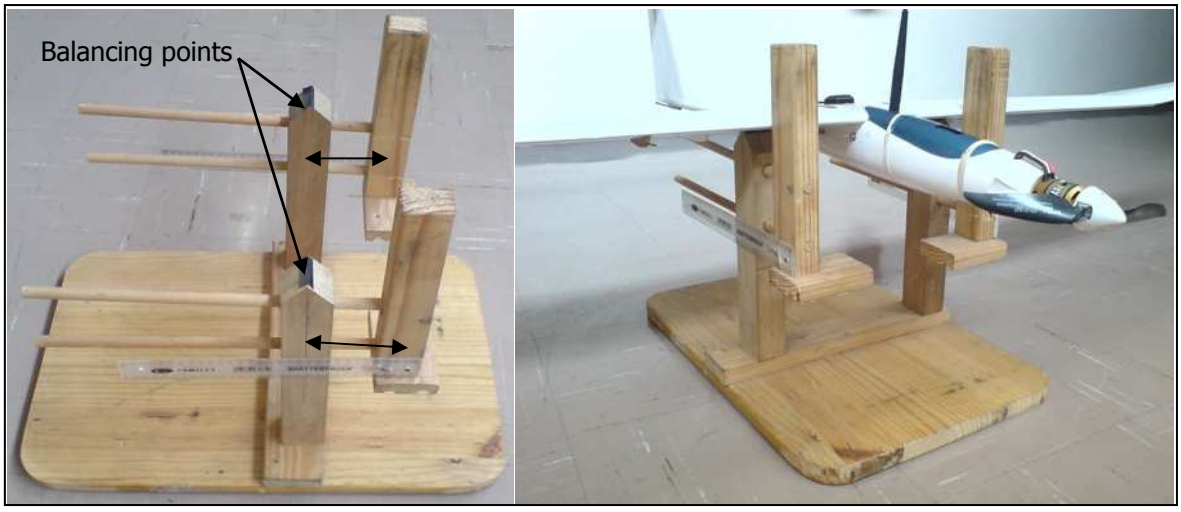

Figure 49: Centre of Gravity (CG) measuring jig

The other important aspects that were required for implementation, to make the launch easier, were:

- Launch only with fully charge batteries.
- The aircraft control surfaces must be set up correctly.
- Always launch into the wind.
- The person that launches the aircraft must be properly trained.
- Make sure that the propeller is not damaged.

These simple precautions should ensure an event free launch every time.

4.3.5.7 Range tests

The range tests were performed at a location where flights can be performed safely within a distance of 15 km from the launch position and line of sight could be maintained during the total flight. As a precaution, the autopilot was programmed to return to the GCS when it looses data link. The aircraft was loaded with fully charged batteries and the day pod with the stationary cameras. The data link indicator on the Horizon software indicated a good link during the total duration of the flight.

The aircraft was fully controllable and a clear video image was captured for the entire duration of the flight. This verified that the aircraft is able to produce quality images when flying a distance of 10 km LOS from the GCS under user control.

4.3.5.8 Operational usage

The aircraft had been used successfully in operations with the client on different occasions. The system was utilised in different locations within South Africa which differ a lot from the hobby airfield where most of the tests were conducted. During the operational usage new knowledge was gained on how to plan and operate the system.

A flat terrain of more or less 50 m x 100 m must be identified within a 10 km radius from the target, that can be used to launch and recover the aircraft. This area can be covered with grass or small bushes not higher than 500 mm, but no trees or hard obstacles. This terrain should preferably not be surrounded by high obstacles.

The wind speed and wind direction must be taken into account especially when flying more than 1 km from the CGS. For example, should a wind of 20 km/h blow towards the target area, the aircraft will fly downwind towards it, which implies a greater ground speed. This will cause the aircraft to reach the target much quicker than when flying back against the wind with a lower ground speed. Enough time on the battery power should be allowed to bring the aircraft back safely.

When flying in mountainous areas, the flight plan must be such that the aircraft flies around or over the high grounds. When the aircraft is behind a mountain, LOS is no longer obtained and this will negatively influence the communications link to the GCS. This can be overcome by flying higher or programming the flight plan so that the aircraft continues the flight path even if the communications link is lost or poor.

4.4 Summary

For all the flight tests with the different payloads, the take-off and landings were successful and satisfactory. The aircraft climbed steadily to the desired altitude after each launch and appeared to be very stable throughout each flight. Each time the aircraft landed within a 50 m radius from the launch position. The video image was also of good quality. Buildings, vehicles and humans can be identified, but not vehicle number plates and human faces.

Unfortunately, the flight endurance with the payloads did not meet the 60 minutes requirement. But it is proven that the COTS MP-Vision aircraft with the modifications can be used to carry the different camera payloads. The aircraft flies steadily enough to produce a stable image with minimal picture distortion. The test results also showed that the selected components can be integrated to develop a complete UAV system that can be used for LOS reconnaissance. The test results validated the modifications and showed that they were beneficial to the system in meeting most of the requirements.

Table 23 summarises the end results for the flight endurance tests of the aircraft with the different payloads and without.

Table 23: Summary of endurance flight tests with different payloads

Payload	Payload dimensions (mm)	Payload mass (g)	Average Throttle (%)	Flight time	Time to climb to 300 m altitude
None	N/A	N/A	31.18 %	60 min	45 sec
Day fixed	330 x 70 x 55	260	38.43 %	44 min	53 sec
Day Pan	340 x 80 x 75	300	41.64 %	38 min	58 sec
FLIR	300 x 90 x 50	309	46.09 %	34 min	57 sec

The next chapter summarises the research and development and highlights the requirements that were not met. It also gives recommendations for further development and improvements that can be made to the system in future.

The final autopilot settings for the aircraft, that was proven to ensure a good launch, stable flight and acceptable landing, are shown in Figure 63 in Appendix C.

5 SUMMARY AND RECOMMENDATIONS

5.1 Conclusion

When this project was started, the SANDF did not have any short range aerial reconnaissance capabilities. The CSIR was tasked to investigate the different options to overcome this shortcoming. Research on this topic was conducted where the different options were considered and presented to the SANDF.

A decision was made at the beginning of this development to design and develop a UAV system using off the shelf items. The development of such a system, rather than purchasing a ready-made commercial system, was shown to be a correct decision. Although the current solution does not meet all the requirements, it is still useful as a reconnaissance tool for most of the possible scenarios. The client applied the end result of this system successfully for several times, in spite of the limitations. This is concrete proof of the success of this development.

The benefits of this system are that it is easy and inexpensive to maintain due to the nature of the components used. Most of the aircraft components required for repairs and maintenance are available at hobby shops. Different payloads, within the weight limitations, can easily be added to the aircraft. The system was developed locally and therefore leaves a large scope for implementing improvements to the system.

The current status of this system is that it is easily portable, can be hand-launched from about any 50 m x 50 m relatively level terrain, can fly for 40 minutes and produce day and night aerial images at a distance of 10 km and more. The requirements that are not met at this stage are:

- Fly for at least 1 hour.
- Carried by foot in backpacks.
- Longest part must not exceed 600 mm in length.
- Facial and number plate recognition.

- Camera platform stabilisation.
- Encrypted data and video links.
- GPS information on video (first aircraft had this).
- Camera stays on target.
- Onboard video recording (first aircraft had this).
- Onboard RF beacon.
- Fly in the rain (IP55) and/or land in sea water (IP57).
- Recovery by net (5 m x 3 m) landing or on narrow road (50 m x 3 m).

The shortcomings do not make the system unusable. The most important requirements are met and therefore the system can be recommended for further operational use within its limitations. The upcoming world cup soccer in 2010 would be an ideal opportunity to use this system. The outstanding items on the specification list can be addressed in the future.

5.2 Recommendations for Future Development

As more experience with this UAV system is gained, many opportunities should present themselves where the user will be able to identify further practical applications. This includes implementing improved enhancements to the existing system. The first improvement should focus on achieving the full specifications which were originally stipulated.

The immediate recommended enhancements and improvements to be made to the existing UAV are:

- Increase the flight duration of the aircraft.
- Modify the fuselage to allow for shorter parts that can more easily be placed into a backpack.
- Different materials can be evaluated for making the airframe more rugged and durable.

- Methods of how to make the aircraft functionally waterproof for water landings and operating in the rain should be given high priority on the research and testing program. If the present airframe cannot be modified, a different airframe can be designed to meet this requirement.
- The aircraft's landing accuracy can be improved for recovery using a net, on a boat or a road that is surrounded by trees or high obstacles.
- A RF beacon can be installed in the aircraft that can assist in recovery when the data link fails.

Recommendations for improvements on the payloads can be the following:

- Develop a payload with a continuous zoom camera that can pan and tilt.
- The GPS data can be overlaid on the video image as with the first aircraft design.
- Stabilised camera payload platforms can be developed to provide a clearer image.
- An onboard video recorder can be installed so that video images can be recorded when the aircraft flies out of video reception range.
- The camera platform can be modified to allow the camera to remain focused on a stationary or moving target while the aircraft is manoeuvring.
- A low light camera can be added to the FLIR payload to provide low light video images during night time.

Encryption of the data and video links is a very important consideration. Present RF links are commercially available and anyone would be able to intercept signals or view the video image.

The option for using more than one aircraft can be considered to increase the observation duration of the system. While the first aircraft turns back to the landing point, another aircraft can be launched to continue with the mission.

The flight endurance can be enhanced by re-evaluating the antennas' placement on the aircraft. The option of using aerodynamically shaped antennas should also be considered.

The type of engine used can also be re-evaluated. Assess the possibility of petrol engines with low acoustic signatures. Measure the acoustic noise levels between a "low noise" petrol engine and the current electrical engine. Compare the flight endurance between a petrol and electrical engine.

Search for alternative methods to increase the accuracy of the landings. Assess the possibilities of adding sensors, i.e. Micropilot acoustic sensor. The flap deflection is currently not set to maximum. Test and evaluate the performance when using different flap settings during the landings.

For training purposes the user manual, which was written for the original aircraft, can be modified to be used with the existing model [28].

6 References

[1] Coffey, T., Montgomery, J.A.; The Emergence of Mini UAV's for Military Applications; Military Technology Magazine, Volume 28, number 7, 2004: pages 28-35, 37.

[2] Poppelmann, J.; UAV Programmes in Germany; Military Technology Magazine, Volume 31, number 10, 2007: pages 106-110.

[3] Anonymous; Unmanned Aerial capabilities and their future utility in NATO; Military Technology Magazine, Volume 31, number 10, 2007: pages 106-110.

[4] Sweetman, B.; Mini-UAV's – the next small thing; Jane's International Defence Review Magazine, June 2005: pages 58-63.

[5] Butterworth-Hayes, P., van Blydenburgh, P.; UAV Systems: The Global Perspective, 2005.

[6] Yenne, B.; Attack of the Drones, A History of Unmanned Aerial Combat; 2004.

[7] Holder, B.; Unmanned Air Vehicles, An Illustrated Study of UAV's; not dated.

[8] Dr. Maziar Arjomandi; Classification of Unmanned Aerial Vehicles; Mechanical Engineering, The University of Adelaide, Australia.

[9] Office of the Secretary of Defense. 2002. *Unmanned Aerial Vehicles Roadmap 2002-2027,* Department of Defense, Washington, D.C., December 2005, Appendix E.

[10] Elbit Systems; Skylark mini UAV; http://www.israeli-weapons.com/weapons/aircraft/uav/skylark/Skylark.html; 12 August 2008.

[11] Lockheed Martin; Dessert Hawk mini UAV system; http://www.designation-systems.net/dusrm/app4/deserthawk.html; 12 August 2008.

[12] Lockheed Martin; Dessert Hawk III mini UAV system overview; http://www.codeonemagazine.com/archives/2003/articles/apr_03/hawk/; 12 August 2008.

[13] Aerovironment; Raven mini UAV system overview; http://www.military.com/soldiertech/0,14632,Soldiertech_Raven,,00.html; 12 August 2008.

[14] Sagem; Merlin mini UAV system overview; http://www.defense-update.com/products/m/merlin-uav.htm; 12 August 2008.

[15] EMT; ALADIN mini aerial reconnaissance system brochure; http://www.emt-penzberg.de; downloaded 20 March 2008.

[16] Becker Avionics Inc.; Casper 250 Manual, Issue 2005/09/27, Revision 1.22.

[17] Aerovironment; Dragon Eye UAV system brochure; http://www.avinc.com; 28 October 2008.

[18] Micropilot official website; www.micropilot.com; 25 September 2009.

[19] UNAV intelligent control for unmanned systems; http://www.u-nav.com/home.html; 8 September 2009.

[20] U-NAV; UNAV3500 *Full-featured* UAV Autopilot brochure, 3500BRCH.pdf

[21] U-NAV; PICOPILOT Miniature Autopilot brochure, PICBRCH.pdf

[22] Micropilot; MP2028g Miniature UAV Autopilot brochure, MP2028g.pdf

[23] Beginners guide for electric motors; http://adamone.rchomepage.com/guide5.htm; 2 September 2009.

[24] Micropilot UAV demonstrators; http://www.micropilot.com/products-mp-visione.htm, 11 August 2009

[25] Vila Mani, M., "A quick overview on rotatory brush and brushless DC motors", Motion control department.

[26] De Villiers, D., "The application of new generation batteries in old tactical radios" Dissertation submitted in fulfilment of the requirements for the degree MASTER of ENGINEERING at the North West University, Potchefstroom, 2007.

[27] Kersop, S.J., "User Requirement Statement and Evaluation Specification for Unmanned Aerial Vehicle", Internal document nr. PH082-000000-501 Rev1, 2008.

[28] Kersop, S.J. "TSO EAGLE User Manual", internal document nr. PH041-000000-805, 2007.

[29] SAFT; *General Characteristics of Ni-Cd and Ni-mH*; 2001 edition; can be found at www.saftbatteries.com, 17 August 2009.

[30] Uniross; Ni-Cd & Ni-MH characteristics, can be found at www.uniross.com, 18 August 2009.

[31] Flight Power, Li-Po batteries, can be found at http://www.flightpower.co.uk/, 21 May 2008.

[32] Dualsky, Li-Po batteries, can be found at http://www.dualsky.com, 13 August 2008.

[33] Yuasa Lead-acid batteries, 0900766b80065ba0.pdf, can be found at http://www.yuasabatteries.com, 8 March 2007.

[34] Duracell, Primary Alkaline batteries, can be found at http://www.duracell.com, 5 November 2003.

[35] Green Robert E.; "Machineries handbook"; 1995: Page 369, Material Densities

[36] Night vision IR cameras, Indigo Omega FLIR A10, can be found at www.flir.com, 16 August 2009.

[37] Micropilot autopilot manual, "Micropilot Autopilot Installation and operation", September 2008.

[38] Micropilot Horizon manual, "Horizon^{mp} User's Guide", June 2007.

[39] Wireless RF communications, RS232 serial data link can be found at www.rfdesign.co.za, 7 September 2009.

[40] Aerocomm antenna tutorial, www.aerocomm.com/docs/Antenna_Tutorial.pdf, 11 September 2009.

Appendix A Battery test measurements

A.1 Aircraft battery tests

Battery tests were performed at different throttle settings on the Micropilot UAV. The following graphs were captured on a calibrated Fluke 199C scope-meter; calibration certificate number 200904-013. See Figure 53 to Figure 59. The throttle settings were chosen according to typical settings recorded during flights:

- 30% - aircraft is flying straight and level at cruise speed.
- 45% - combination of straight and level flight and turning.
- 60% - aircraft is turning (banking).
- 90% - aircraft climbing to a higher altitude.
- 100% - aircraft takes off.

The bench tests were performed with a new battery pack (Figure 50) supplied with the aircraft by Micropilot. The batteries were fully charged at the beginning of each test. The bench test setup is shown in Figure 51.

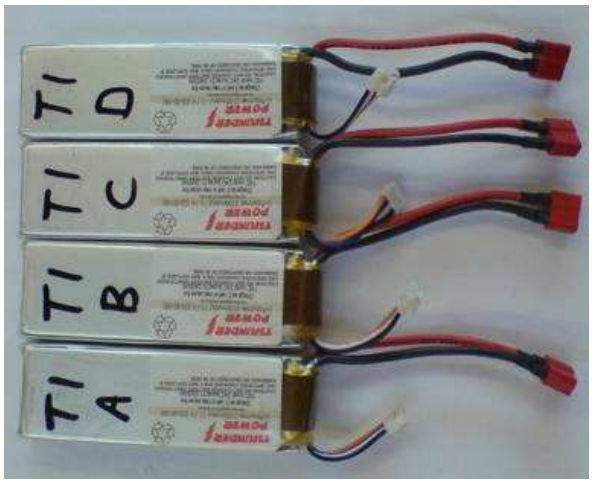

Figure 50: Aircraft Battery pack

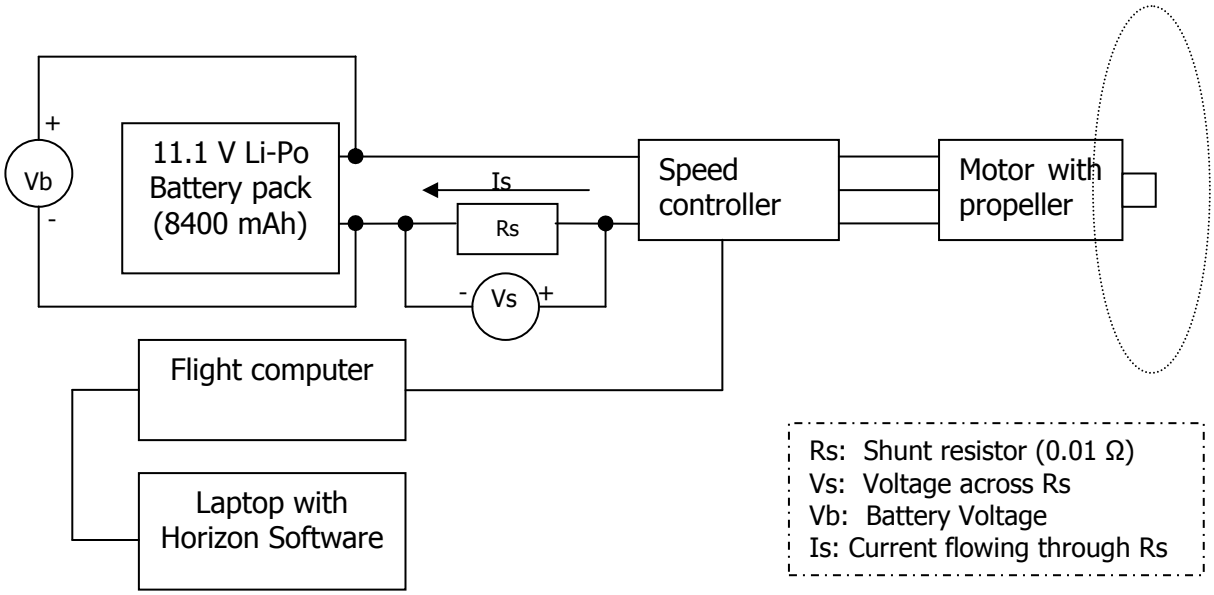

Figure 51: Bench test for measuring the running motor power consumption

On the two inputs of the scope-meter, Vs was measured on Input A and Vb on Input B. A picture of the battery tests setup is shown in Figure 52.

Figure 52: Picture of Bench setup for battery tests

By measuring the battery voltage and current, the power consumption could be calculated for different throttle settings. Equation 2 is used to calculate the current by measuring the voltage (Vs) across the shunt resistor (Rs) in Figure 51.

$$Is = \frac{Vs}{Rs} \qquad (2)$$

On the scope meter, the measured current is represented by the voltage measured on Input A of the scope-meter, where 10 mV represents 1 A. This is derived from the voltage measured across the 0.01 Ω shunt resistor (Rs).

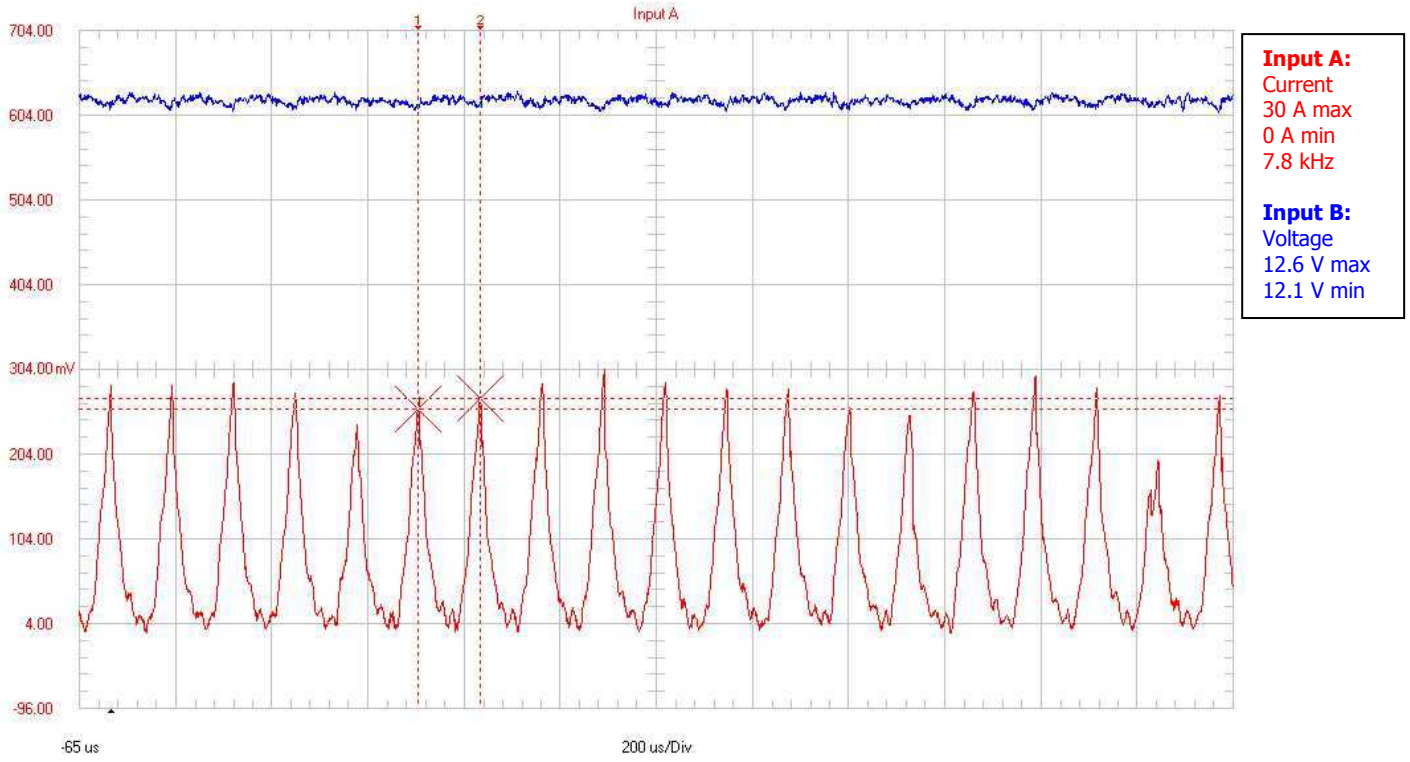

Figure 53: Battery Voltage & Current measurement with a throttle setting of 30 %

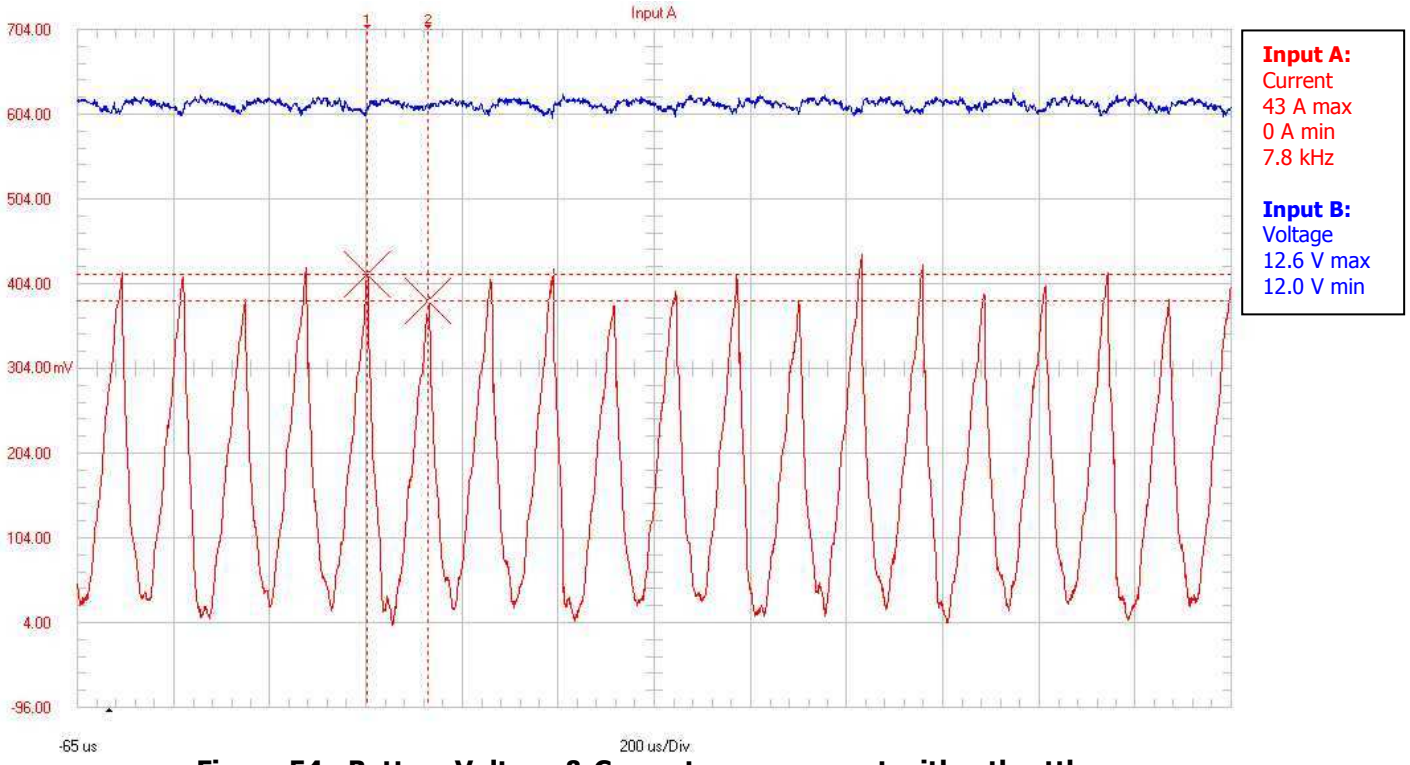

Figure 54: Battery Voltage & Current measurement with a throttle setting of 45 %

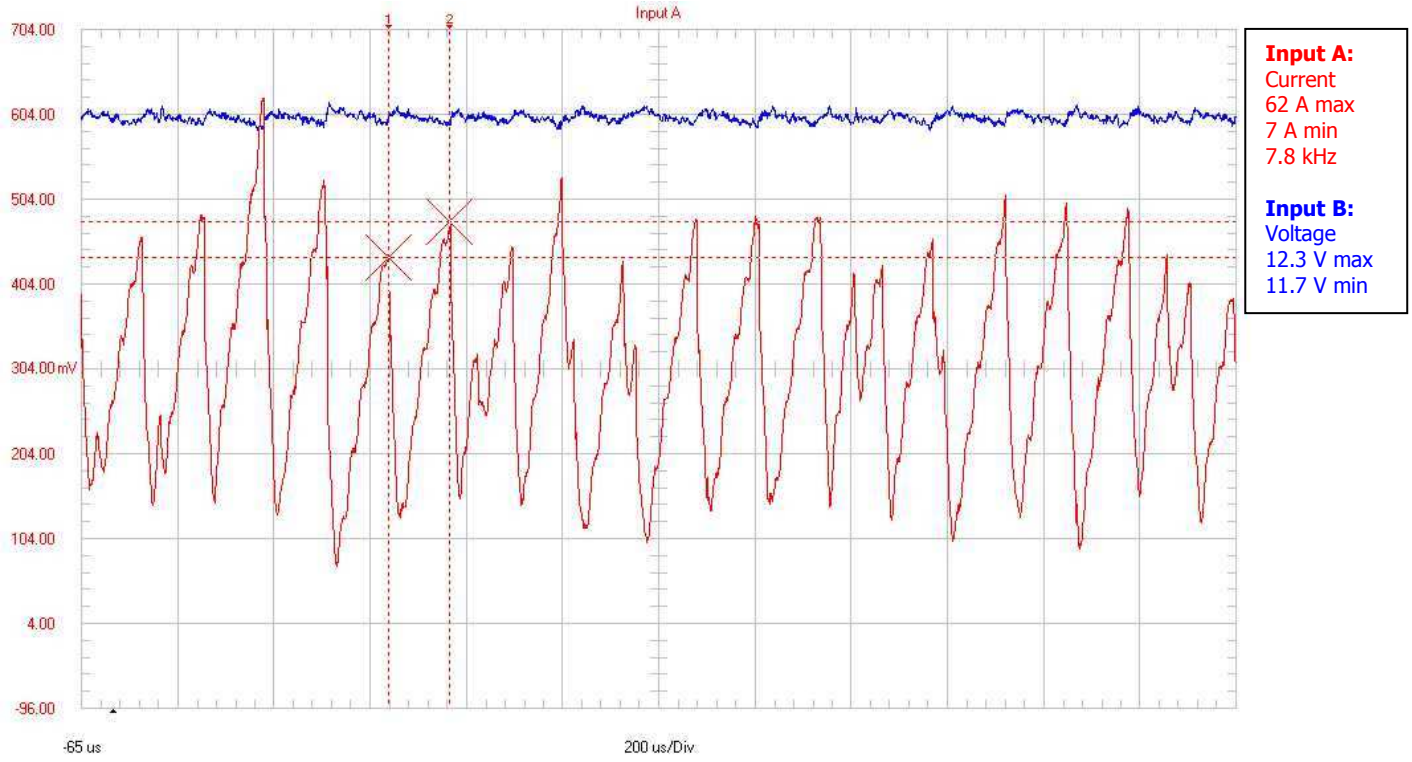

Figure 55: Battery Voltage & Current measurement with a throttle setting of 60 %

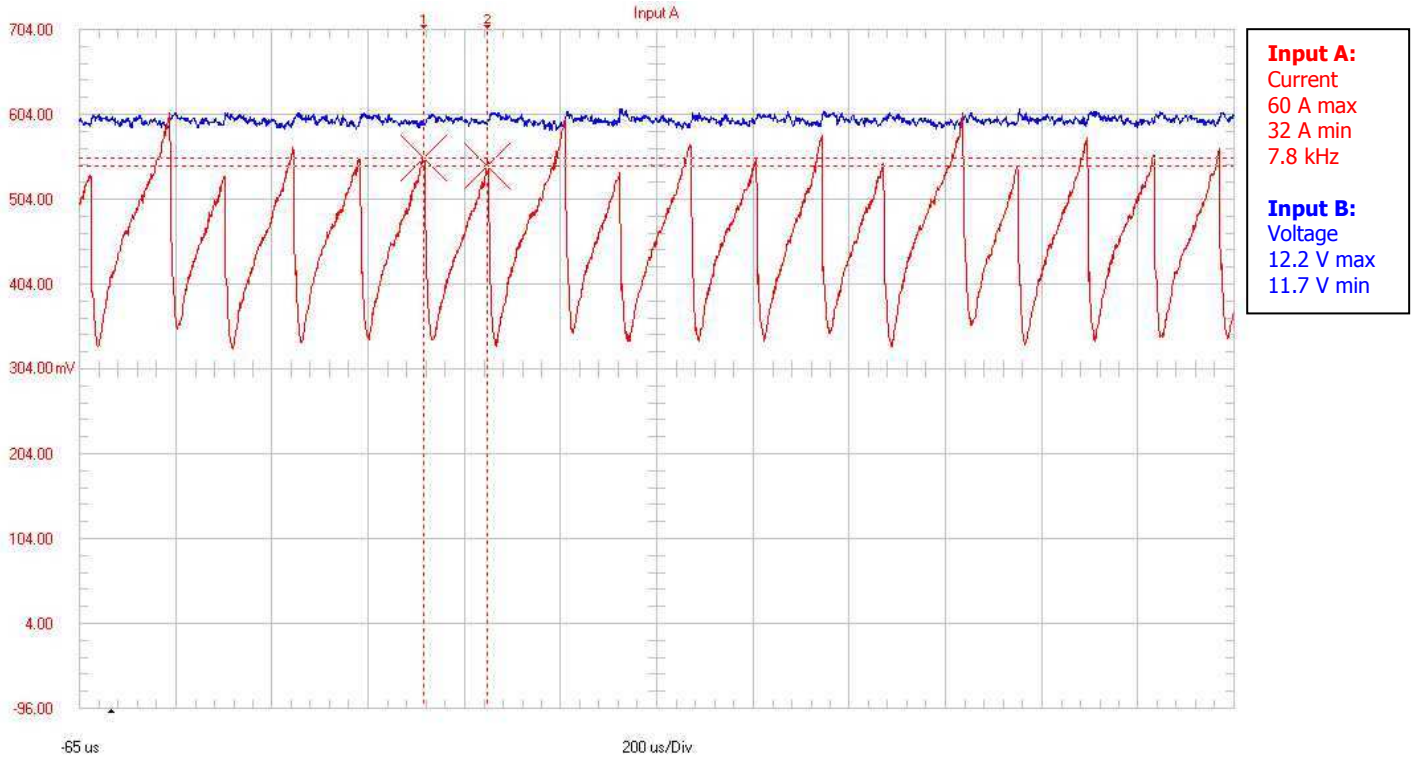

Figure 56: Battery Voltage & Current measurement with throttle set to 75 %

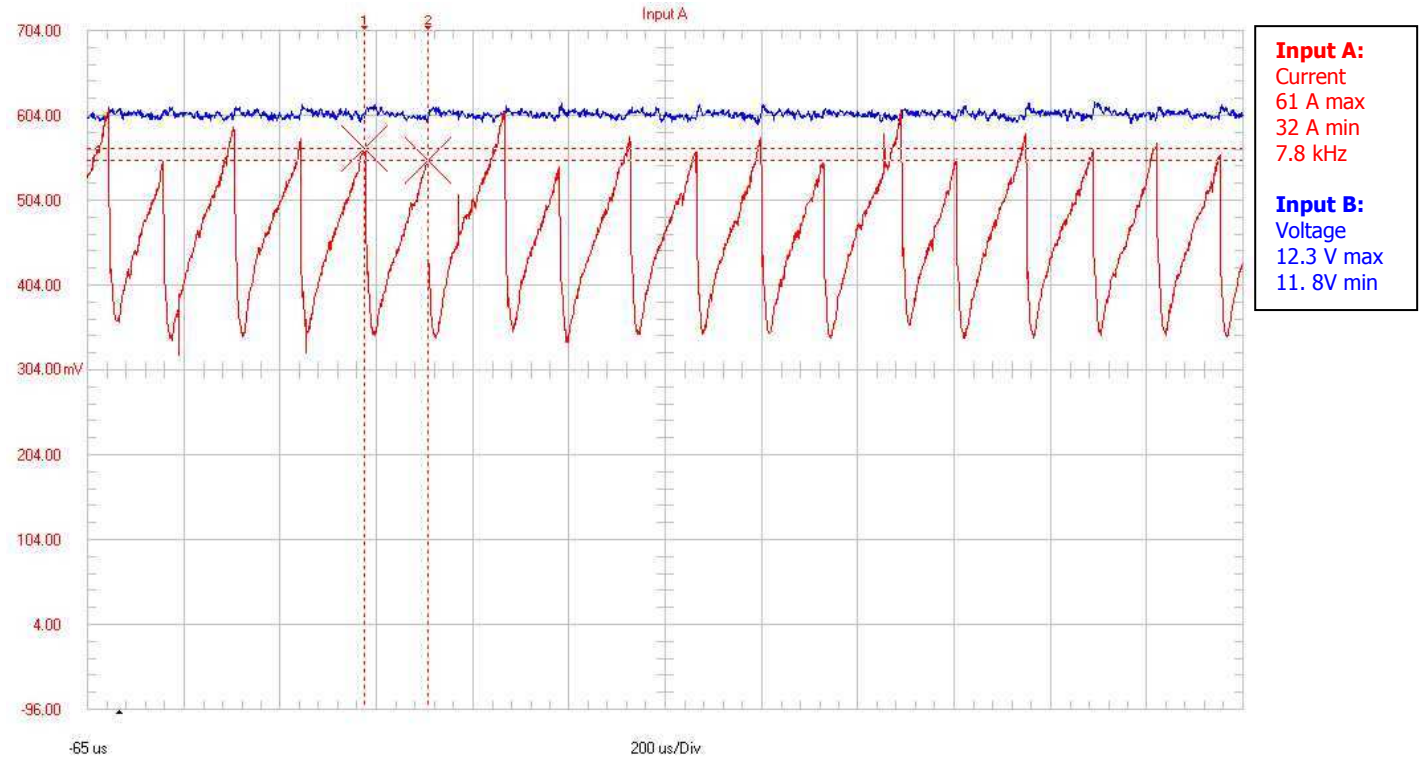

Figure 57: Battery Voltage & Current measurement with throttle set to 90 %

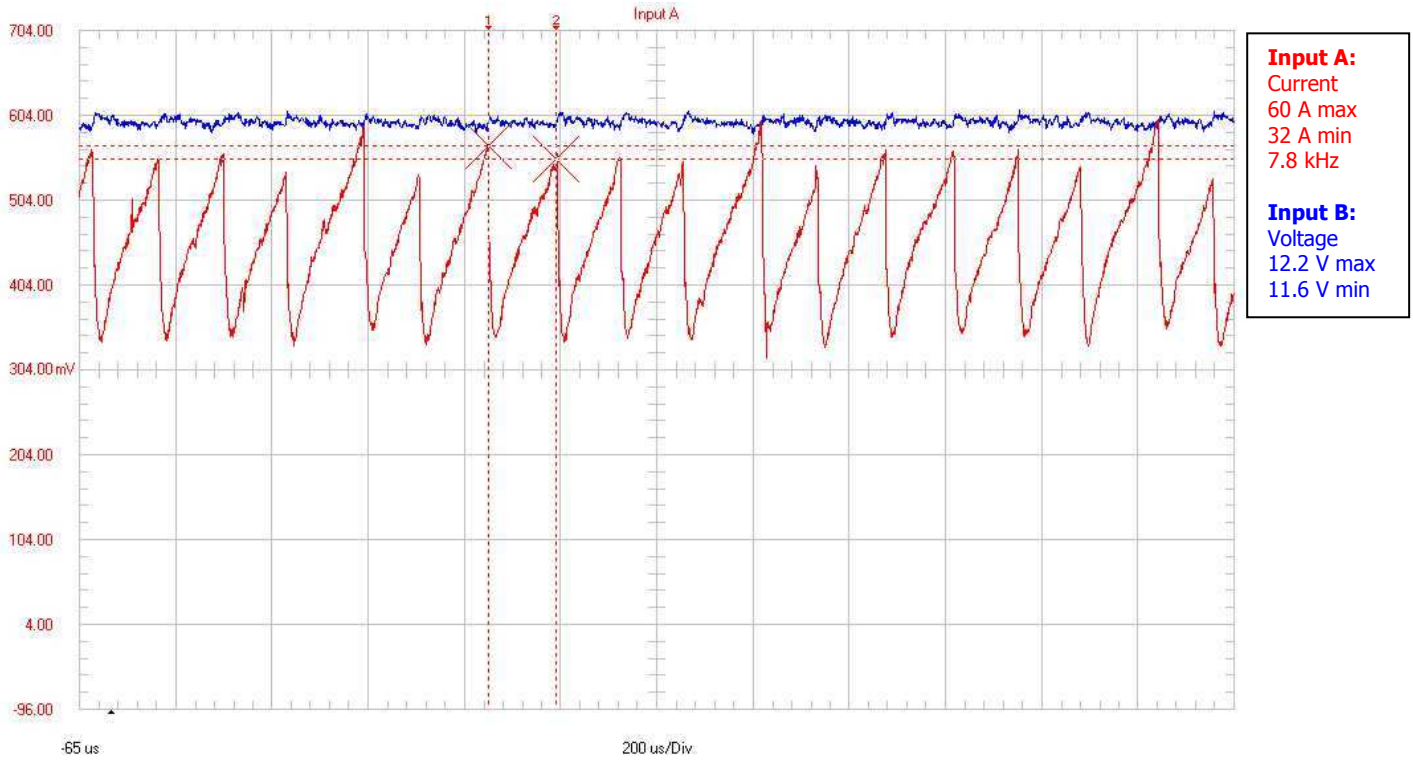

Figure 58: Battery Voltage & Current measurement with a throttle setting of 100 %

Figure 59 shows a scope meter reading of the voltage measured between the battery ground and servo board ground while the motor is running at full power. No payload was connected to the aircraft during this measurement. A noise floor in the order of 300 mV is measured here. This is caused by the high currents flowing through the ground wires. Also see Figure 12 for information regarding the wiring of ground loops.

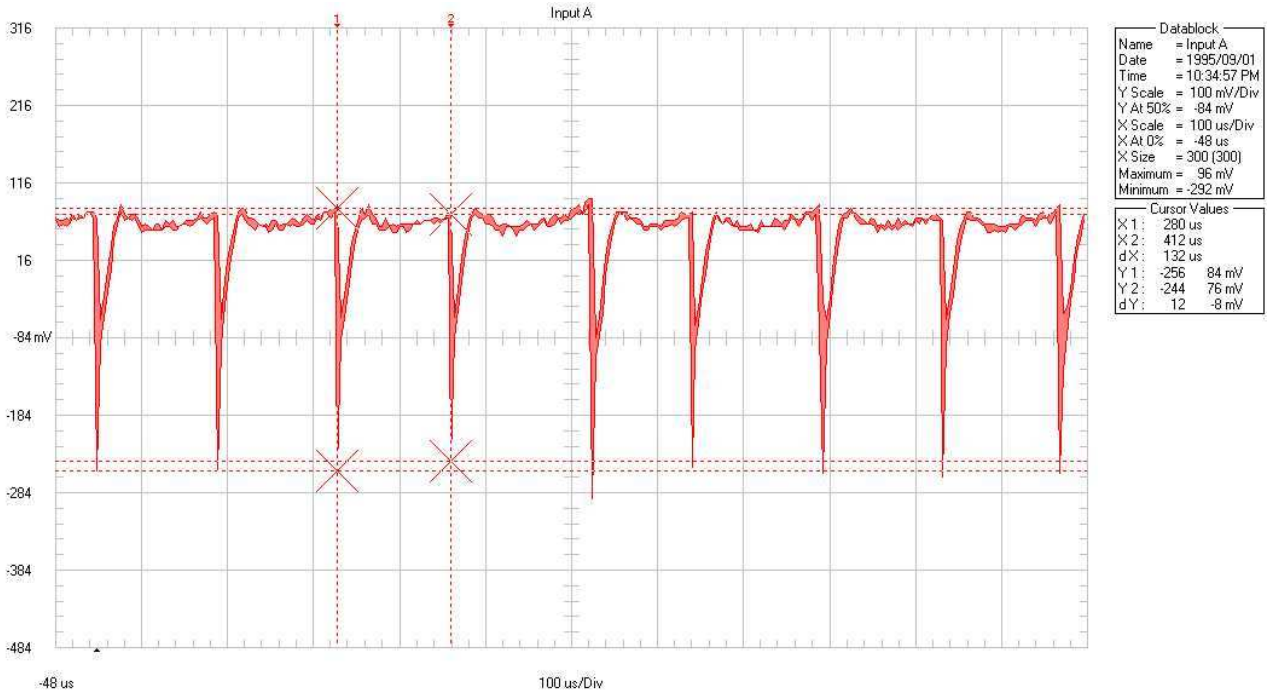

Figure 59: Ground voltage between battery and servo board

Appendix B Camera & LED switch circuit design

The MP2028g & MP2128g autopilots from Micropilot use servo controls to control the camera payloads. This can be controlled by either a slider or button icon on the Horizon software. The output signals for the servo controls produce between 1 ms and 2 ms pulses every 20 ms, as shown in Figure 60. This signal is used as the input to control the switching between the two cameras. The camera switch was designed that when the pulse is 1 ms, the one camera signal is relayed to the video transmitter and when the pulse is 2 ms, the other camera signal is relayed. Figure 61 shows the circuit diagram used for switching the cameras with the servo signal.

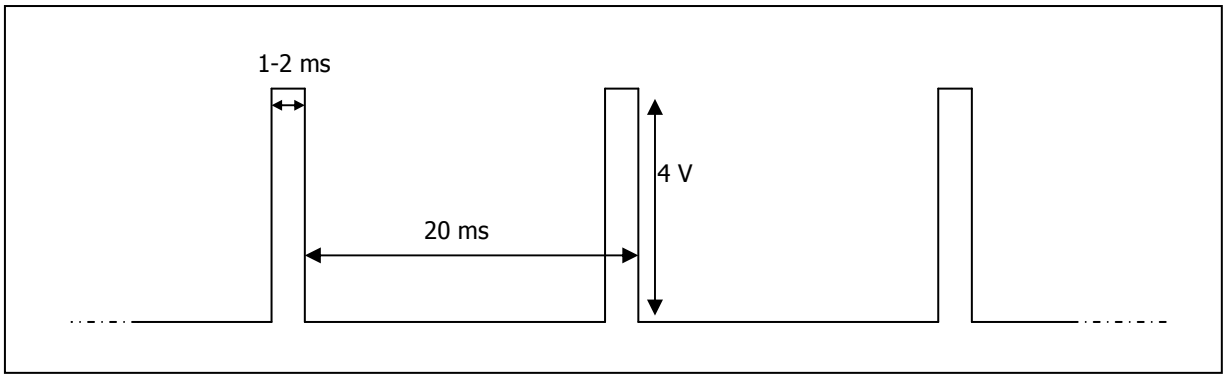

Figure 60: RC servo control pulses

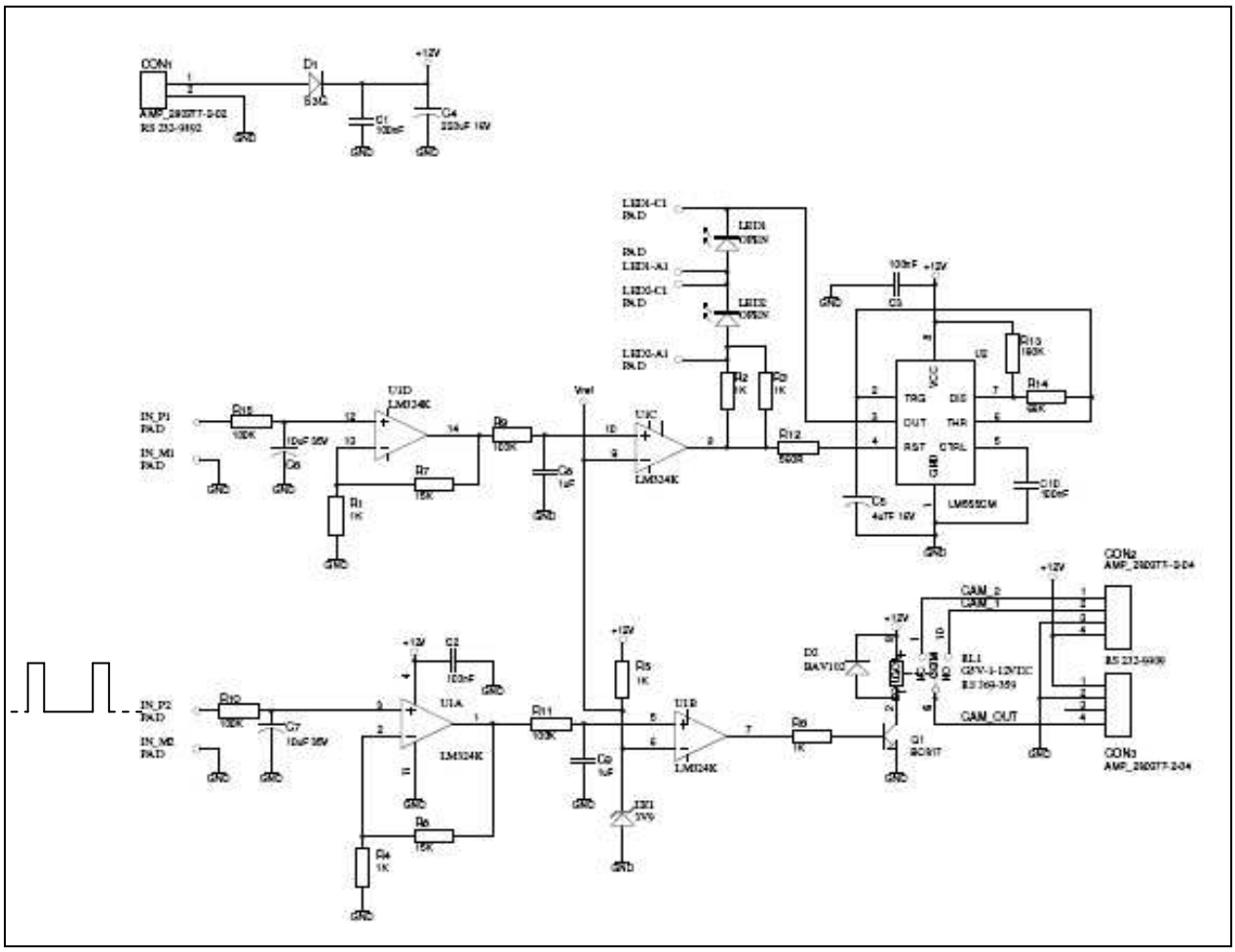

Figure 61: Schematic circuit design for the payload camera & LED switch

Appendix C Horizon software

Screen shots have been captured from Micropilot's Horizon software to show what the GCS graphical user interface looks like. These screen shots are also used to indicate various functions and features that are explained in this dissertation. Figure 62 shows the screen from where the aircraft is controlled. The aircraft is placed on a geo-referenced map as soon as a GPS lock is obtained on it. The waypoints are also placed on the map. This indicates the flight route that is currently loaded on the aircraft.

The aircraft controls are found on the left hand side of the screen. The buttons to launch the aircraft, pre-defined flight patterns and the camera controls are all located here. Pre-defined flight patterns can be used as in-flight commands at any stage during the flight. The patterns currently programmed can be used to bring the aircraft back to the launch point, land the aircraft, fly circles or fly figure 8 manoeuvres. These patterns can be cancelled by clicking the button again and the aircraft will continue the pre-set flight plan.

Figure 62: Screenshot of Horizon software

Figure 63 shows the window within Horizon that is used to set up the flight parameters of the autopilot. These flight parameters can only be changed while the aircraft is on the ground and must be uploaded onto the autopilot.

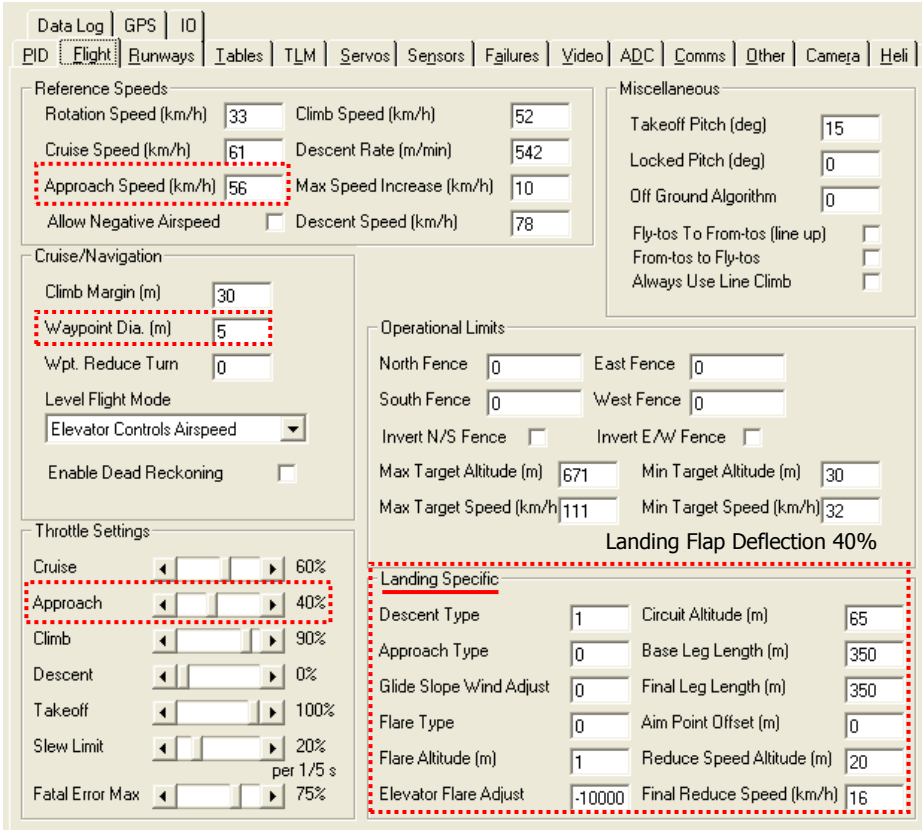

Figure 63: Screenshot of autopilot flight parameters setup

Figure 64 shows the window within Horizon that is used to set up tables. This table is used to control the spoiler of the aircraft during the final approach of the landing circuit. The condition on the left of the table (gsAlt with field ID 1037) will cause the effect on the right hand side (fServo with field ID 1234). The variable gsAlt is measured in feet x -8. Therefore, a value of -240 is equivalent to 9 m above and the value 260 to 10 m below glide slope. This table is disabled by default and is only activated during the final approach of the landing. The spoiler should never be deployed during normal flight.

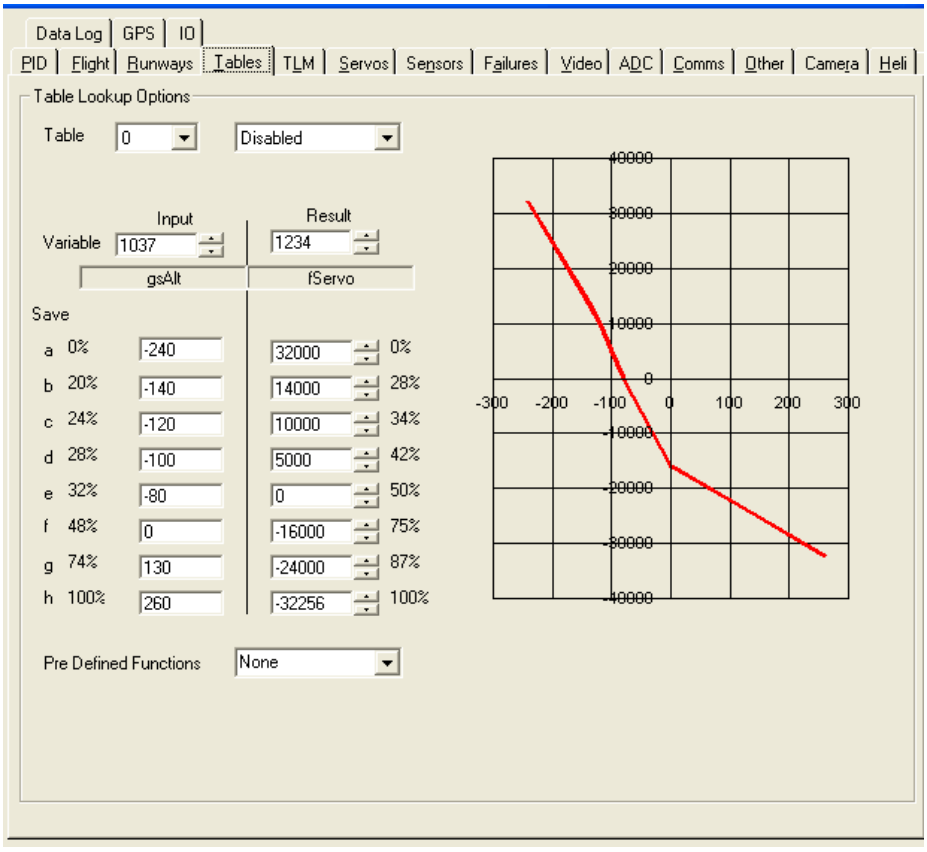

Figure 64: Screenshot of Spoiler activation table

Appendix D Flight logs

The autopilot stores 52 different parameters 5 times a second, that can be downloaded after each flight ([37], p149). This data can be used to determine how effective the aircraft's control loops are reacting and can be used to enhance it. The figures given in this appendix were used to analyse and enhance the aircraft's performance.

D.1 Flight log data for benchmark tests

This paragraph shows the flight log data that was retrieved after the endurance flight test, without any payloads. Figure 65 shows a picture of the aircraft that was used to set the benchmark on performance. The aircraft was also used like this, with the payloads attached later on. Notice that the spoiler is attached to the wing.

Figure 65: Photo of aircraft used for benchmark test (with spoiler on wing)

Figure 66 shows a screen shot of the Horizon software that was taken during the endurance test. The aircraft was flying a path by following the waypoints on the map. A small black line is drawn behind the aircraft as it flies (flight trail). This shows

how accurate the aircraft navigates. Notice how the aircraft passes through the waypoints and how straight the flight path is between the waypoints.

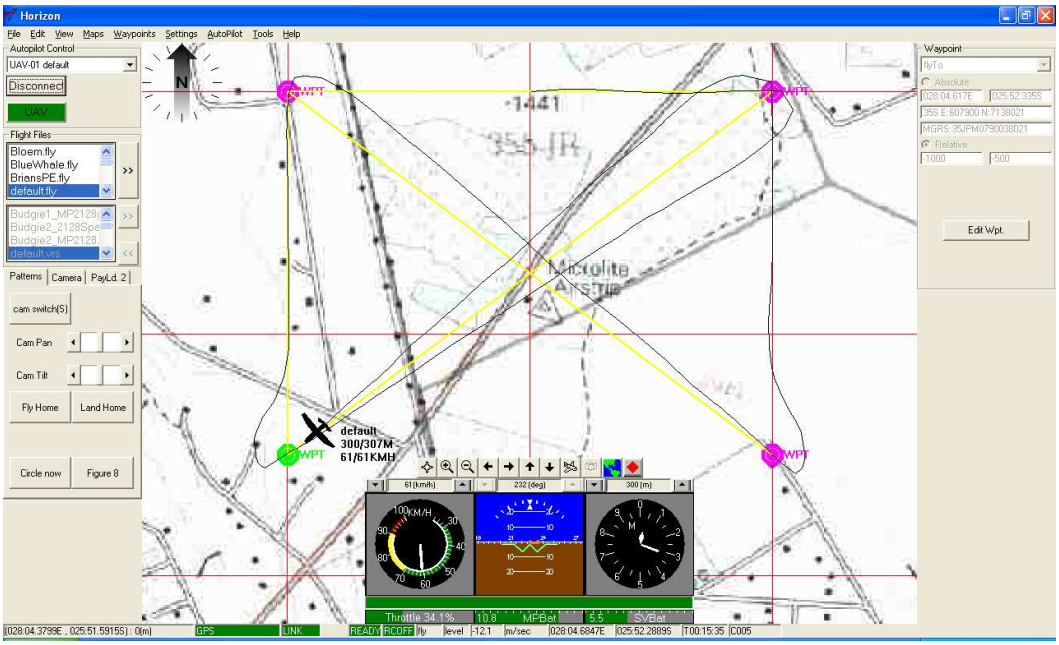

Figure 66: Screen shot of aircraft flight trail during benchmark test

Figure 67 shows the graph of the desired altitude versus the current altitude of the aircraft during the entire duration of the 1 hour endurance test flight. This information indicates how accurate the aircraft is able to maintain the set altitude (desired altitude) during flight.

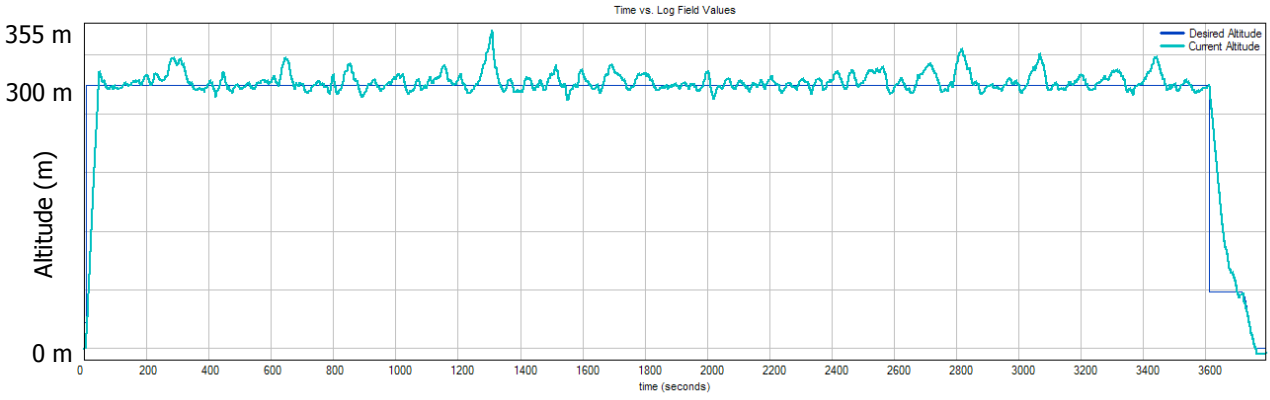

Figure 67: Desired Altitude vs. Current Altitude over time

Figure 68 shows the graph of the desired speed, current speed and GPS speed measured by the aircraft during the entire duration of the 1 hour flight. Notice that the current speed is a bit higher (up to 10 km/h) than the desired speed when the

GPS (ground) speed is below the desired speed. The autopilot was configured to correct for ground speeds that are slower than the set air speed, by increasing the speed up to a maximum of 10 km/h. This typically happens when the aircraft experiences a head wind. In this case it happened every time the aircraft flew from South to North. On the down wind stretches, it can be seen that the aircraft maintained airspeed very well.

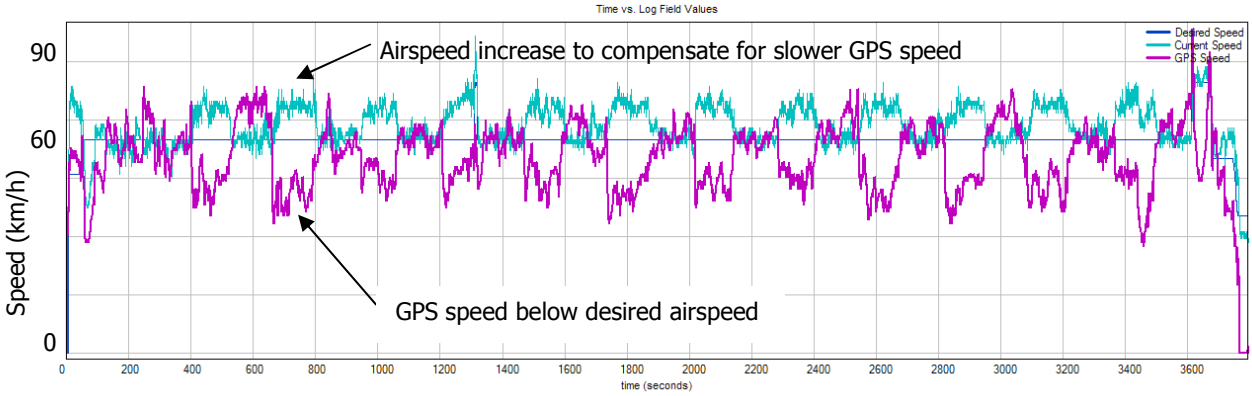

Figure 68: Desired speed, current speed and GPS speed plotted against time

Figure 69 shows only a part of the test flight, to get a more zoomed-in view to indicate how the throttle is used to control the aircraft's altitude. When the aircraft is below the desired altitude, more throttle is applied to pull the aircraft up and visa versa.

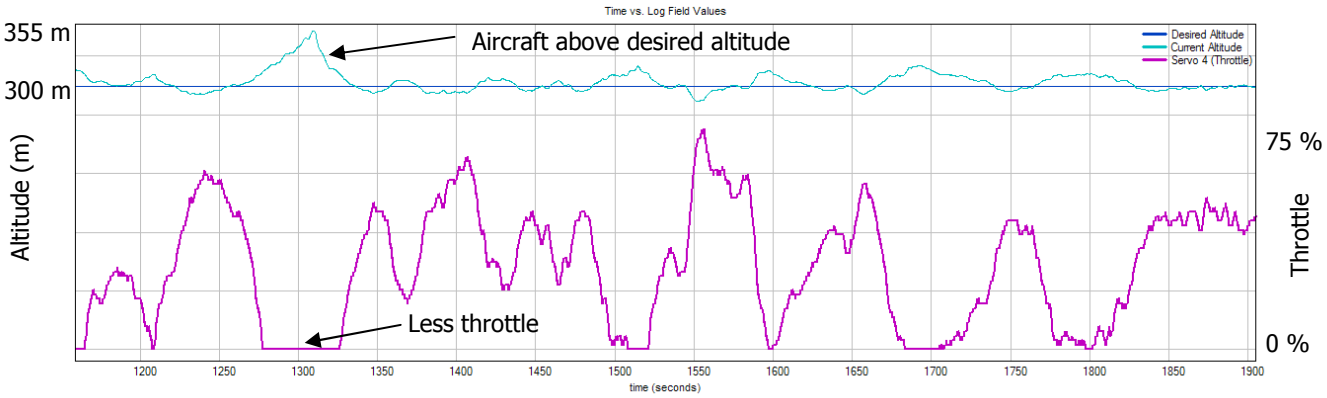

Figure 69: Throttle settings during altitude control

Figure 70 shows how the aircraft maintains altitude during the descent of the landing. Towards the end the aircraft goes above the desired glide path, indicated by 1, 2 & 3.

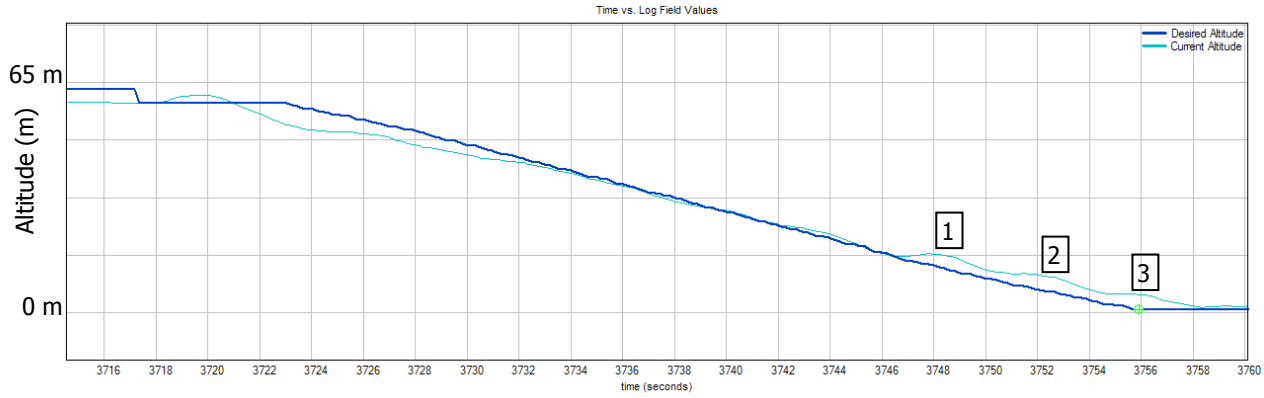

Figure 70: Current altitude vs. desired altitude during the descent of the landing

Figure 71 shows the spoiler activation (lifts up) as soon as the aircraft is above the glide path. 0 % is when the spoiler is lying flat on the wing and 100% is when it stands upright. Three areas where the altitudes are higher (4 m) than the glide path are indicated as 1, 2 & 3 and correlates with Figure 70.

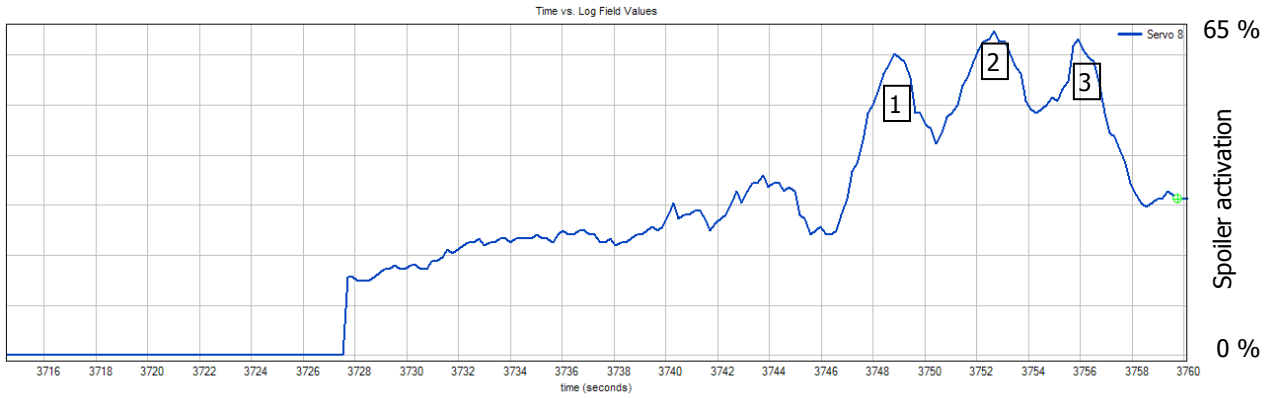

Figure 71: Spoiler activation during the landing descent.

D.2 Flight log data for landing tests

The flight log data of the tests performed to better the landing accuracy are shown in this paragraph. Nine tests were performed. At this stage, the spoiler was not designed yet. Figure 72 indicates that the aircraft was flying below the glide path on the final approach and landed short. The GPS and current speed are also shown on the graph to indicate that the aircraft was flying in a head wind of about 15 km/h.

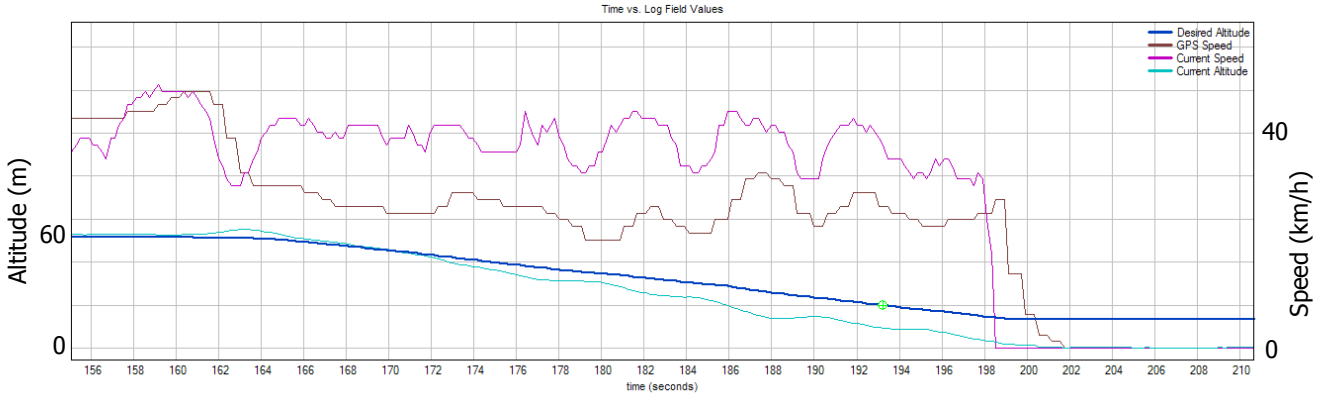

Figure 72: Landing test flight 1

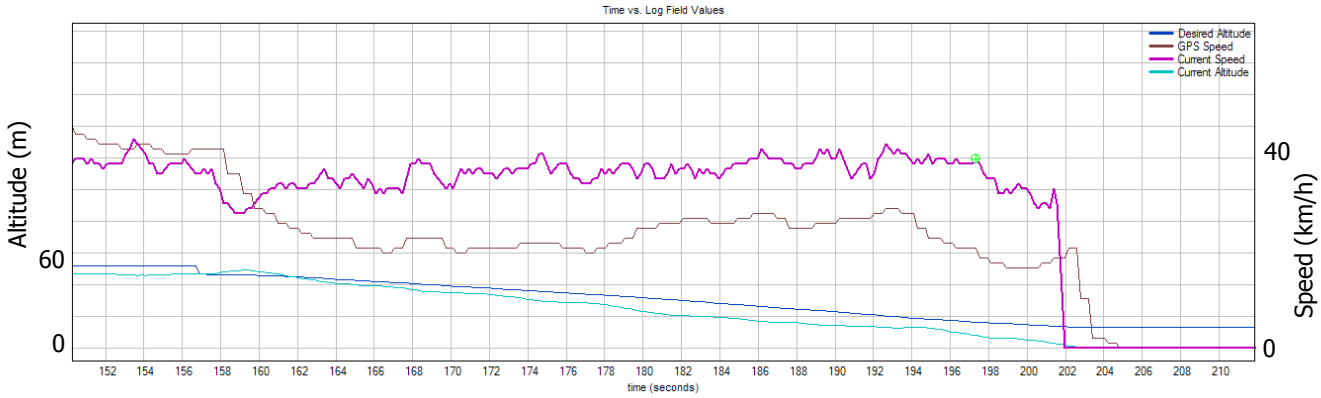

Figure 73: Landing test flight 2

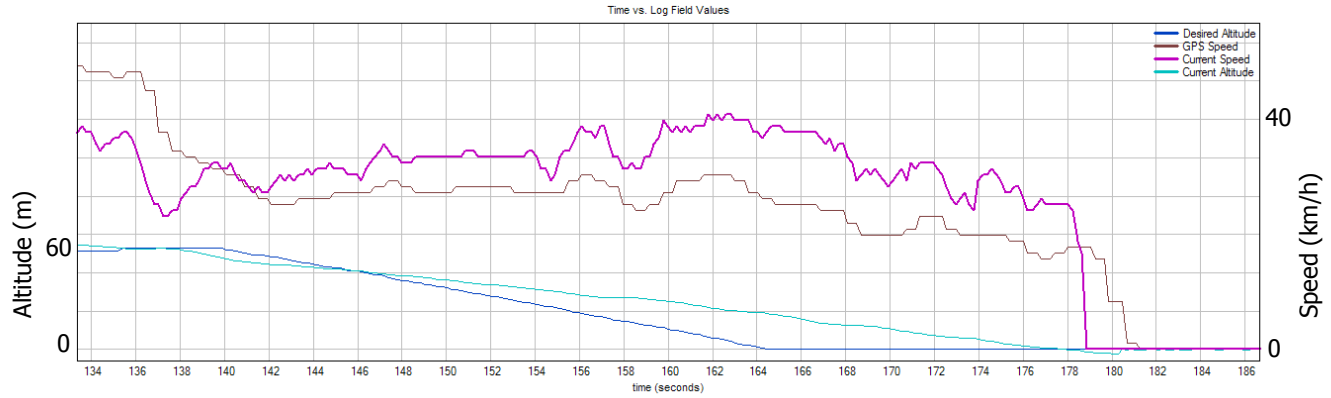

Figure 74: Landing test flight 3

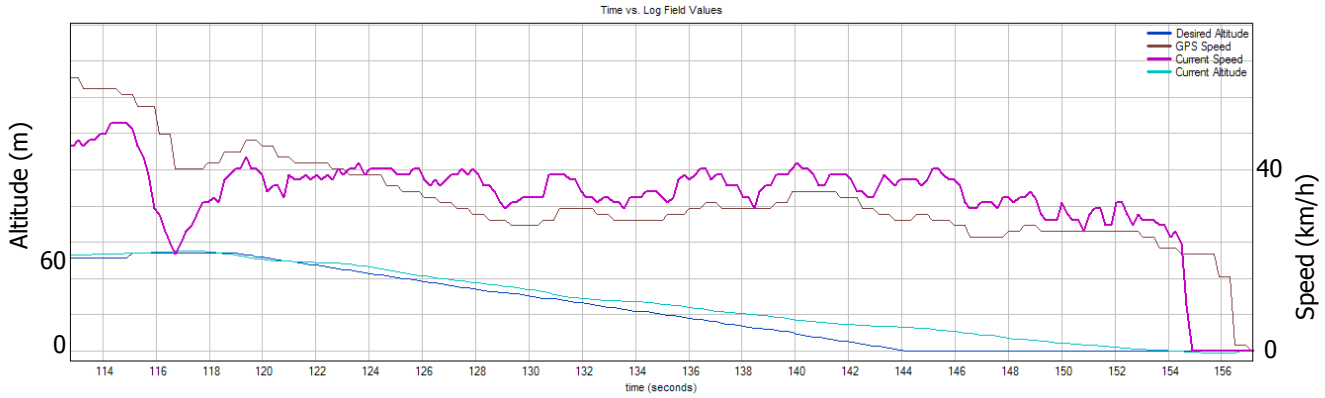

Figure 75: Landing test flight 4

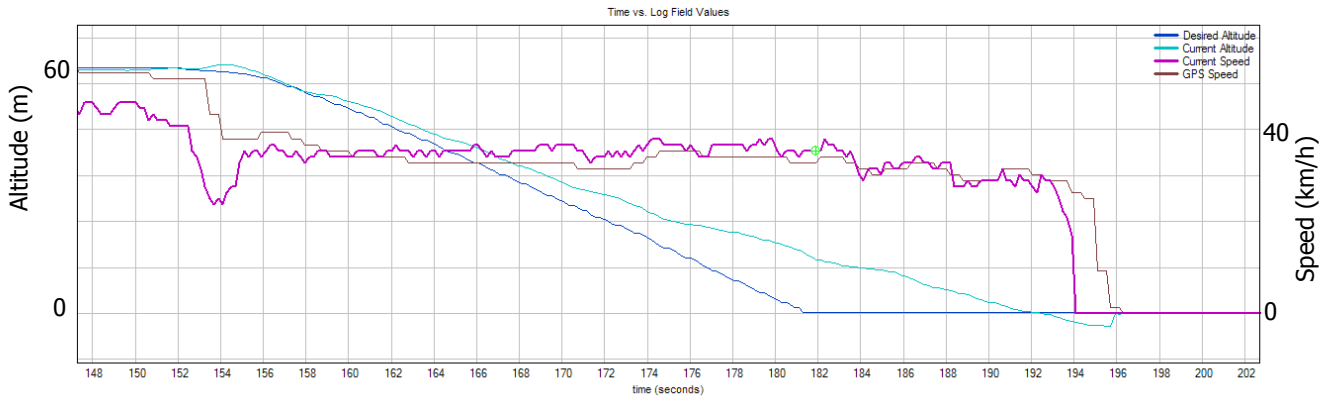

Figure 76: Landing test flight 5

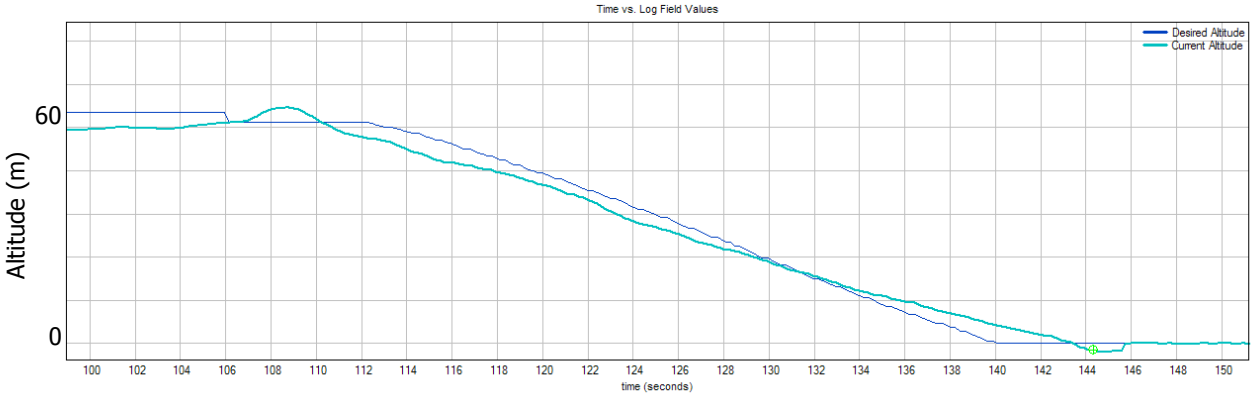

Figure 77: Landing test flight 6 *(Speed data not available)*

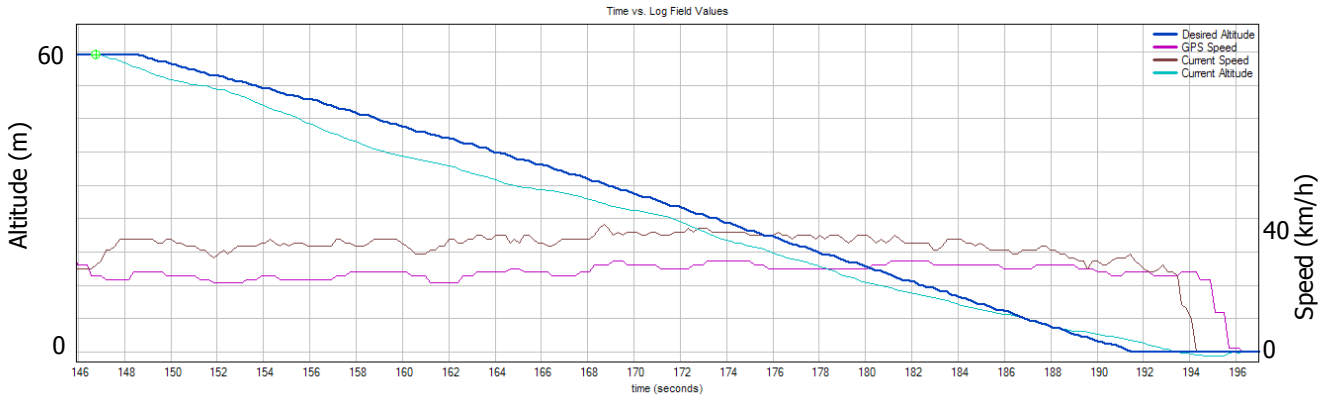

Figure 78: Landing test flight 7

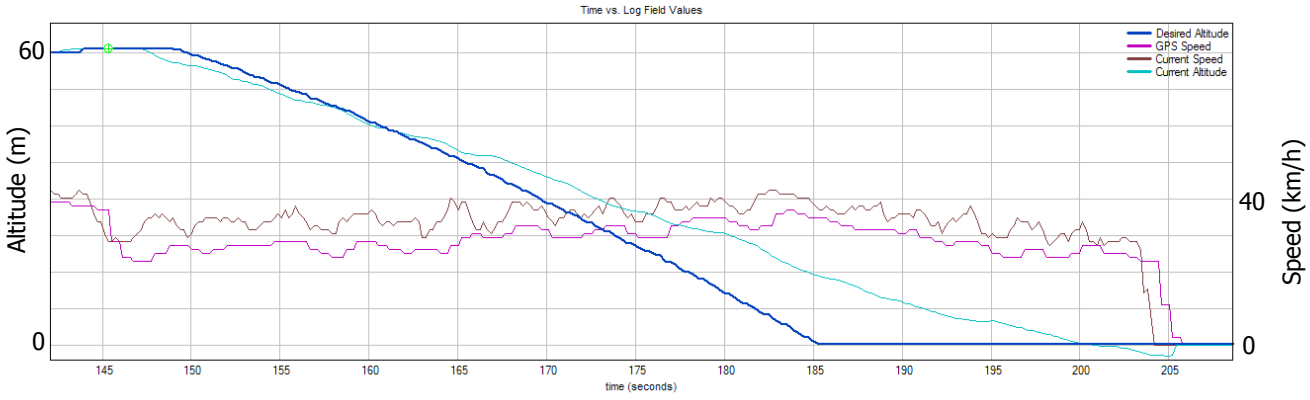

Figure 79: Landing test flight 8

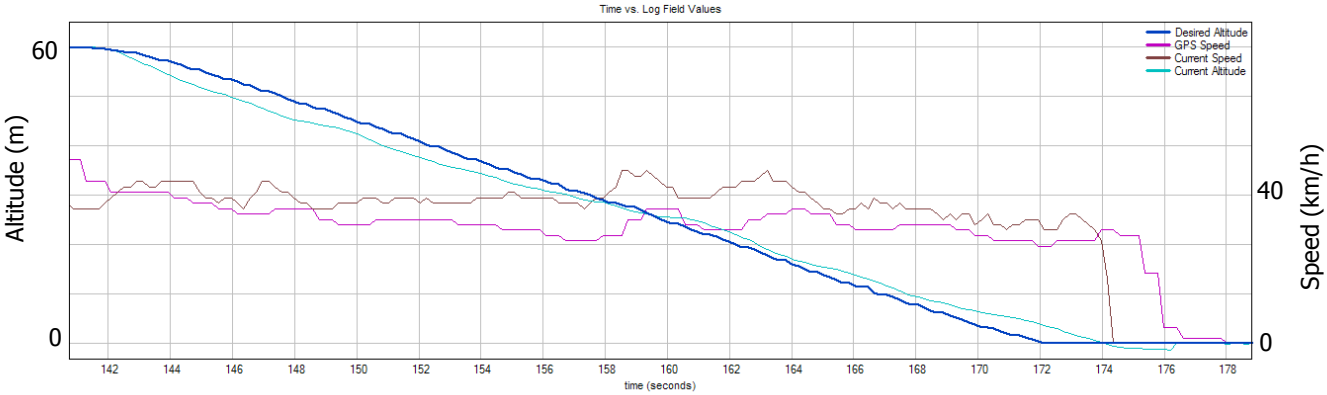

Figure 80: Landing test flight 9

D.3 Flight log data for flight stability tests

The flight log data from the endurance flight without any payloads attached, but with the spoiler, were used to analyse the flight stability of the aircraft. The autopilot's ability to keep the aircraft's wings level is analysed by comparing the desired roll with the current (actual) roll and how the ailerons are controlled to rectify the error.

Figure 81 shows how the aircraft uses its ailerons to maintain roll stability on a straight and level flight path. The autopilot measures the difference (error) between the roll angle it needs to be (desired) and its current angle. The control loop reacts on the error by moving the aileron control surfaces in the opposite direction to compensate for this. When the aircraft's roll angle is more than the desired angle, the aileron reacts in such a way that the aircraft rolls back to the desired angel. In Figure 81 a maximum roll error of 5 % can be seen.

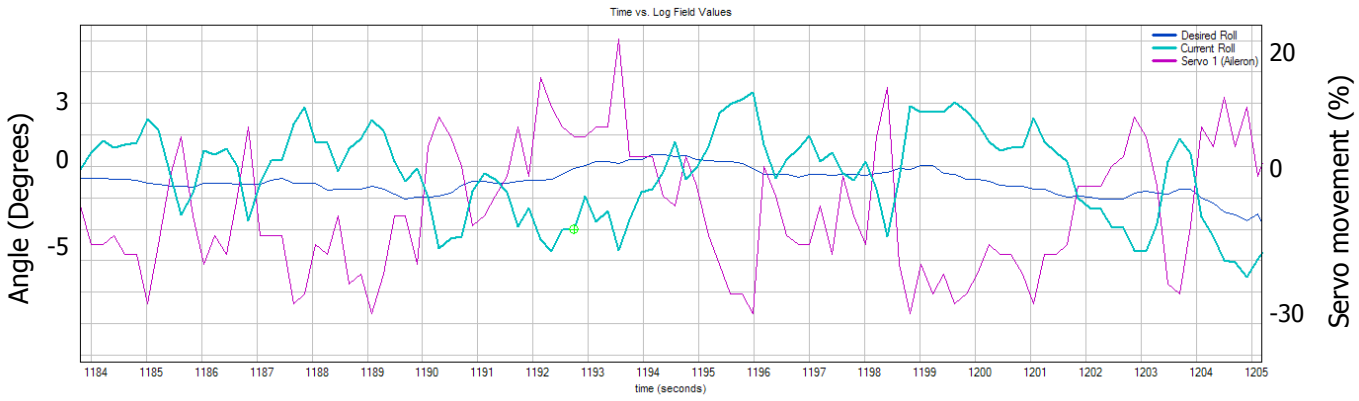

Figure 81: Desired Roll vs. Current Roll and Aileron control

Figure 82 shows how the aircraft uses its elevator to maintain pitch stability on a straight and level flight path. The autopilot measures the difference (error) between the pitch angle it needs to be (desired) and its current angle. In Figure 82 a maximum pitch error of 5 % can be seen. The control loop reacts on the error by moving the elevator control surfaces in the opposite direction to compensate for this. When the aircraft's pitch angle is more than the desired angle, the elevator reacts in such a way that the aircraft corrects itself to the desired angel. The elevator is also used to control the airspeed and is therefore controlled by two control loops.

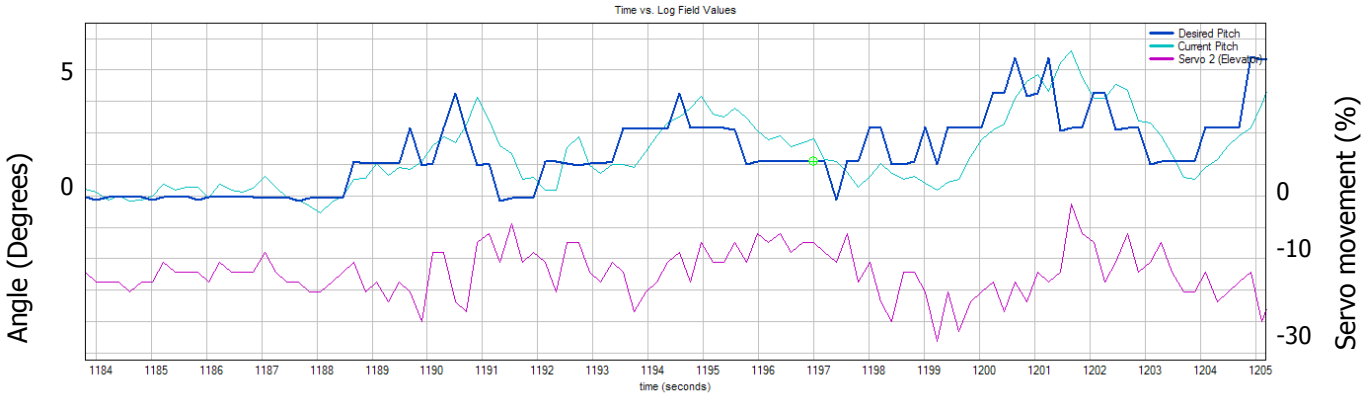

Figure 82: Desired Pitch vs. Current Pitch and elevator control

The main functions of the rudder is to help steer the aircraft in cross winds and to push the nose up while banking. The log file does not contain the desired yaw and therefore the yaw-stability cannot be analysed.

Figure 83 shows the GPS-, air- and desired speeds for a test flight performed at sea level in wind speeds greater than 30 km/h. The wind speeds can be calculated by subtracting the GPS speed from the measured airspeed where the difference is the greatest. This implies that the aircraft was flying directly into the wind at that stage. It was found that when the ground speed of the aircraft is slow (5 km/h) as a result of flying into strong winds, the aircraft's navigation is not that good. The GCS can be used to increase the flying speed of the aircraft in flight. This was proven to have a positive result.

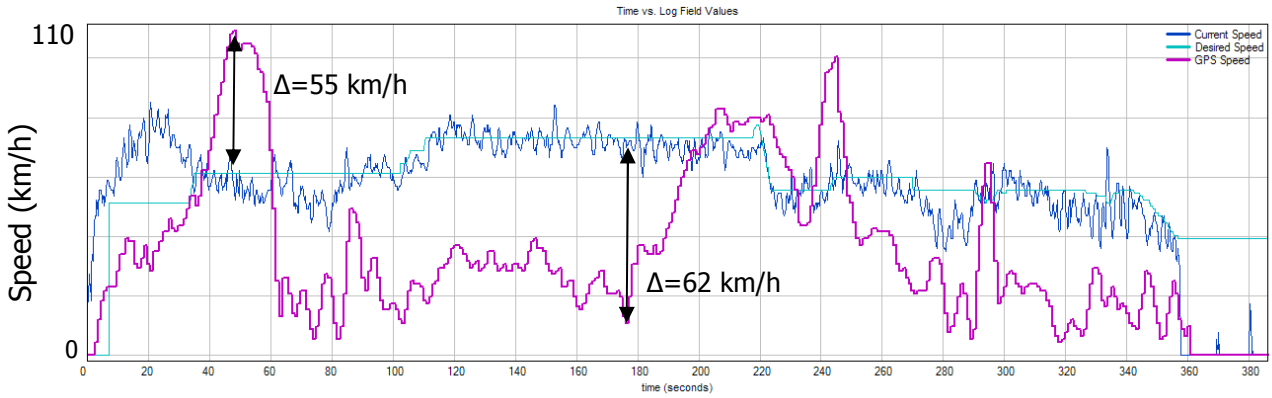

Figure 83: Log data for flight in winds > 30km/h at sea level

Appendix E Payloads wiring block diagrams

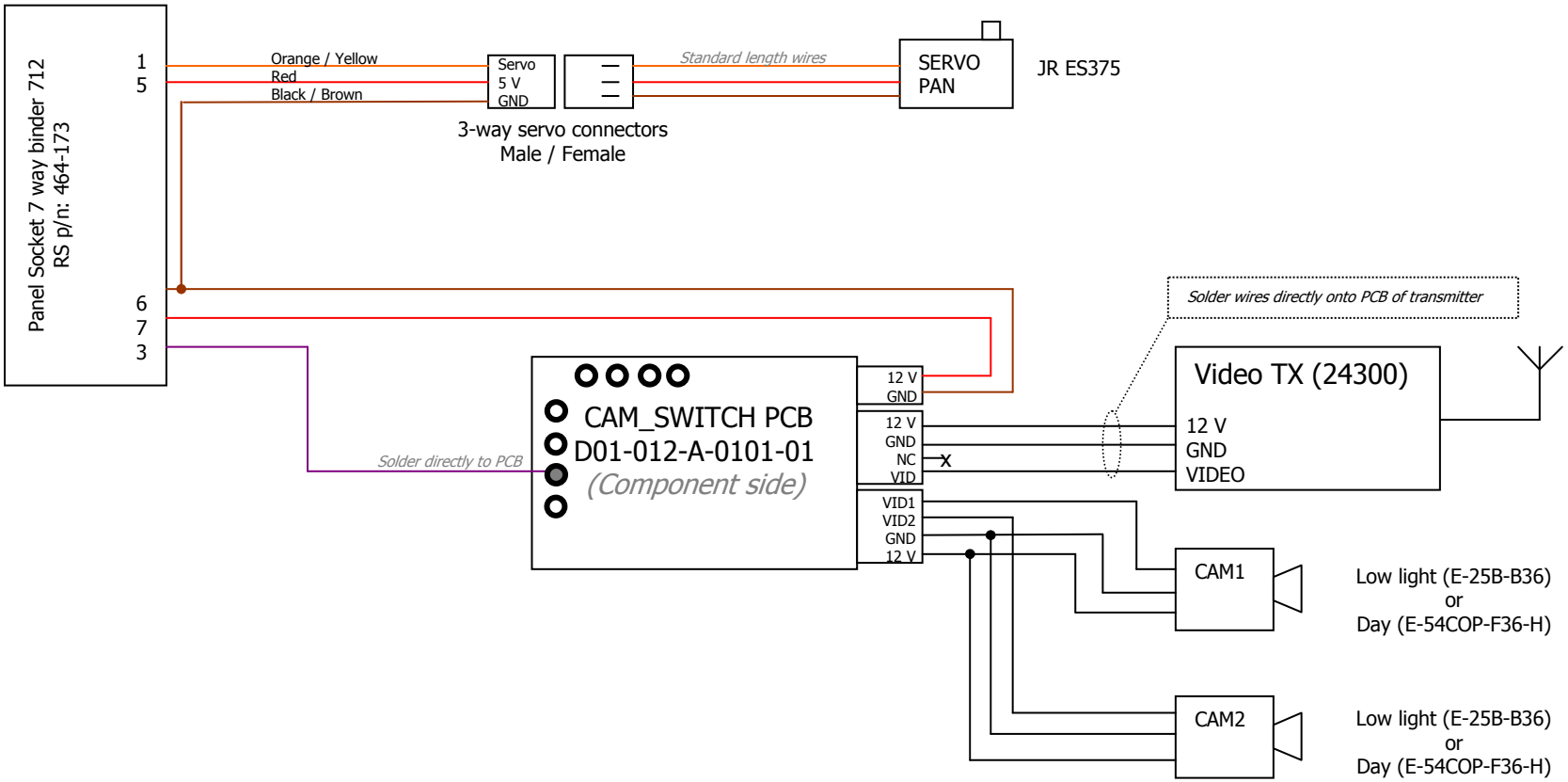

Figure 84: Wiring block diagram for payload with cameras that can pan side-to-side

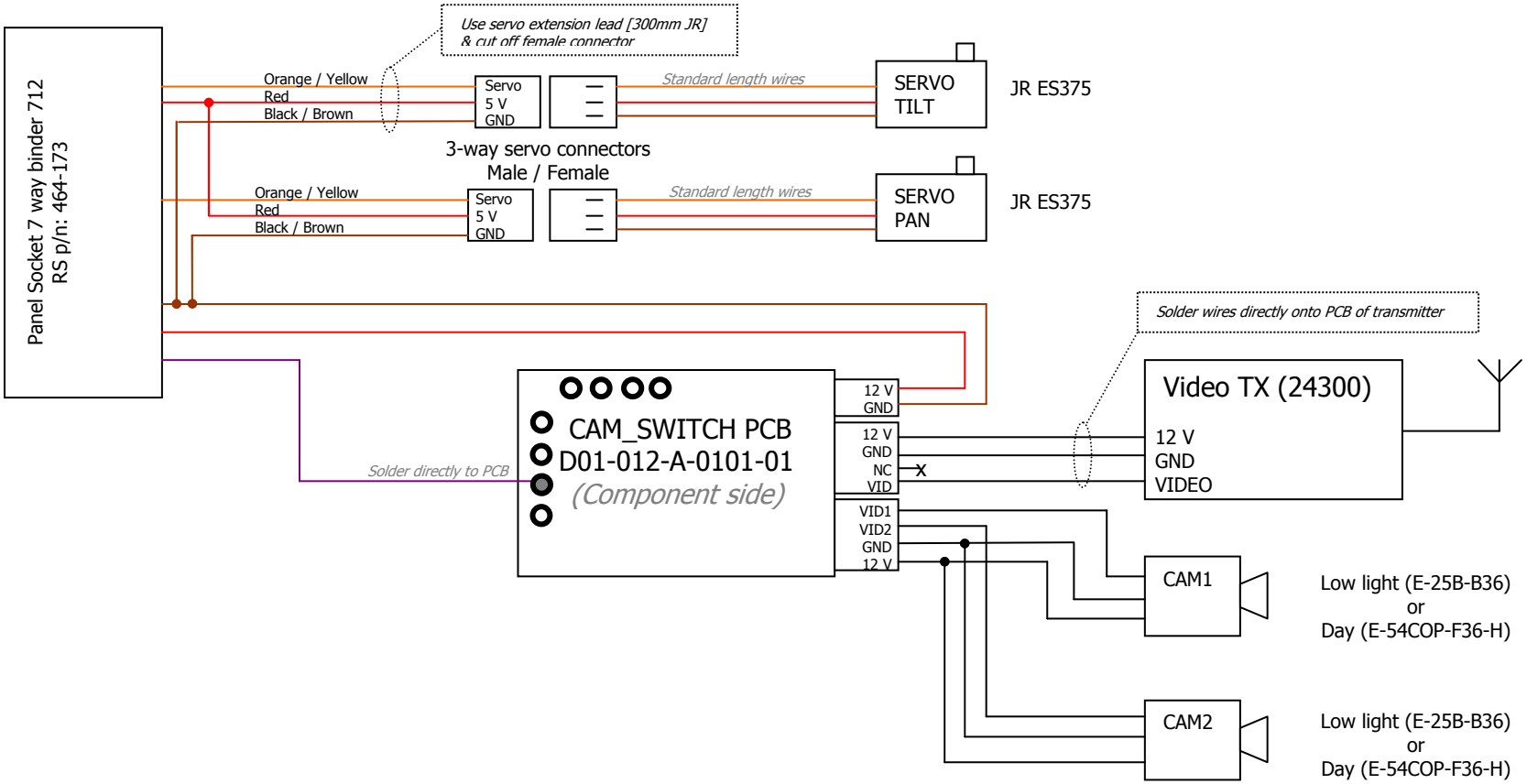

Figure 85: Wiring block diagram for payload with cameras that can pan and tilt

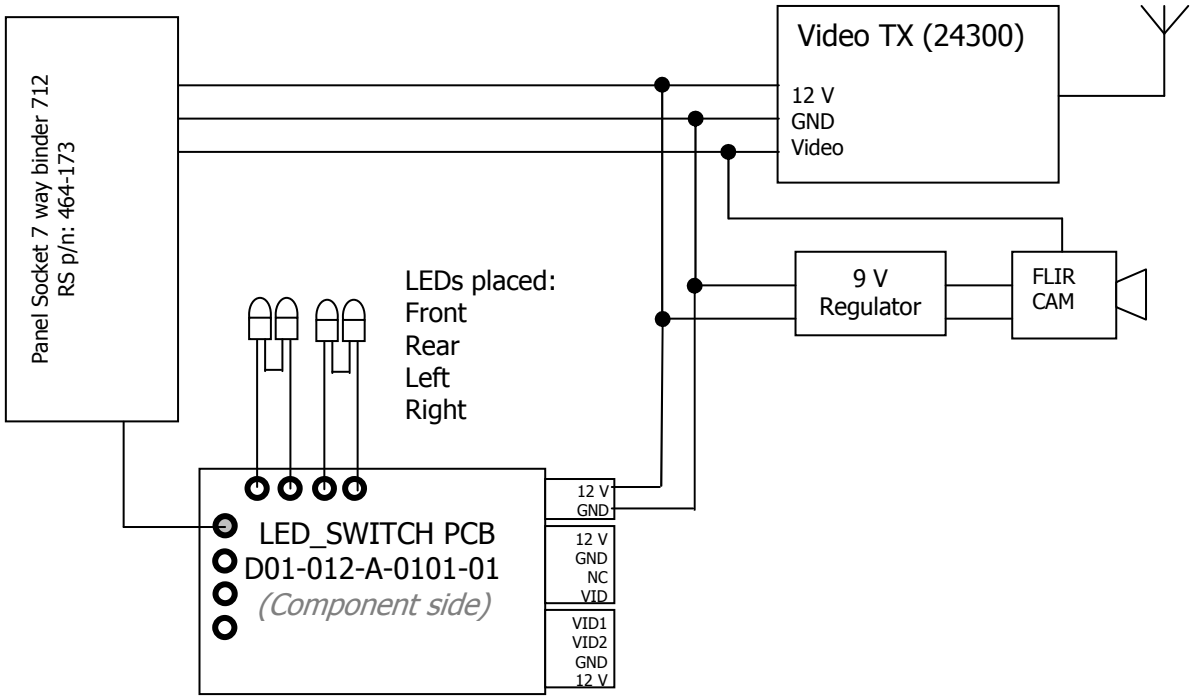

Figure 86: Wiring diagram for payload with FLIR camera and LEDs

Appendix F Autopilot specifications

F.1 Micropilot MP2128g [18]

Servos & Mixing	MP2128g	Tick off
elevon	yes	
flaperons	yes	√
4 servo flap/aileron	yes	
separate flaps	yes	√
v-tail	yes	
x-tail	Yes	
split aileron	Yes	√
rudder throttle	Yes	√
split rudders	yes	
number of servos	8/16/24	√
servo update rate	50 hz	
separate servo and main battery power supply	Yes	√
separate voltage monitor for main and servo battery power supplies	Yes	√
integrated RC override	Yes	√
servo resolution	11 bit	
extra ADC channels and 3-axis magnetometer available	Yes	
Control System	**MP2128g**	
gain scheduling for optimum performance	Yes	√
rudder aileron feed forward for improved turn performance	Yes	√
aileron elevator feed forward for improved altitude hold during turns	yes	√
autonomous takeoff and landing	Yes	√
user definable PID feedback loops (for camera stabilization etc)	8	
user definable table lookup	8	

functions		
MP plugin compatible	Yes	√
Sensors	MP2128^{g}	
airspeed sensor range (kph)	500	√
altimeter range (meters above launch point)	12000	√
3-axis rate gyro	Yes	√
Navigation	**MP2128^{g}**	
1Hz GPS update rate	Yes	√
optional 4 Hz GPS update rate	Yes	
move servo at waypoint	Yes	
change altitude at waypoint	Yes	√
change airspeed at waypoint	Yes	√
user definable holding patterns	Yes	√
user definable error handlers (loss of GPS, low battery etc.)	Yes	√
RPV and UAV modes	Yes	√
supports DGPS accuracy	Yes	√
waypoints	1,000	√
Telemetry, Datalog & Video	**MP2128^{g}**	√
telemetry (user defined fields transmitted each second)	100	
telemetry update rate	5 Hz	
video overlay (number of user definable fields)	16	√
Ground control station	**MP2128^{g}**	√
HORIZON^{mp} 2128 ground control software included with system	yes	√
MP2028^{g} autopilot simulator for operator training	yes	√
ground control station developer's kit	yes	√
gains can be adjusted in-flight	yes	√
change waypoints in-flight	yes	√
payload servos controlled from ground station	yes	√
fly in RC mode via datalink (both stabilized and normal)	yes	√
point-and-click waypoint editor	yes	√
Physical Characteristics	**MP2128^{g}**	
weight (including GPS receiver, gyros, and 26 grams sensors)	(not including GPS antenna)	√
power (including GPS receiver, gyros, all sensors and GPS antenna)	140 mA @ 6.5 V	√

supply Voltage (volts)	4.2 – 26 V	√
size - length (cm)	10.0 cm	√
size - width (cm)	4.0 cm	√
size - height (cm)	1.5 cm	√
software upgradable in the field	yes	√

F.2 UNAV3500FW

This information is directly copied from the brochure and added as an appendix for simplifying the reading of this dissertation.

The 3500 autopilot features an onboard IMU, full-duplex telemetry link and a feature rich Ground Station. 7 RC channels are available, 4 flight control and 3 payload control. Advanced features include integrated camera stabilization, 5 user analog channels and a real-time map display and waypoint control. The 3500 was specifically designed for commercial UAVs and its feature set supports FAA proposed guidelines for Group II, III & IV sUAS operations. The 3500 is capable of operating in any weather, on any fixed-wing aircraft.

- Small Size: 4.0” x 2.0” x 0.8” @ 1.5 oz (PCB).
- (7) RC input channels.
- (7) RC servo outputs.
- AHRS: 5DOF IMU @ 50Hz.
- Onboard sensor suite.
- Onboard servo switching: electronic servo command transfer.
- GPS waypoint navigation: accepts NMEA0183 (GGA & RMC) from any GPS receiver.

- Smart Waypoint sequencer: ignores invalid waypoint data or SPD & ALT out of limits.
- Waypoints: 64 non-volatile waypoint storage (LON, LAT, ALT, SPD).
- Data logging: FDR (20 channel data recorder @ 1Hz).
- Program storage: allows embedded program to be updated in the field.
- Sensor Calibration: on command sensor calibration stored in FLASH.
- Robust design: All data backed in FLASH, transparent recovery from a power failure in 1 sec.
- Fault detection: fault detection, reporting and compensation.
- Payload Trigger: (2) TTL triggers controlled from groundstation or automatically.
- Camera mount servos; (3) integrated camera mount stabilization or manual control.
- Semi-autonomous mode: autopilot stabilizes airplane, ground pilot controls flight path.
- Map: real-time map display and waypoint creation.

Specifications:

- Dimensions: 4.0" x 2.0" x 0.8".
- Weight: 1.5 oz. (PCB).
- Power: 5.5v to 6.5v @ 100ma.
- Operating Temperature: 0 C – 60 C.
- Processor: 16 bit @ 40MIPS.
- FLASH memory: 256K.
- Din: (5) discrete in (5v).
- Dout: (5) discrete out (5v @ 5ma).
- Serial ports: (2) RS232 ports.
- RC: (7) In (7) Out.
- Servos: (4) flight control, (3) payload.

- Analog: (8) onboard sensors, (5) user analog in.
- Max waypoints: 64 Max.drift rate: 0.1 deg/sec.
- Autopilot Parameters: 21 Max. roll rate: 150 deg/sec.
- GPS data: 1 Hz Max. pitch rate: 150 deg/sec.
- Attitude control loop: 50 Hz Attitude accuracy: +/- 2 deg.
- Servo pulse rate: 50 Hz Max. linear acceleration: +/- 5 g's.
- Max. airspeed: 120 mph Max. turn rate: 90 deg/sec.
- Max. range: 25 miles Max. altitude: 16,000 ft MSL.

F.3 UNAV PICOPILOT-NA

This information is directly copied from the brochure and added as an appendix for simplifying the reading of this dissertation.

- Size: 2.0"L x 1.0"W x 0.5"H (-NA).
- PCB Weight: 18g (-NA).
- Max. Altitude: 15,000 ft MSL.
- Altitude Hold: +/- 50 ft.
- Max Airspeed: 50 mph (depends on airframe).
- Min. Airspeed: 5 mph.
- Attitude control loop: 3 Hz.
- Power: 5.0v - 7.0v @ 100ma.
- Roll attitude control: MEMS rate sensor.
- Turn Radius: 100 ft @ 35mph.
- Pitch attitude control: barometric pressure sensor.

- Speed control: +/-2mph sample and hold (-NAT).
- Altitude hold: +/-20ft sample and hold (-NA).
- GPS interface: Any commercial GPS receiver. NMEA0183v2.
- Route storage: 32 waypoint storage (FLASH memory).
- Auto takeoff and landing: no.
- Safety features: 1) circle when GPS reception is lost.
  2) power-up sensor test (BIT).
  3) status LED for each controller.

Waypoints Editor:

- Line item editor permits editing of all 32 waypoints from a display table.
- Pull-down tools for copying and pasting rows, saving and reading route files.
- Note: telemetry can be added by installing a radio modem which sends onboard GPS serial data to a
- groundstation laptop, running moving map software. Another telemetry option is to add an OSD-GPS
- (video text board) to your TV system.

Physical

- Dimensions: 2.0" x 1.0" x 0.5".
- Weight: 1.0 z (-NA).
- Power: 5.0v to 7.0v (from RC receiver).
- Packaging: shrink wrap.
- Temp range: 0F to 100F.

Performance

- max. roll angle: 45 deg.
- max. pitch angle: 20 deg.

- Turn rate sensitivity: 0.1 deg/sec.
- Altitude resolution: 6 in.
- max. airspeed: 50 mph typical (depends on airframe).
- min. airspeed: 5 mph (required for GPS heading data).
- max. turn rate: 20 deg/sec.
- max. altitude: 15,000 ft MSL.
- Turn radius: 100 ft @ 35mph (depends on airframe).
- Positioning accuracy: 15 meters CEP (commercial GPS receiver).